Eutectic Freeze Crystallization of Lactose

Ruben Halfwerk

Eutectic Freeze Crystallization of Lactose

A novel separation technology for food systems at sub-zero temperatures

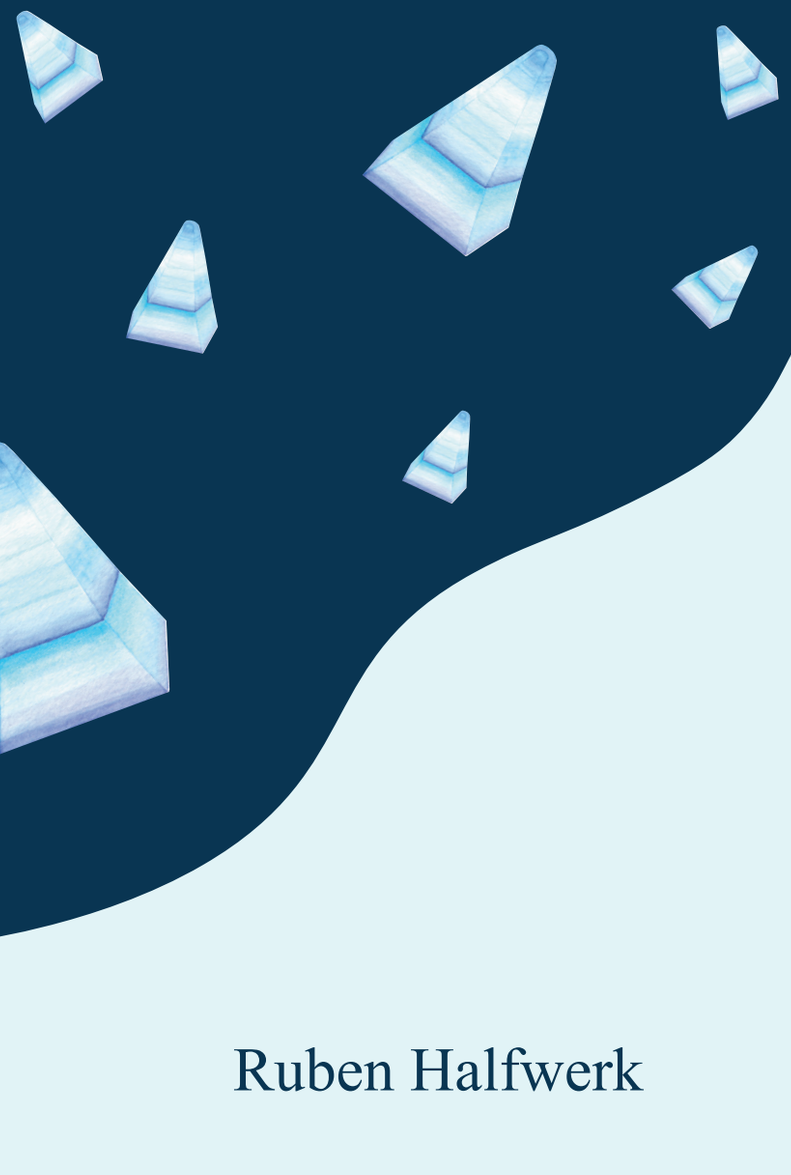

Ruben Halfwerk

Propositions

1. The generalization that processes at low temperatures are slow compared to processes at high temperatures is incorrect.
   (this thesis)
2. Pure systems do not describe reality.
   (this thesis)
3. Supervision determines the productivity of students.
4. Mindset determines the viability of a technology.
5. Life cycle costing of products and services will lead to a different society.
6. Nature protection can only be successful if it is in everyone's way of living.

Propositions belonging to the thesis, entitled:

Eutectic Freeze Crystallization of Lactose
A novel separation technology for food systems at sub-zero temperatures

Ruben Halfwerk

Leeuwarden, 02 June 2023

Eutectic Freeze Crystallization of Lactose

A novel separation technology for food systems at sub-zero temperatures

Ruben Halfwerk

Thesis committee

Promotor

Prof. Dr Albert Van der Padt

Special professor Sustainable Production of Food

Wageningen University & Research

Co-promotor

Dr Doekle Yntema

Scientific Project Manager

Wetsus, European Centre of Excellence for Sustainable Water technology, Leeuwarden

Other members

Prof. Dr P. J. A. van Heijster, Wageningen University & Research

Dr K. van der Voort Maarschalk, Avebe Innovation, Groningen

Dr S.Y. Wong, Singapore Institute of Technology, Singapore

Dr M.L.F. Giuseppin, Giuseppin Technology Advice, Gieten

This research was conducted under the auspices of VLAG Graduate School (Biobased, Biomolecular, Chemical, Food and Nutrition Sciences)

Eutectic Freeze Crystallization of Lactose

A novel separation technology for food systems at sub-zero temperatures

Ruben Halfwerk

Thesis

submitted in fulfilment of the requirements for the degree of doctor
at Wageningen University
by the authority of the Rector Magnificus,
Prof. Dr A.P.J. Mol,
in the presence of the
Thesis Committee appointed by the Academic Board
to be defended in public
on Friday 2 June 2023
at 1:30 p.m. in De Harmonie, Leeuwarden.

Ruben Halfwerk

Eutectic Freeze crystallization of lactose
A novel separation technology for food systems at sub-zero temperatures
195 pages

Cover design by Tamara and Ruben Halfwerk, the lactose crystals and the bird were created by watercolour drawings by Tamara Halfwerk. The bird is a nutcracker bird that connects Ruben's love of nature to this research. Furthermore, it represents the many different challenges solved during this research, some of which were a though nut to crack.

PhD thesis Wageningen University, Wageningen, the Netherlands (2023)
With references, with summaries in English and Dutch

ISBN: 978-94-6447-597-5
DOI: 10.18174/587958

Table of Contents

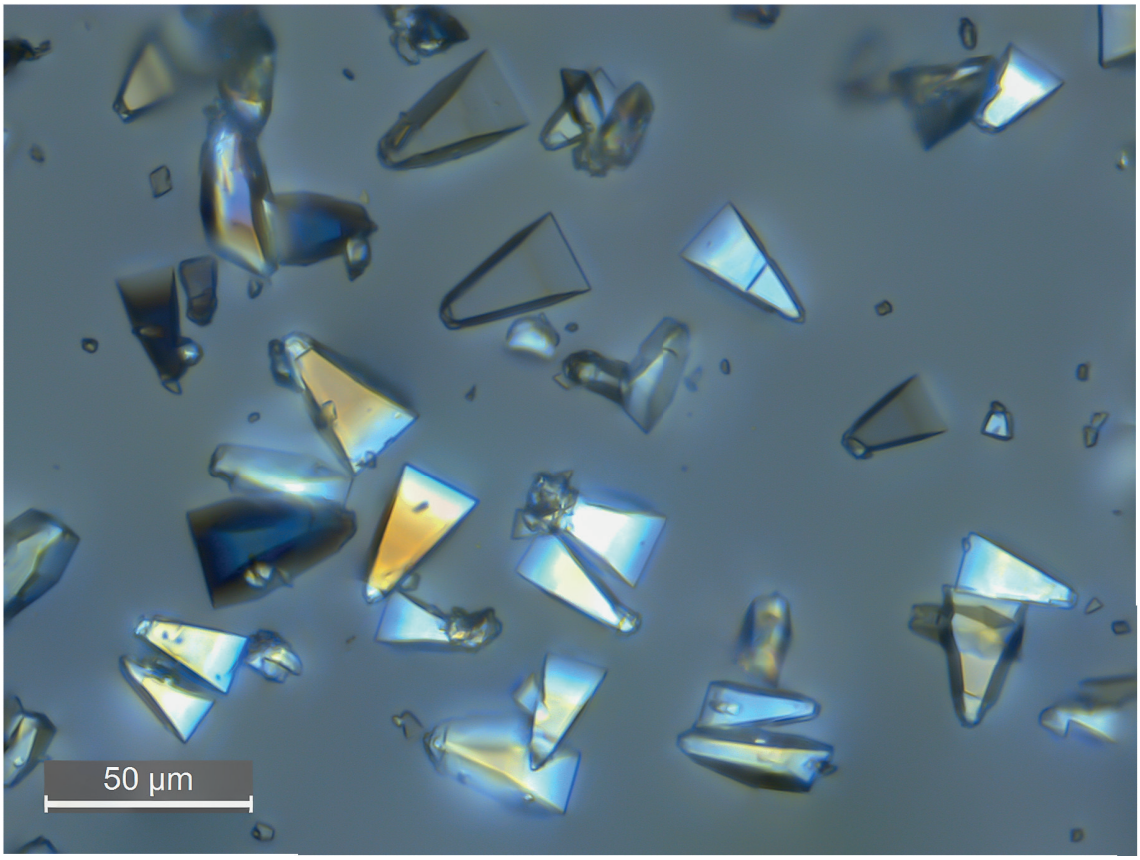

*Tomahawk shaped lactose crystals produced at sub-zero temperatures

Chapter 1

General Introduction

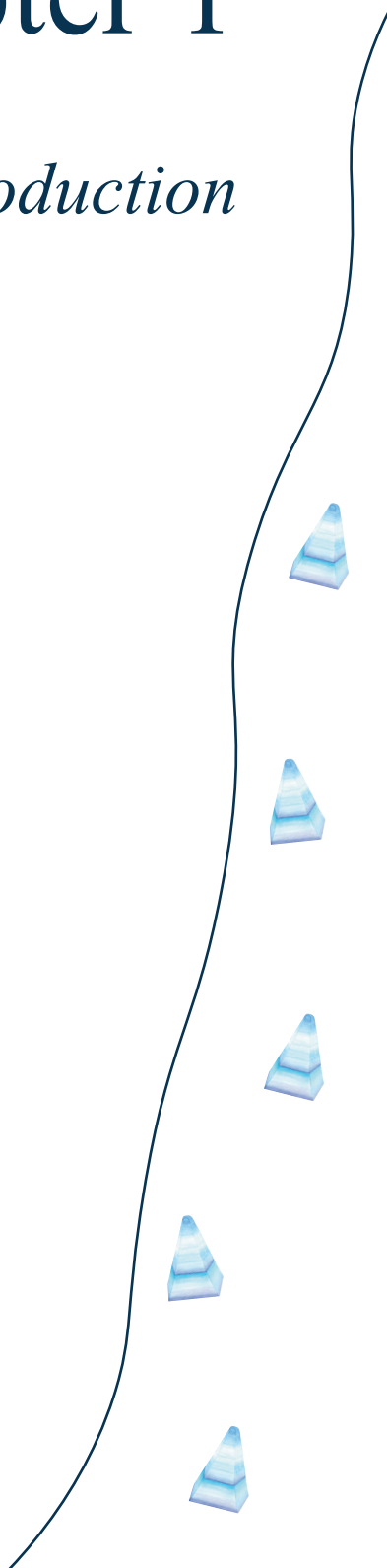

1.1 Crystallization in the food industry

1

Today, crystallization in the food industry is used for the production of many raw materials, like sugars, ice, lipids and proteins (Hartel, 2019). Generally, crystallization from an aqueous solution occurs in two steps: dewatering, producing a concentrated liquid, and slowly cooling this liquid to create a driving force for crystallization. The properties of the crystals are the result of the crystallization process and are strongly affected by the fluid properties, operating conditions, and reactor type. Although highly optimized, the current crystallization processes used in industry have some significant disadvantages: 1. After crystallization, a dilute residual stream is produced, which usually has low economic value and is considered waste. 2. Most crystallization processes are at high temperatures (evaporation), leading to high energy consumption, risk of heat degradation of valuable compounds, high biological activity and fouling of heat exchangers.

An example is the production of lactose from whey permeate, one of the larger streams that is crystallized in the food industry. Lactose is infamous as a problem component for people with lactose intolerance. However, it is used in many everyday products like infant formula, as an ingredient in food products and in the pharmaceutical industry as a filler for drugs in tablets and aerosols (McSweeney and Fox, 2009). Typically, evaporation is used for concentrating whey permeate. At high temperatures, lactose can degrade into lactulose (Berg, 1993). Although this effect is mainly seen at alkaline conditions, still 0.5-3 % of lactose isomerizes to lactulose during UHT processing or sterilization of milk (Gänzle, 2011). It can be expected that during the concentration step of whey permeate a certain amount of lactose is lost as lactulose.

Moreover, the lactose production process suffers from fouling/scaling with calcium phosphate, requiring the need for chemicals and cleaning steps. After

the production of lactose, a residual stream is produced: delactosed whey permeate. This stream still contains around 20wt.% lactose but due to high mineral content and viscous nature it is economically not feasible to have further recovery (Oliveira et al., 2019).

The energy transition and awareness of sustainability, minimization of water usage and the possibility of a higher yield give manufacturers incentive to look at further recovery of these streams. Thus, new technologies are needed to further reduce waste streams at a low energy cost. An alternative to the evaporation process would be to use a process at a temperature below zero, converting water into pure ice. By doing so, the liquid below the ice becomes more concentrated until it is so supersaturated that the solute will also start to crystallize as well: eutectic freeze crystallization (EFC)

In this thesis, eutectic freeze crystallization is investigated for the recovery of lactose. In this chapter, first, conventional lactose production will be explored, next the EFC process and finally the research gap and the goal of this thesis will be defined.

1.2 Conventional production of lactose

Industrially, lactose is recovered from whey, which is a by-product from the cheese manufacturers. Proteins are first retrieved from the whey using ultrafiltration; the resulting whey permeate contains around 5wt.% lactose. Figure 1-1 shows an overview of the different steps, the main steps are concentrating, crystallization and purification (Wong and Hartel, 2014). Whey permeate is first concentrated by reverse osmosis to around 20 wt.%. Subsequently, it is further concentrated to around 55 wt.% lactose. Next, the solution is transferred to a jacket reactor where the solution is slowly cooled from 70°C to around 20°C (Wong and Hartel, 2014). By doing so a driving force for crystallization is created; slow-cooling crystallization. Slow cooling is required to maintain a low supersaturation to maximize growth and limit nucleation. The filling of the tank and the slow cooling process can take up to 24h (Yuping et al., 2006). The residual mother liquid (delactosed whey permeate or DLP) still contains around 20wt.% lactose. In the next stage, the crystals are separated and washed with water. Next, the crystals are ready to be dried in a fluidized bed dryer and packed. Ussually a second crystallization step is applied to remove impurities before drying.

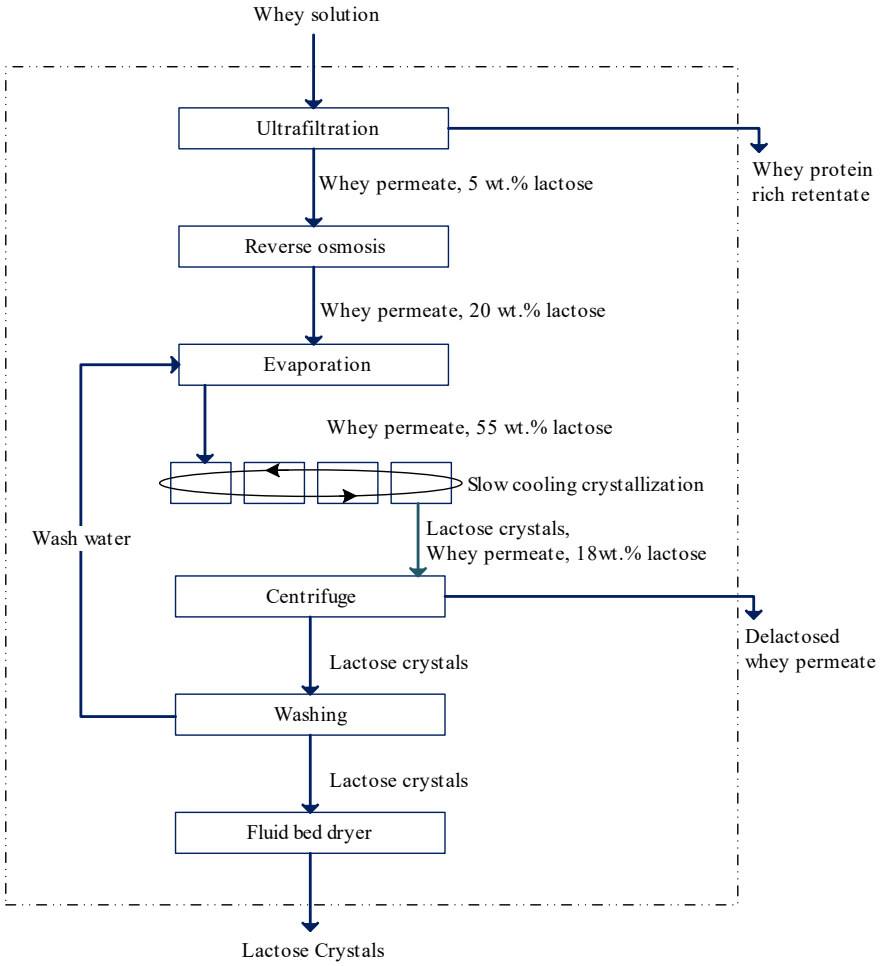

Figure 1-1 Schematic overview of the lactose production process based on (Wong and Hartel, 2014) *and* (Paterson, 2017)

The aim of an industrial lactose process is to grow large crystals with a minimum of fines as further processing will be easier and yields will be higher (Paterson, 2017). In addition to size, an important parameter for the separability of crystals is the morphology of the crystal. Lactose can exist in a wide range of morphologies, the most common types are tomahawk, prism, and needle-like crystals, see Figure 1-2. Tomahawk shaped crystals are preferred as they have the most developed body and are thus more easily separable. The type of morphology that will develop is mainly dependent on the supersaturation and the impurities present in the solution (Parimaladevi and Srinivasan, 2014)(Paterson, 2017). As the final crystal properties depend on many different variables, a major part of lactose research has been focused on crystal growth at different conditions.

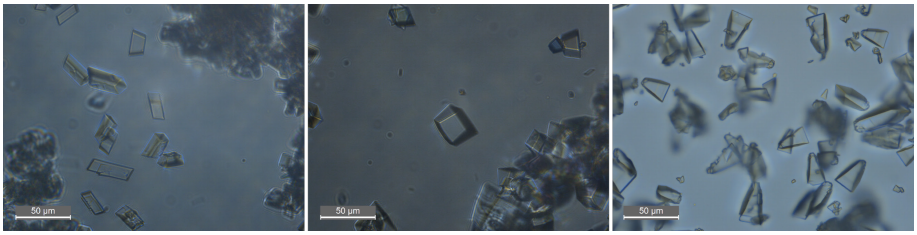

Figure 1-2 Overview of different types of crystal morphologies, 1.) needle like, 2.) prism and 3.) Tomahawk crystals

1.3 Eutectic freeze crystallization

The eutectic point of a solution is the point where both the solute as the solvent start to crystallize simultaneously, hence the name eutectic freeze crystallization. By using this point, a binary solution can in principle be fully converted to ice and crystals(van der Ham et al., 1999). Figure 1-3 shows a simplified binary phase diagram: the lines are the freeze point line and solubility line; the intersection is the eutectic point. Depending on the initial concentration, the solvent or solute will start to crystallize if the temperature is set to the eutectic

temperature. When a lower concentration is used, the solvent will first start to crystallize first, until the concentration reaches the saturation point (path A→B→C). Whereas, if a higher concentration is used, solute will first crystallize until it reaches the eutectic point, after which the solvent will start to crystallize (path D→E→C). Note that by operating at the eutectic temperature, in theory, the whole solution can be converted into ice and salt, in practice, the system will be stopped earlier on or operated in continuous mode, adding a continuous new solution, and removing ice and crystals. Due to the density difference between the solvent and solute, separation by gravity is possible.

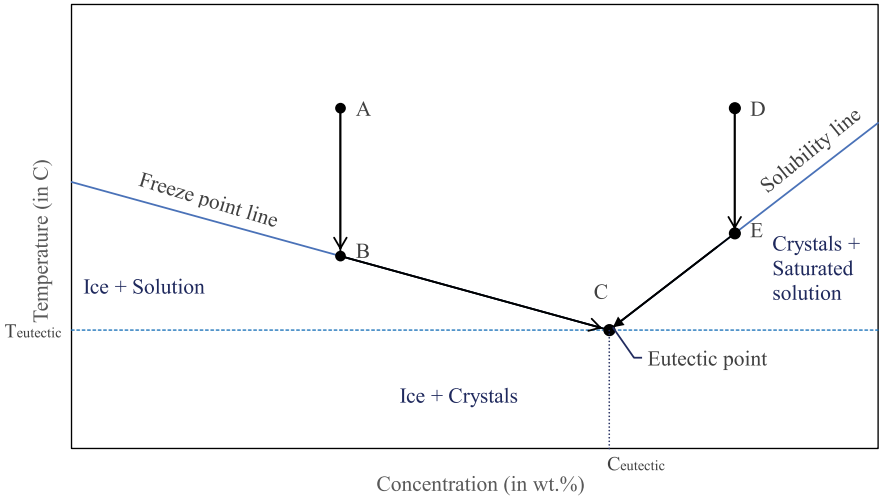

Figure 1-3 Binary phase diagram to show the eutectic freeze crystallization principle

1.3.1 Origin

The use of the eutectic point was first proposed as a separation technique by (Stepakoff et al., 1974), who mixed refrigerant and a NaCl solution together. They found that the solution could be separated into 5 phases: ice, brine, NaCl dihydrate, liquid Freon and Freon vapor (Stepakoff et al., 1974). After this discovery, different researchers worked on the use of eutectic freeze

crystallization for different types of brine streams, among which brine streams from the mining industry, reverse osmosis brine and textile wastewater (Lewis et al., 2010)(Randall et al., 2011) (Randall and Nathoo, 2015) (van der Ham et al., 1999)(Van Spronsen et al., 2010).

1.3.2 Physical implementation

An EFC crystallizer is usually cooled indirectly by cooling fluid flowing through plates in the reactor or on the outside of the reactor. The total surface area that is needed for cooling is a key parameter, as well as the heat transfer coefficient (van der Ham et al., 1998). As the temperature of the coolant and thus surface area is normally lower than that of the solution, the degree of supersaturation for both solvent as solute will be higher at the surface. Thus, there is a large risk of solute and ice scaling on the surface of the heat exchanger which reduces heat transfer and thus slowing down cooling. The rate of ice scaling on a surface depends on the temperature difference of the solution/surface area and the operating conditions like agitation, viscosity, and concentration. Therefore, a major part of the research has been on developing different types of crystallizes (Genceli et al., 2005)(Rodriguez Pascual et al., 2010)(van der Ham et al., 2004)(Vaessen et al., 2004). The most common concept is the use of scraped crystallizer, where scrapers take care of the removal of ice from the cooling plates as well as agitation of the solution.

In addition to the crystallizer an EFC process requires a separator which settles the slurry, ice will float to the top and crystals sink to the bottom. The ice and salt crystals are recovered by two centrifuges/belt filters. To increase the purity of the crystals they can be washed simultaneously in the centrifuge. Figure 1-4 shows an overview of the steps. After separation, the crystals are further processed similarly to the slow-cooling crystallization process for lactose described in section 1.2.

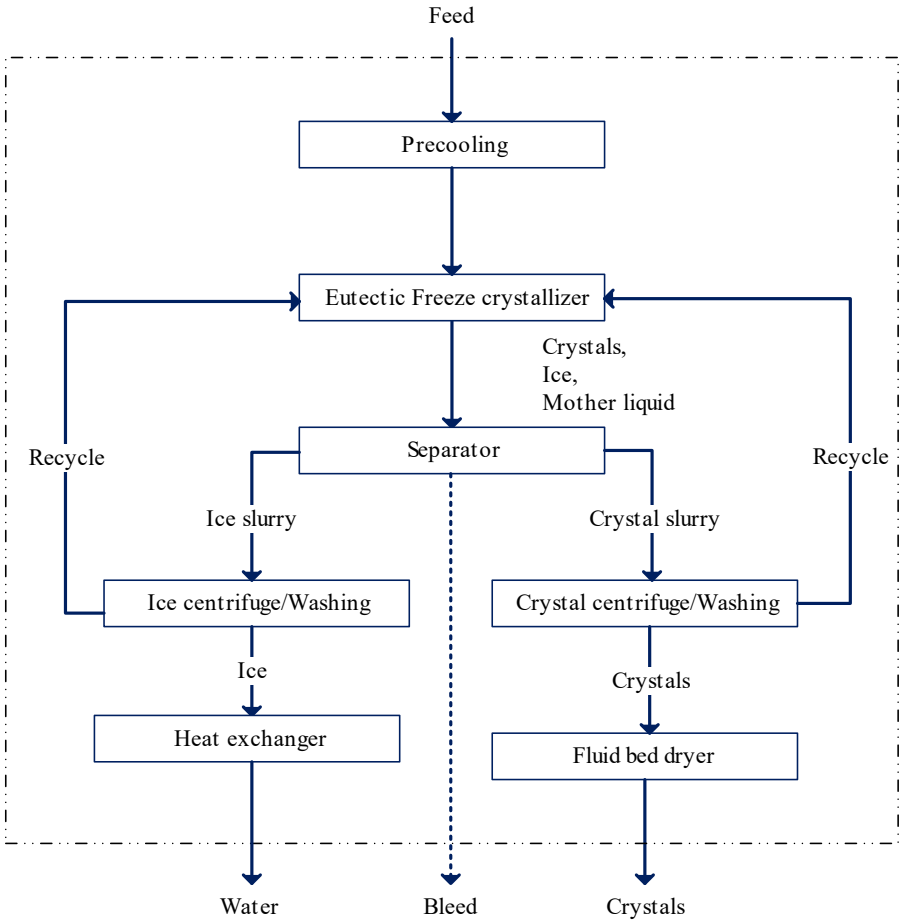

Figure 1-4 Schematic overview of an EFC process

In comparison with other separation technologies like evaporation, EFC has a low energy requirement and has in theory the ability of complete conversion of feed into water and crystals, but only if no bleed is needed, e.g. in case of binary systems. It has therefore been suggested as a good alternative to the existing technology (Fernández-Torres et al., 2012)(Himawan, 2005) (Vaessen et al., 2004)(van der Ham et al., 1998).

1.4 Knowledge gap

Most of the research on EFC has been focused on brine streams, recovering different types of salt. However, in theory, this method could also be applied for organic crystalline substances, for example sugars. Using low temperatures for food application is very beneficial. At temperatures below zero, heat-sensitive compounds are not affected, preserving taste and quality (Sánchez et al., 2011). In addition, biological activity is low at temperatures below zero. Moreover, fouling, scaling and corrosion issues will be less (Williams et al., 2015).

Although the use of EFC is proven for brine streams it cannot easily be extrapolated for food streams as generally they are more complex. Typically, food streams are a mixture of minerals, acids, sugars, and proteins. Crystallization of food streams can therefore be challenging, as the composition is complex and exact interactions are not always known. Moreover, like many sugars, lactose can exist in two isomeric forms: alpha and beta lactose. When dissolved, an equilibrium of the two isomeric forms is formed (Wong and Hartel, 2014). The effect of temperatures below zero on the crystallization process, and how it influences growth, nucleation, and the isomeric forms, is largely unknown. Knowledge about the eutectic point and best operating regime is lacking.

In food industry, EFC is a relative new technology and replacing the current/conventional technology is challenging. Therefore, this technology is particularly interesting for treating residual streams, as it can still add value to them. Further recovery of lactose from delactosed whey permeate could still give value to this stream. Insight is needed if a low-temperature crystallization process can handle the high viscosity and high mineral content.

Furthermore, EFC is a continuous process operating at a constant concentration, the eutectic point, simultaneous converting solvent, and solute. The question is whether EFC for food systems can be operated continuously and whether enough yield could be obtained within a limited process time.

1.5 Goal of this research

The aim of this research was to show the applicability of EFC for streams in the food and agricultural industry, as model system lactose was used. Based on section 1.4 the main objectives were determined as:

1. To show the proof of concept of using EFC for lactose, to find the best operating regime and to assess the quality of crystals based on their morphology and size.

2. To identify and describe the kinetics of lactose crystallisation at sub-zero temperatures, determining the effect of mutarotation, nucleation, and the growth of crystals at these kinetics.

3. To assess the possibility of using EFC for the recovery of lactose from a residual stream from the dairy industry: delactosed whey permeate. And to determine the effect of minerals on the crystallization process.

4. To assess the viability of scaling up a eutectic freeze crystallization process, to determine the effect on yield and energy consumption

1.6 Thesis outline

Chapter 2 shows the use of eutectic freeze crystallization as a separation technology for the recovery of lactose. A proof of concept was demonstrated for both freeze concentration and eutectic freeze crystallization. Furthermore, a detailed analysis was performed into the effect of seeding on the morphology and crystal size of the crystals.

Subsequently, the kinetics of a lactose crystallization process at temperatures below zero was investigated **in chapter 3**. A population balance model combining mutarotation, nucleation and crystal growth was used to describe the growth of crystals over time. Different operating conditions were analysed, with varying stirrer rates and initial concentrations. The model results were compared with the experimental results.

In **chapter 4** it is explored whether a low-temperature crystallization process is suitable for the recovery of lactose from delactosed whey permeate, which is currently a waste stream from the dairy industry. The lactose from delactosed whey permeate was compared with lactose obtained from pure solutions with respect to yield, crystal size, morphology, and kinetics.

In **chapter 5** a realistic system was used, comprising of a continuous eutectic freeze reactor of 315l. In this pilot test it was shown that lactose and ice could be recovered simultaneously from whey permeate. An evaluation of all mass and energy balances is made.

In **Chapter 6,** we present a general discussion of the results found in this thesis. Furthermore, it assesses the viability of the EFC process compared to conventional techniques, and an outlook is described for future research.

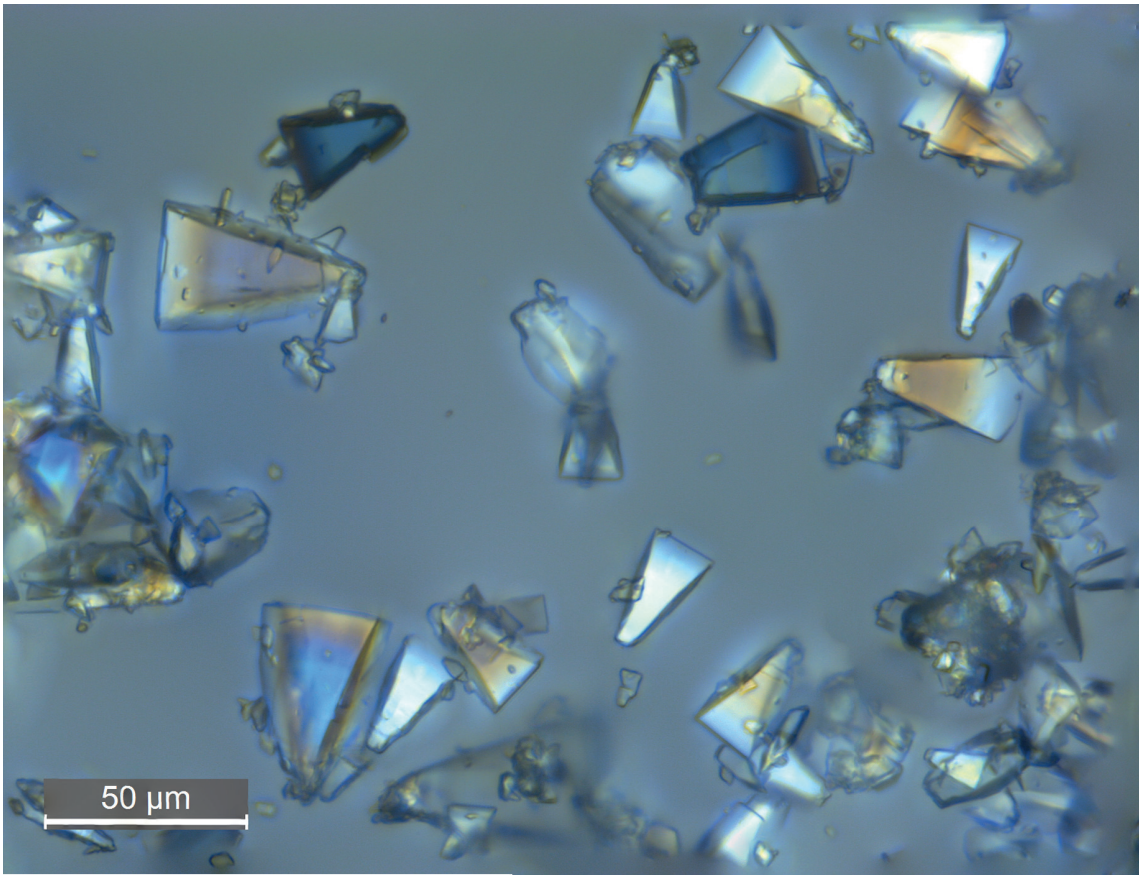

*Tomahawk shaped lactose crystals produced at sub-zero temperatures

Chapter 2

A sub-zero crystallization process for the recovery of lactose

This chapter has been published as:
Halfwerk, R., Yntema, D., Van Spronsen, J., Van der Padt, A., (2021).
A sub-zero crystallization process for the recovery of lactose.
Journal of Food Engineering

Abstract

In industry, lactose is generally produced by concentrating whey permeate by evaporation followed by a slow cooling process where lactose is crystallized. Here, an alternative method is presented whereby the concentration and crystallization steps are combined at sub-zero temperatures, so-called eutectic freeze crystallization. It was discovered that simultaneous crystallization of lactose and water (ice) is possible. The obtained lactose crystals had an average size of 10 µm and a thin triangular or tomahawk morphology.

The process was analysed in detail in two steps: freeze concentration and lactose crystallization at sub-zero temperatures. Freeze concentration experiments showed that concentrating to supersaturation was possible without excessive lactose crystallization. In the second step, lactose was crystallized at temperatures below zero from a 30 wt.% lactose solution, without observation of significant primary or secondary nucleation. The amount of seed material had a large influence on the final yield, crystal size and morphology. The optimum seed amount was found to be at 0.08% of the total lactose; the resulting crystals had an average size of 26 µm and a tomahawk morphology. Although highly supersaturated conditions are present in the sub-zero crystallization of lactose, crystal growth is found to be the predominant process rather than nucleation.

2.1 Introduction

Lactose has a wide range of applications ranging from additives in the food industry to products for the pharmaceutical industry. Lactose is the main sugary compound in human and mammalian milk where, among others, it acts as a source of energy. It is a key ingredient for the production of infant formula from cow milk where the amount of lactose in cow milk (4.6%) is increased to the concentration of human milk (7%) (McSweeney and Fox, 2009). Furthermore, lactose is used as a free-flowing or agglomerating agent to accentuate/enhance the flavour of some food applications (McSweeney and Fox, 2009). In the pharmaceutical industry, it is used as a filler for drugs in tablets, capsules and aerosols.

Industrially, lactose is sourced from whey, a side product from cheese and casein production. The lactose production process can be described in three stages: increasing concentration, crystallization of lactose and purification (Wong and Hartel, 2014). Proteins in whey are first removed by ultrafiltration; producing a whey protein concentrate and whey permeate. Whey permeate has a lactose concentration of 5%; in a second stage, it is concentrated by evaporation to 39%–56% (Wong and Hartel, 2014). The lactose in concentrated whey permeate is subsequently crystallized as α-lactose monohydrate; the supersaturated whey permeate leaves the evaporator at a temperature between 65°C and 70°C and is slowly cooled down to 20°C–25°C. While the solution is cooled, supersaturation is created and so the driving force for crystallization is increased. Industrial crystallization by gradual cooling generally takes up to 14–18 h (Yuping et al., 2006). After crystallization, the lactose crystals are separated from the mother liquor by centrifugation and an additional washing and centrifugation step is used to remove any remaining impurities (Wong and Hartel, 2014). The liquid that is separated by centrifugation

is called de-lactosed whey permeate. Any remaining water content in the lactose crystals is removed in a fluidized bed dryer.

2.1.1 Lactose crystallization

Figure 2-1 shows part of the lactose–water phase diagram constructed from data published by different authors (Hudson, 1908)(Wong et al., 2011)(Vu et al., 2003). The rate of nucleation can be characterized by the induction time, i.e. the time elapsed between the initiation of supersaturation and the initial formation of nuclei (Karpinski and Wey, 2002). The induction time can be used to divide the graph into different regimes: an under saturated solution regime, a metastable regime and a labile zone. In the under saturated regime, no crystal growth or nucleation occurs and it is a transparent solution. In the labile zone, supersaturation is high, which results in a relatively short induction time of between 10 and 36 h (Herrington, 1934) (Wong and Hartel, 2014). In the metastable zone, crystallization without the addition of seeds will not occur quickly. The induction time reported for crystallization without stirring in the metastable zone was 136 h (Herrington, 1934) (Wong et al., 2011). When lactose crystals are present, crystal growth and secondary nucleation are possible in the metastable regime (Wong and Hartel, 2014).

For industrial crystallization processes, it is important to produce relatively large and uniform crystals because this makes further separation and handling of the crystals easier. The optimum size of lactose crystals is 200–300 µm with a tomahawk shape (Durham, 2009). The size, size distribution and shape of the crystals depends on the type of solution and the operating parameters. Furthermore, the size and size distribution of lactose seeds have a large influence on the nucleation and growth rate during crystallization. Ideally, seed material has a small crystal size distribution with a minimal amount of aggregation and is free of small crystals (<20 µm)(Wong et al., 2011). (Yuping et al., 2006)

studied the effect of seed amount for lactose crystallization and reported an optimum amount of nuclei (27 mg/100 g).

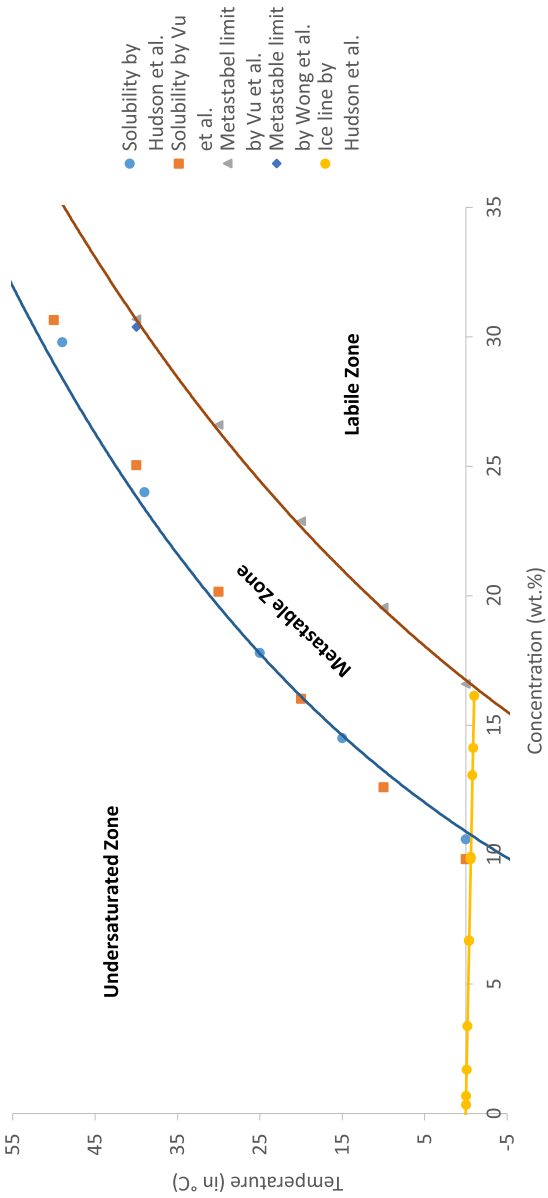

Figure 2-1 Phase diagram of lactose–water solution (only α-lactose monohydrate). Data used from (Hudson, 1908) (Wong et al., 2011) *and* (Vu et al., 2003)*).*

In industrial crystallization, generally a large amount of fines is produced due to secondary nucleation; this limits the separation efficiency, resulting in low recovery rates (Paterson, 2009). There is a trade-off between the amount of supersaturation, rate of crystallization and the amount of secondary nucleation. Operating close to the solubility of lactose reduces the amount of nucleation, however it results in a lower crystallization rate. (Wong et al., 2012) compared an industrial crystallization process with an improved process based on the metastable limit. The authors found that in order to minimize secondary nucleation or the production of fines, a cooling profile needs to be selected such that the concentration profile of the crystallization process lies within the upper metastable zone. They found that using a cooling profile based on the medium metastable regime produced 28% less fines than an industrial process.

Supersaturation ratios of α-lactose solutions depend on temperature, concentration and mutarotation equilibrium of α-/β-lactose, (Visser, 1983) developed a method to determine the supersaturation ratio:

$$S = \frac{C}{C_s - FK_m(C - C_s)} \tag{2-1}$$

where F and K_m are factors to account for β-lactose in the solution. In an industrial process, a supersaturation ratio between 1.5 and 2 is generally used (Wong et al., 2012)(Visser, 1983).

2.1.2 Low-temperature crystallization

Industrial lactose crystallization from whey is an energy-intensive process because of the evaporation step. Furthermore, high temperatures and long residence times, up to 18 h, are needed during cooling crystallization. Evaporators and crystallizers can suffer from fouling. Whey permeate contains about 370 ppm calcium and 440 ppm phosphorus; at these concentrations whey permeate is already saturated with calcium and phosphate (Durham, 2009). When whey is heated above 60°C, calcium and magnesium phosphates and residual proteins, fat, etc. precipitate and form scaling on the evaporators and heat exchangers; this leads to higher energy and maintenance costs (Bylund, 2015).

Several studies have been performed involving methods for improving the lactose crystallization process. Ultrasound is known to lower the induction times for lactose nucleation due to cavitation of the (lactose) solutions, this results in an increase in crystallization rate (Dincer et al., 2014b)(Zisu et al., 2014). Similar, gas addition, like nitrogen or carbon dioxide, during lactose crystallization increases the nucleation rate and yield. A larger amount of gas will result in a decrease in crystal size (Adhikari et al., 2018)(Xun et al., 2017). Antisolvents, like methanol, acetone or ethanol can lower the solubility of the solute thus increasing the supersaturation. (MacFhionnghaile et al., 2017) studied the effect of different antisolvents in combination of lactose crystallization. Mixtures of α-lactose monohydrate and β-lactose were crystallized under most conditions with β-lactose content increasing with increasing amount of antisolvent. (Patil et al., 2020) investigated the recovery of lactose with a combination of antisolvent and sonication. They found that the highest lactose recovery was obtained using a mixture of acetone and ethanol as antisolvent.

In this research, a new crystallization method is investigated to produce lactose at sub-zero temperatures: eutectic freeze crystallization (EFC). The eutectic point of a solution is the point at which both the solvent and the solute start to crystalize. Although EFC has been used for the separation of brine streams (Lewis et al., 2010; Randall and Nathoo, 2015, 2018), limited research has been found by the authors for the recovery of heat-sensitive products in the food industry. In a patent by (Spronsen, 2017) freeze concentration is used to concentrate a lactose solution well below the eutectic point. They found that it was possible to freeze concentrate a solution up to 27wt% without crystallization of lactose. After this concentration step lactose is crystallized at a constant temperature of 10-20°C, the remaining mother liquid could be recycled to the reactor. In our research it is investigated if it is possible to combine the concentration and crystallization step at sub-zero temperatures.

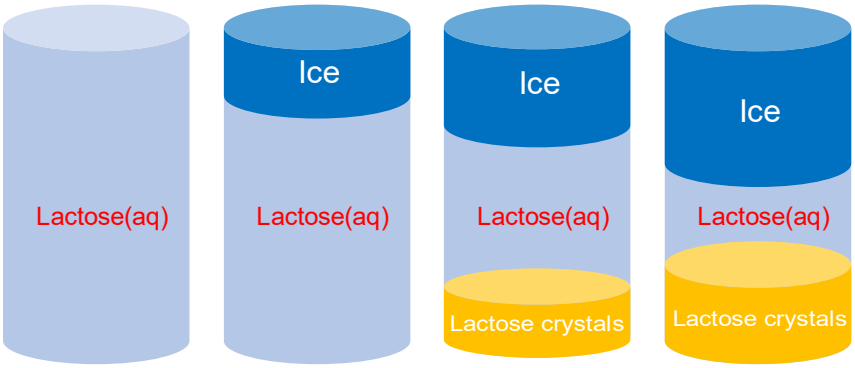

Figure 2-2 An ideal development of an EFC process: 1. A lactose solution is cooled to temperatures below zero 2. The temperature drops below the freeze point and ice crystallizes, the concentration of lactose in the solution increases 3. Lactose crystallizes when the solution is saturated with respect to lactose, this is the eutectic point. Due to density differences ice floats to the top and lactose crystals sink to the bottom 4. The simultaneous crystallization of ice and lactose will continue until the process is stopped.

From Figure 2-1, the eutectic point of an aqueous lactose solution can be determined at 11 wt.% and −0.7°C. Using this, in theory, the solution can be converted into pure ice and lactose (Figure 2-2). Based on primary energy demands, converting water into ice is favourable over evaporation. The heat of solidification of ice produces 334 kJ/kg, whereas the heat of evaporation consumes 2265 kJ/kg. In practical operation, the energy consumption levels are closer. Fouling by calcium phosphate when using freeze concentration is limited because calcium phosphate precipitation is favoured by higher temperatures (Durham, 2009).

Lactose crystallization at sub-zero temperatures is not unique, it does occur in ice-cream production as well, where lactose crystals can cause a sandy texture if they become too large. At temperatures below zero, lactose has greatly exceeded its solubility saturation and, from a thermodynamic point of view, could easily crystallize (McSweeney and Fox, 2009). However, nucleation is strongly dependent on temperature and viscosity. Where the higher supersaturation increases the driving force for crystallization, it is counter affected by the low nucleation rate due to the decreased temperature and increased viscosity of ice cream. Once nucleation has occurred, crystallization can proceed quickly (McSweeney and Fox, 2009). Nickerson (1954, 1956) investigated the effect of seeding on the rate and quantity of lactose crystallization in ice cream, they found that lactose crystallization is slow without the presence of initial nuclei (Nickerson, 1956). Furthermore, they found that if a small amount of lactose crystals was present initially, they caused the ice cream to become sandy more quickly than when a large number of nuclei were present. Livney et al. (1995) investigated the induction time and initial growth rate of lactose crystals in ice cream. They found that the induction time initially decreased when the temperature was lowered until a minimum time of 3 hours was found between -10°C and -12°C. Further decrease of the storage

temperature caused the induction time to increase again. The initial growth rate increased when the temperature was decreased from -5°C to -10°C. Further decrease would result in a lower initial growth rate.

The dependency on the amount of seed on crystal growth plus the slow nucleation kinetics found in ice-cream production provides an opportunity, it is an indication that crystallization of lactose from a solution, without excessive nucleation, is possible at sub-zero temperatures.

2.2 Materials and methods

2.2.1 Experimental setup

Experiments were performed using a crystallizer consisting of a double walled vessel with cooling fluid inside the vessel and cooling fluid circulating through the wall (Figure 2-3). A glass beaker with a solution was placed inside the vessel. The cooling fluid between the vessel and glass beaker ensures good thermal contact between the wall of the vessel and the glass beaker. Essentially, liquid could be poured directly into the reactor, however, for experimental reasons, e.g. to look through and for easy removal of slurry, a glass beaker is used. The contact fluid was stirred with a magnetic stirrer at 200 rpm to ensure good heat transfer to the glass beaker. The cooling fluid in the jacket was cooled by a chiller with a flow of 10 L/min. Agitation of the lactose solution was done by an anchor stirrer inside the glass beaker. The use of an anchor mixer ensures that the area at the wall is well mixed and that a uniform temperature is created. The temperature inside the glass crystallizer beaker was measured using a precision temperature sensor (Tempcontrol PT 6180 with ASL F200 indicator), which has (calibrated) accuracy of 0.02K. Data acquisition and equipment control of the temperature indicator was done via an RS-232 connection and a program running in Python.

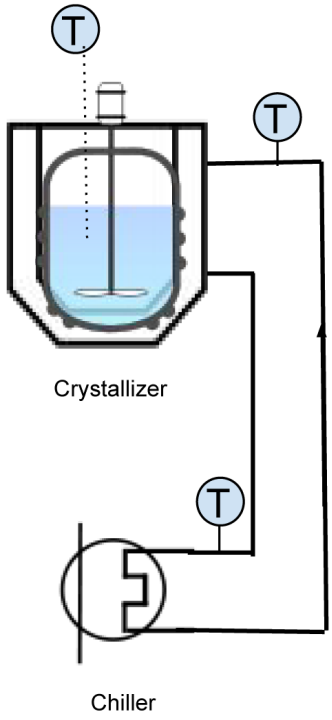

Figure 2-3 Crystallization reactor for eutectic freeze crystallization.

2.3 Materials

2.3.1 Lactose concentrate

Lactose solutions were prepared by dissolving analytical grade lactose monohydrate (≥99% α-lactose) in hot (60°C–80°C) MilliQ water. During dissolution, the solution was stirred with a magnetic stirrer. The concentration of the solution was determined using a refractometer (Krüss AR4), and any evaporation was compensated by adding MilliQ water.

2.3.2 Seeds

Micronized lactose from DFE Pharma (Lactohale 300) was used as seed. Fifty percent of the particles are smaller than 5 µm and ninety percent of the particles are smaller than 10 µm. The material does not have a defined morphology. The seeds were produced by milling and fractionated by air classification. Figure 2-4 shows the particle size distribution of the seed crystals.

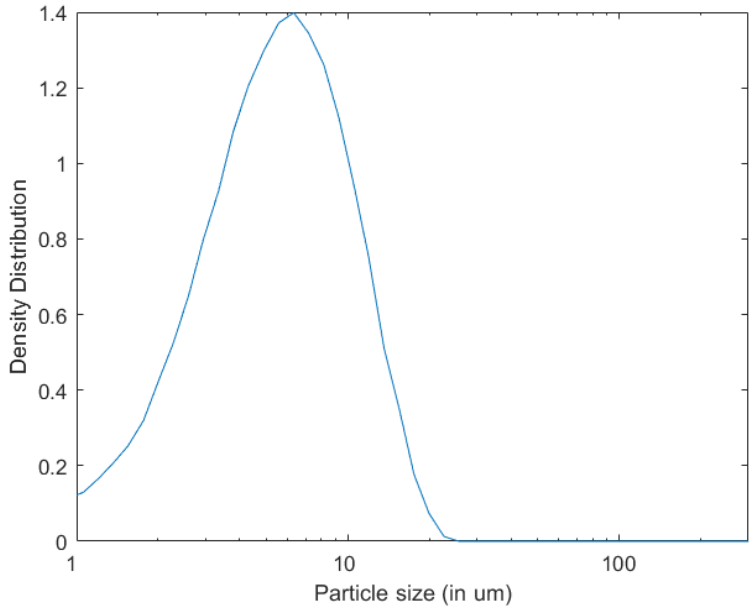

Figure 2-4 Particle size distribution of seed (DFE Pharma, Lactohale 300).

2.4 Crystallization methods

The effect of low-temperature crystallization on the quality and quantity of lactose was investigated by two methods. First, a sub-EFC process whereby both ice and lactose are produced simultaneously, secondly, a freeze concentration process with removal of the ice and a low-temperature lactose crystallization step.

2.4.1 Eutectic freeze crystallization

A 900 ml solution of 30 wt% lactose was used to investigate EFC of a pure lactose–water system. The solution was cooled in ± 4h with a chiller temperature of −4.5°C, resulting in a liquid temperature before ice nucleation of −3°C. A lower temperature than the eutectic temperature was chosen as there would be no supersaturation of ice and lactose above the eutectic temperature and thus no driving force for crystallization. When the temperature dropped below -2.7°C, 0.08% seed material based on the total amount of lactose (250 mg/kg solution) was added, and the operation was kept at constant temperature for ~22 h. This was chosen to exceed the time used in an industrial lactose crystallization process (14–18 h) to get more insight in the full development of the process. The low seed amount was based on the optimum amount reported by Yuping et al. (2006); due to the small crystal size of the seed, a relatively small amount resulted in a large number of crystals.

The concentration of the solution was measured by sampling a few millilitres and measuring the brix value using a refractometer (Krüss). After 22 hours, the reactor was filed with ice/lactose and the operation was stopped. Continuing for a longer period was impossible because the stirrer would not be able to stir the thick slurry. For our 1-L batch process, the large volume of ice made it impossible to effectively separate the slurry into ice, lactose crystals and mother To still be able to separate the slurry, we took a step back and first

melted the ice, leaving only lactose crystals and mother liquid. The final concentration of the mother liquid (after ice melting) was well above the solubility concentration; with no dissolution and, as crystallization occurs slowly, no addition of mass was expected.

With the ice melted, the slurry was allowed to settle and was filtered over a sintered glass filter with pore size 16–40 µm. The lactose was subsequently washed with 2-propanol to remove any moisture. The so washed lactose crystals were dried at 45°C for 24 h to remove any remaining free water (not the hydrate). The overall mass balance was evaluated by determining the final concentration in the solution as well as the recovered lactose, enabling the calculation of the amount of ice. See appendix 2.A for a detailed description of the mass balance. The lactose crystals were investigated under a microscope (Leica dm750 with polarized light) and a particle size analyser (Sympatec laser diffraction).

2.4.2 Uncoupled system: freeze concentration and sub-zero lactose crystallization

To investigate the process in more detail, the system was uncoupled into two steps: (1) freeze concentration and (2) crystallization at sub-zero temperatures without ice formation.

Freeze concentration

Before crystallization, a concentration step is generally used to produce a supersaturated liquid to create a driving force for crystallization. For this research, five different solutions with a lactose content ranging from 5 to 30 wt%, were investigated to check if it was possible to concentrate the solutions by freeze concentration without the development of lactose nuclei. A lactose solution (800 mL) was poured into the crystallizer, and the temperature of the chiller was set to −5.5°C. The solution was agitated with an anchor stirrer at

70 rpm. When the temperature of the solution stabilized, ice spontaneously nucleated after 1–2 h. The experiment was stopped when the glass beaker was filled with ice. The slurry was filtered over a sintered glass filter with pore size 40–100 µm. Three washing steps with 50 mL of cooled (0°C) MilliQ water were applied before removing the ice from the filter. Melting of ice by the washing fluid is expected to be neglectable as heat transfer from washing water of ± 0°C is low. A mass balance was made, and the final concentration of the solution, ice and wash water was determined using a refractometer (Krüss AR4). A sample of the concentrate was investigated under the microscope to check if there was spontaneous nucleation. The growth rate of ice at constant chiller temperature (−5.5°C) was determined for different start concentrations; the growth rate was defined as the mass of pure ice divided by the residence time.

Crystallization of lactose at sub-zero temperatures without ice formation

A 30 wt% lactose solution was used to investigate crystallization of lactose after freeze concentration; 950 mL of lactose solution was added to the crystallizer. After dissolving the lactose at 50°C the solution was cooled as fast as possible. The temperature of the chiller was set to −3°C, resulting in a final temperature of the solution of −1.9°C and a supersaturation ratio of 4.1 (determined by the method described by Visser, 1983). As crystallization proceeded, the supersaturation decreased because the temperature was constant. Different amounts of lactose seeds, namely 0.08, 0.2 and 5 wt% based on the total lactose content, were added when the temperature of the liquid reached −1.85°C. The amount of 0.08wt% was based on the optimum reported by Yuping et al. (2006). Seed was added from room temperature; the temperature increase for 5% was 0.19°C, 0.04°C for 0.2% and there was no effect observed for 0.08%. The temperature of the chiller was kept stable for 22 h, which is

relatively close to the residence time in an industrial process. The extent of crystallization was determined by sampling a few millilitres of solution and measuring the brix degree using a refractometer (Krüss).

The crystallized slurry was filtered over a sintered glass filter with pore size 16–40 µm. The filtrate was subsequently washed with 2-propanol to lower the water content. The lactose crystals were dried until constant weight at 45°C in an incubator to remove any remaining water. An overall mass balance was evaluated by determining the final concentration and the amount of lactose recovered. The lactose crystals were investigated under a microscope (Leica dm 750 with polarized light) and a particle size analyser (Sympatec laser diffraction) to determine the shape and size of the particles.

Accuracy of experiments

Eutectic freeze crystallization, freeze concentration and sub-zero crystallization of lactose solution were investigated in a batch reactor. From initial experiments (not shown here) the optimum operating conditions were determined. During the experiments the chiller temperature and agitation rate was kept constant to ensure constant conditions. All crystallization experiment were done in duplicate and the freeze concentration experiments in triplicate to ensure that the results are reliable. The resulting standard deviations for the freeze concentration experiments were determined and added to the figure. Every sample was checked three times by manual refractometer to ensure that the same value was obtained. Refractive measurements with known amounts of lactose were used to make a calibration curve to relate the refractive index (°Brix) to the lactose concentration. Particle size analysis of the solid sample were performed in duplicate or triplicate, were applicable the standard deviations were given.

2.5 Results and Discussion

2.5.1 Crystallization under sub-eutectic conditions

In two experiments, with the same operating conditions, 30wt% lactose solutions were cooled to sub-eutectic conditions (−3°C). At these conditions the solution is already supersaturated with respect to both lactose as ice. It was found that it was possible to crystallize lactose and water (i.e. ice) simultaneously. The final slurry was a mixture of lactose, ice and remaining liquid. Figure 2-5 shows the two temperature profiles of the lactose solutions during an EFC experiment at a constant chiller temperature of −4.5°C. Due to the stochastic nature of the process, the temperature profiles have slight differences although the same operating conditions were used. The point of ice nucleation of the two curves was chosen to overlap by shifting the second curve in time.

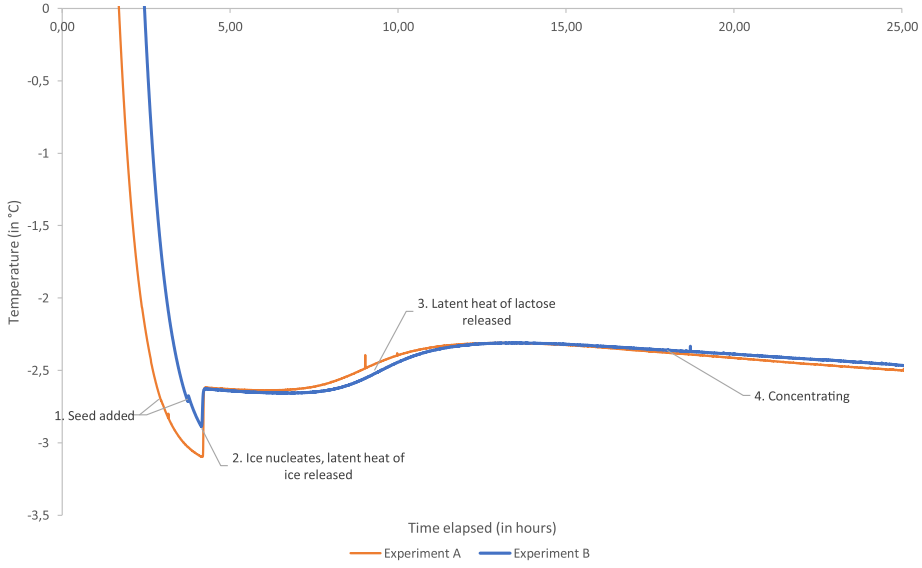

Figure 2-5 Temperature profiles of the solutions during sub-eutectic freeze crystallization.

At −2.7°C, lactose seeds were added (1). One could expect that the crystallization of lactose would start immediately after seeding, however, the temperature still drops after adding seed and the seed does not seems to have a pronounced effect. After seeding lactose, ice spontaneously nucleated (2). A rapid increase in temperature occurred due to the release of latent heat of ice crystallization (2). After ice nucleation, the temperature decreased slightly by 0.02°C. After 2.5 hours of ice nucleation, the temperature increased, indicating that lactose was being crystallized, latent heat was released and the concentration decreased (3). If only ice was being crystallized, then a decrease in temperature would be expected because the freeze point decreases with concentration. Nine hours after ice nucleation, the temperature of the solution decreased again, indicating that the concentration of the solution increased (4). The final concentration of the solution was found to be 29.5 wt% and 29 wt% lactose for experiments A and B, respectively, which is only slightly below the starting concentration of 30 wt%. Although steady state was not yet achieved, the experiment was stopped because the 1-L batch reactor was filled with ice, lactose and mother liquid, and the stirrer would not be able to stir the thick slurry.

Figure 2-6 shows a polarized light image of the lactose crystals extracted from the reactor from the first experiment. The seed material does not have a clear morphology, whereas the crystals produced by the process have a triangular or tomahawk shape. The particles are crystals because they alter part of the polarized light, but the polarized light is only slightly altered by the crystals, which indicates that they must be thin.

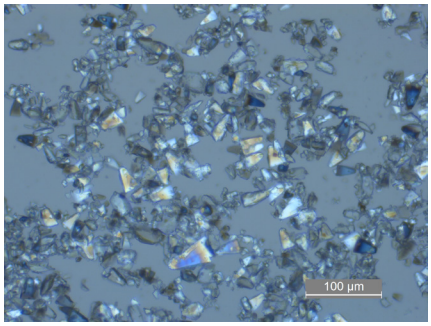

Figure 2-6 Lactose crystals after 22 h produced under sub-eutectic conditions.

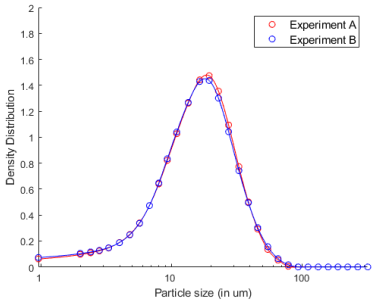

Figure 2-7 Particle size distribution of the lactose crystals produced by eutectic freeze crystallization.

The volumetric mean diameter particle size of the crystals was for both experiments 18 µm; see Figure 2-7 for the full particle size distributions. Although the filter has a pore size of 16–40 µm, it was able to separate the slurry properly; the final products were a clear solution and a solid cake. Due to the efficiency of the filter and the self-filtering effect of the solid cake, it was possible to separate particles smaller than 16 µm. When viewed under the microscope, only a few crystals were visible in the solution; in comparison with the lactose recovered (115 g), this is insignificant.

For our 1-L batch process, the large volume of ice made it impossible to effectively separate the slurry into ice, lactose crystals and mother liquid. The mass balances were therefore determined based on the description in Section 2.3.1. The total amount of solid lactose recovered was 42% and 41% of the initial lactose amount for experiments A and B, respectively. The ice fraction was calculated based on the initial mass of the solution and found to be 26% and 24%, respectively.

A possible solution for the difficult separation of ice/lactose and mother liquid would be to go from a batch process to a continuous process. Continuous removal of ice and lactose would make the separation easier, because a lower

slurry density can be applied. Also, the residence time in the crystallizer and the amount and size of the lactose seeds could be optimized to create larger lactose crystals.

2.5.2 The uncoupled system: freeze concentration and sub-zero lactose crystallization

In Section 3.1, it was shown that simultaneous crystallization of lactose and ice is possible. However, separation of the different fractions in a batch system is difficult. To investigate EFC in more detail and to improve the lactose crystal quality (size and shape), the process was separated into two parts: freeze concentration and crystallization at sub-zero temperatures without ice formation.

Freeze concentration part

Five different solutions, with a lactose content ranging from 5 to 30 wt%, were investigated to check if it was possible to concentrate the solutions by freeze concentration without nucleation of lactose. The point of ice nucleation can be easily determined by the sudden increase of in the temperature due to the heat released by ice crystallization just after 1 h (Figure 2-8). The temperature after initial ice nucleation is the freezing temperature of the solution. The Hudson's freeze line in Figure 2-1 could be extended by our measurements as given in Figure 2-9. The freeze line produced by Hudson et al. showed a close fit with these results.

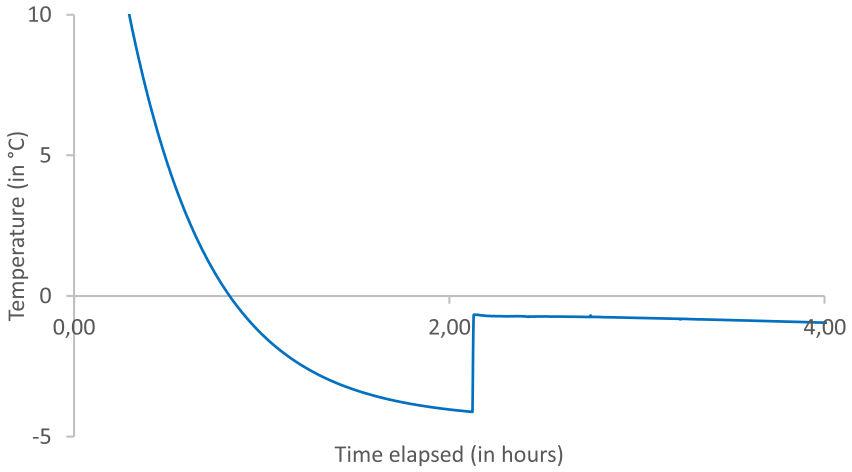

Figure 2-8 Temperature profile of the freeze concentration batch operation of a 10 wt% lactose solution.

In Figure 2-9, the metastable limit reported by (Vu et al., 2003) is extrapolated to make an intersection with the determined freeze point line; the intersection lies at −1.2°C and 16 wt%. Although this interpolation must be done with caution, because the exact shape of the metastable limit below zero is unknown, it is expected that lactose will spontaneously nucleate below this value. For a start concentration up to 15%, lactose did not crystallize during the freeze concentration experiments. However, when a start solution of 20 wt% and 30 wt% lactose was concentrated, a small amount of small lactose crystals (<10 µm) were visible when viewed under a microscope. This is in accordance with the extrapolated metastable limit. It is expected that the presence of a small amount of nuclei/crystals will not affect the overall process, because they can serve as initial nuclei in the lactose crystallization process.

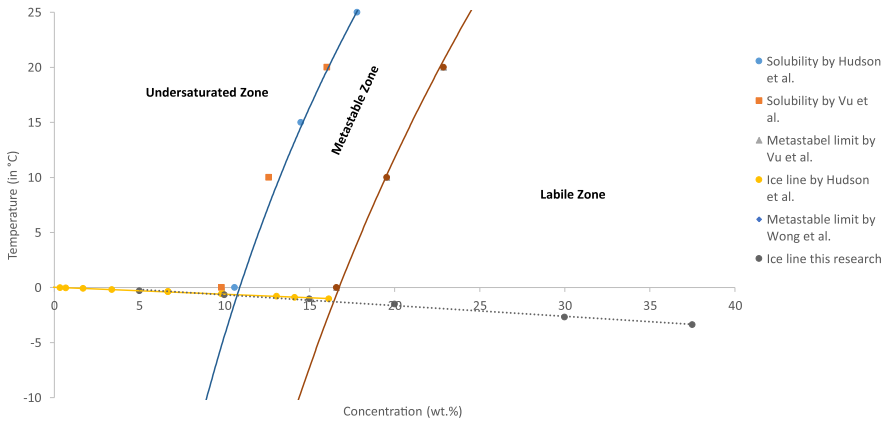

Figure 2-9 Extended and zoomed in version of the phase diagram of lactose. Data used from (Hudson, 1908)(Vu et al., 2003) *and* (Wong et al., 2011)

In the different experiments, lactose solutions were concentrated 1.1–1.5 times the start concentration with an initial concentration between 5 and 30 wt% (Appendix 2.B). For a low lactose concentration, a relatively large amount of water needs to be converted to slightly increase the concentration. To increase the lactose concentration from 5 to 7.5 wt%, 47% of water needs to be removed from the solution, whereas to increase the lactose concentration from 20 to 26 wt%, a similar 46% of water needs to be removed (Appendix 2.B).

The growth rate of ice decreases with increasing concentration at constant temperature (Figure 2-10). As the freeze point temperature decreases with increasing concentration, the driving force for ice crystallization decreases when a constant coolant temperature is used.

From the experiments, it can be concluded that an aqueous lactose solution can be concentrated to 30 wt% by freeze concentration without significant nucleation of lactose.

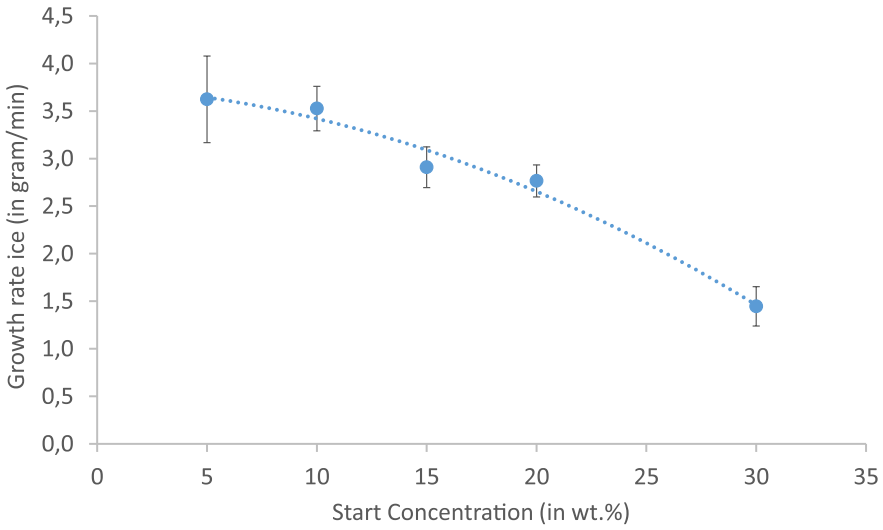

Figure 2-10 Growth rate of ice as a function of the start concentration of lactose at a chiller temperature of −5.5°C.

Sub-zero crystallization of lactose without ice formation

To study the sub-zero crystallization of a 30 wt% lactose solution, a chiller temperature of −3°C was chosen so that only lactose will crystallize and no ice will be formed. Initial experiments showed that crystallization was possible; however, operating conditions, seed type and the amount had to be optimized to obtain large uniform crystals.

The influence of seeding was investigated by varying the seed amount from 0.08% up to 5% DFE Pharma lactose. Figure 2-11 shows microscope images with polarized light of lactose crystals produced after 22 h for 5%, 0.2% and 0.08% seed, respectively. The influence of different amounts of seed can be clearly seen. Five percent seeds result in small crystals with a mixture of shapes: triangles and particles without a clear crystal structure. The particles

are crystals because they alter part of the polarized light. Seeding with 0.2% DFE Pharma led to larger crystals with triangular morphology. The crystals are thin as they hardly change the polarization. When 0.08% seed is used, the crystals have a much larger and a clear tomahawk morphology and can be detected clearly under polarized light.

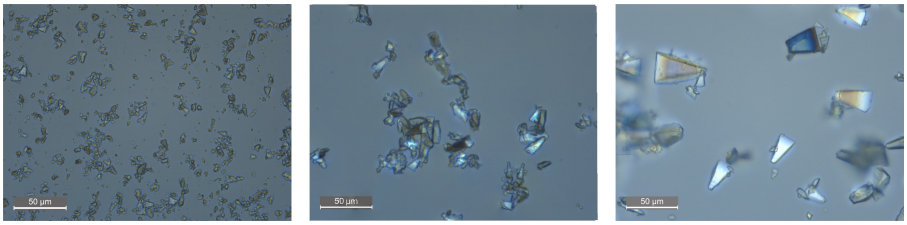

Figure 2-11 Lactose crystals produced with 5%, 0.2% and 0.08% seeds (left to right). The second and third images were created by focus stacking different pictures from a microscope with polarized light.

Figure 2-12 shows the particle size distributions for the experiments above; all results are based on volumetric distributions. The second peak of the 0.08% graph in Figure 2-12 was further investigated by dynamic image analysis. It was found that this peak in the volumetric distribution was due to the formation of aggregates. A two-term Gaussian distribution was used to determine the mean of the first peak of the 0.08% graph. Also, the difference in the height of the peaks can be explained by the presence of aggregates. From Figure 2-12 and Figure 2-13, an evident increase in particle size can be seen, from a volumetric mean diameter of 7 µm for 5% seed up to 26 µm for 0.08% seed. It can be concluded that lactose crystals produced with a low seed amount grow larger in size. This is in agreement with the results found by Nickerson (1954, 1956), where a small amount of nuclei caused ice cream to become sandy more quickly than with a large amount.

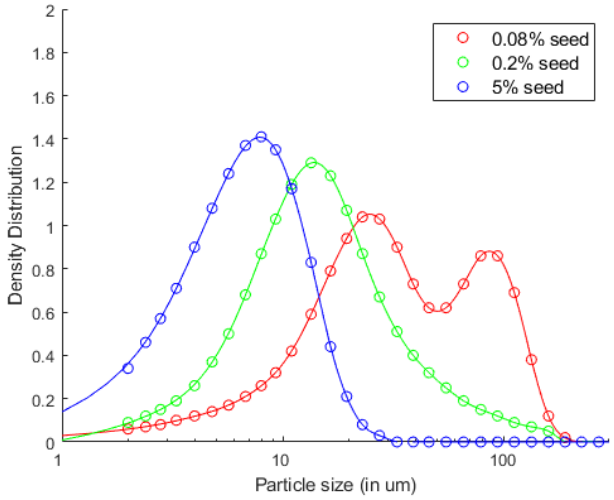

Figure 2-12 Particle size distribution for crystallization below zero with 0.08%–5% seed.

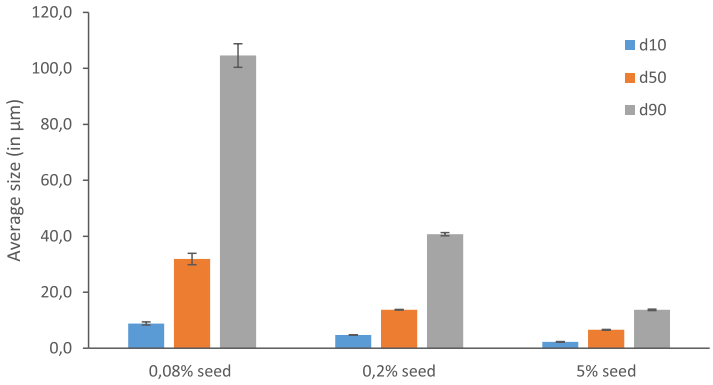

Figure 2-13 Particle size d10, d50 and d90 as function of seed amount

The differences in the shape and size of the crystals resulted in different filtration behaviour. Filtration of the larger tomahawk crystals produced with 0.08% seed were easy to filter within a minute, and the final product was a wet powder. Filtration of the small crystals from the experiment with 5% seed was cumbersome, filtration took a long time and removing the filtrate was difficult because it was a hard paste.

During the experiments, the concentration of lactose in the solution was continuously monitored. In Figure 2-14 the concentration is given as a function of the elapsed time; the missing data points between 5 and 20 h are because the concentration was not measured overnight. When the temperature of the solution was −1.85°C, seeds were added to initiate the crystallization process. For 5% seed, the concentration decreases fast after adding seed, indicating a high crystallization rate. When the concentration decreases, i.e. supersaturation decreases, the crystallization rate also decreases. For 0.08 wt% seed, the concentration initially does not change; after 2 hours there is a slight decrease in concentration. The concentration decrease is slower and constant over time, indicating a slow crystallization rate. The influence of the amount of initial surface area can be clearly seen in Figure 2-14; a higher seed surface area resulted in a higher mass deposition rate.

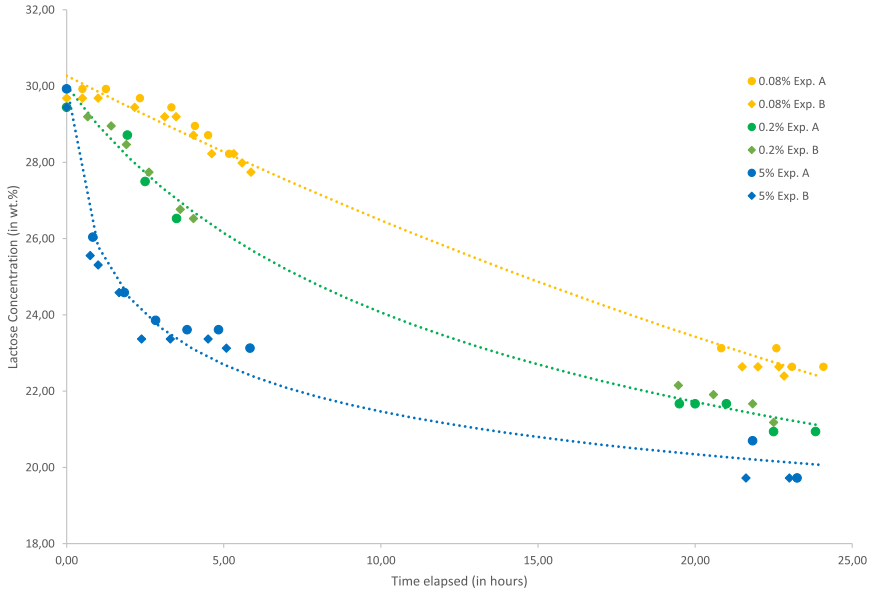

Figure 2-14 Concentration profiles during low-temperature crystallization, t = 0 is the time of seeding. The lines between the points was added for guiding the readers eye, the regression was based on the general expression for crystal growth ($G = \frac{d\Delta c}{dt} = K_g \Delta c^g$).

In an industrial process, the temperature profile is selected such that supersaturation is small, generally 1.5–2. This to minimize the amount of (secondary) nucleation resulting in a process that is governed by crystal growth producing large uniform crystals. If a higher supersaturation is used, it would result in excessive nucleation and thus many small crystals. At sub-zero crystallization of lactose, the start concentration is 30 wt% at a temperature of −1.85°C, resulting in a supersaturation ratio of 4.1. The final concentration of the mother liquid after crystallization increases from 21% up to 22.8% for 5% and 0.08% seed, respectively; under these conditions, the final supersaturation ratios are still 2.7 and 3, respectively. When the crystallization is allowed to run longer, the concentration still decreases until ice nucleates as the concentration drops below the freezing point (see Appendix 2.C, Fig. 2, experiment 2). In comparison with an industrial process, the initial and final supersaturation are extremely high. Under these conditions, it would be expected that nucleation will govern the crystallization process. However, similar to an industrial process, the crystallization at sub-zero temperatures is controlled by the available surface area rather than the amount of supersaturation. Apparently, the effect on the nucleation rate with high supersaturation is counter affected by the low temperature used. Furthermore, the final size of the crystals is dependent on the amount of crystals present initially, e.g. with less particles, every particle can growth bigger in size. From this, we can conclude that for sub-zero crystallization of lactose, although high supersaturations are used, crystal growth is the predominant process rather than nucleation.

The overall yield of the process, based on recovered material versus the initial amount of lactose, was 32%, 35% and 42% for 0.08%, 0.2% and 5% seed, respectively. Paterson (2009) reported a theoretical yield for a slow cooling crystallization process of 82.6%. In practice, however, there are losses during separation and washing of the crystals; industrial yields are reported to be

around 60%–65% (Paterson, 2009). The yield for the batch system in this paper is relatively low, however the system is not optimized. One way for optimizing the yield would be to treat the mother liquor again in a second batch process. Furthermore, if the process would be made continuously and part of the liquid after crystallization would be recycled, then the yield is expected to increase.

2.6 Conclusion

This study presents a low-temperature crystallization method for the separation of lactose. Two methods were presented: (1) a sub-eutectic process where simultaneous ice and lactose is formed and (2) concentrating by freeze concentration and subsequently a low-temperature crystallization process.

It was found that simultaneous crystallization of lactose and water (ice) was possible under sub-eutectic conditions. The lactose crystals had an average size of 18 µm and they had a thin triangular or tomahawk morphology.

Experiments show that it is possible to concentrate a lactose solution up to 30 wt% without significant nucleation. The freeze points determined in these experiments were added to the phase diagram of lactose–water. For the lactose crystallization step, it was found that the amount of seed has a large influence on the final morphology, crystal size and yield. Seeding with a larger amount of 5% led to a small amount of crystal growth with tomahawk crystals as well as particles without a clear structure. Seeding with a small amount (0.08%) ensured more crystal growth leading to crystals with an average size of 26 µm and a tomahawk shape. Although the supersaturation was large at sub-zero temperatures, no excessive primary or secondary nucleation was apparent during the process. A larger available surface area increased the crystallization rate substantially. From this, it can be concluded that, although highly supersaturated conditions are used in sub-zero crystallization of lactose, crystal

growth is the predominant process rather than nucleation. The yield found for the batch system used in this paper was 32%–42%.

Acknowledgements

This work was performed in the cooperation framework of Wetsus, European Centre of Excellence for Sustainable Water Technology (www.wetsus.eu). Wetsus is co-funded by the Dutch Ministry of Economic Affairs and Ministry of Infrastructure and Environment, the European Union Regional Development Fund, the Province of Fryslân, and the Northern Netherlands Provinces. The authors would like to thank the participants of the research theme Dehydration for fruitful discussions and financial support. In addition, the authors would like to thank Prof. Dr. Ir. K. van der Voort Maarschalk for his scientific input and reviewing this paper.

2.A Appendix Mass balances

For our 1-L batch process, the large volume of ice made it impossible to effectively separate the slurry into three phases, i.e. ice, lactose crystals and mother liquid. To separate the slurry into three phases, we took a step back and first melted the ice. The final concentration of the mother liquid (after ice melting) was well above the solubility concentration; with no dissolution and, as crystallization occurs slowly, no addition of mass was expected.

When the ice was melted, the slurry was allowed to settle and was filtered over a sintered glass filter with pore size 16–40 µm. The lactose was subsequently washed with 2-propanol to remove moisture. The washed lactose crystals were dried at 45°C for 24 h to remove any remaining free water (not the hydrate). The overall mass balance was evaluated by determining the final concentration in the solution as well as the lactose recovered. The following equations were used to determine the different fraction of lactose, ice and mother liquid.

Overall mass balance:

$$m_{initial\ solution} = m_{lactose.H_2O} + m_{mother\ liquid} + m_{ice} \qquad 2.A\text{-}1$$

Lactose balance:

$$m_{initial\ solution}(liq) \cdot x_{lactose,start} = m_{lactose.H_2O}(s) \cdot \frac{M_{lactose}}{M_{lactose.H_2O}} + m_{mother\ liquid}\ (liq) \cdot x_{lactose,final} \qquad 2.A\text{-}2$$

We measure the total recovered solid lactose, final concentration and we know the initial amount from this we can calculated the amount of mother liquid after crystallization:

$$m_{mother\ liquid} = \frac{m_{initial\ solution}(liq) \cdot x_{lactose,start} - m_{lactose.H_2O}(s) \cdot \frac{M_{lactose}}{M_{lactose.H_2O}}}{x_{lactose,final}} \qquad 2.A\text{-}3$$

From equation 1 and 3 we can then determine the amount of ice that has crystallized. Table 2A-1 shows the results of the eutectic freeze experiments

Table 2A-1 Overview/Mass balances of EFC experiments

	Experiment 1	Experiment 2
Total mass (in gram)	900	900
Initial concentration (in wt.%)	30.5	30.5
Lactose.H2O recovered (in gram)	115	113
Final concentration (in wt.%)	29.5	29.0
Amount of concentrate	525	545
Amount of ice (in gram)	228	213
Ice fraction (in %)	26.2	24.4

2.B Appendix Freeze concentration data

Table 2B-1 shows the different start and final concentration values achieved in the different batch freeze concentration experiments, column three of Table 2B-1 shows the achieved concentration ratio which is defined as the final concentration divided by the initial concentration. Table B2-2 shows the lactose concentration of ice after washing and the concentration of the washing fluid is.

Table 2B-1 Initial and final concentrations of the different batch experiments

Start concentration (in wt.%)	Final concentration (in wt.%)	ratio
5	7.25	1.5
5	6.75	1.4
5	7.00	1.4
10	14.25	1.4
10	14.00	1.4
10	14.00	1.4
15	20.75	1.4
15	22.00	1.5
15	22.75	1.5
20	26.25	1.3
20	26.00	1.3
20	26.50	1.3
30	33.25	1.1
30	35.00	1.2
30	34.25	1.1

Table 2B-2 The different remaining concentration of lactose in Ice and wash water.

Start concentration (in wt.%)	Lactose in ice after washing (in wt.%)	Lactose in wash Water (in wt.%)
5	0	6.5
5	0	2.75
5	1	4.5
10	1	13.5
10	1	8.5
10	0.75	10.50
15	2	21
15	2.5	21.5
15	5.5	19.25
20	4.5	25
20	2	21.25
20	4	24.5
30	3	23
30	5.25	24.25
30	3.25	25

2.C Appendix Sub-zero crystallization

Figures 2C-1 to 2C-3 show the temperature and concentration profile of the lactose crystallization experiments at sub-zero temperatures, there is no ice crystallization in these experiments. Every experiment with different amounts of seed (0.08, 0.2 and 5%) has been performed in duplicates to iron out any irregularities or logistical problems. Table 2C-1 shows an overview of the final results (Concentration, yield) achieved in the different experiments.

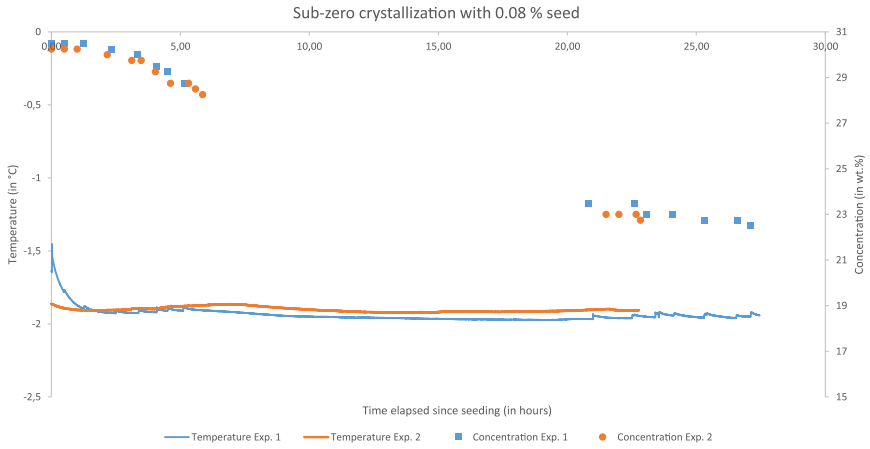

Figure 2C-1 Temperature and concentration profile for sub-zero crystallization with 0.08% seed

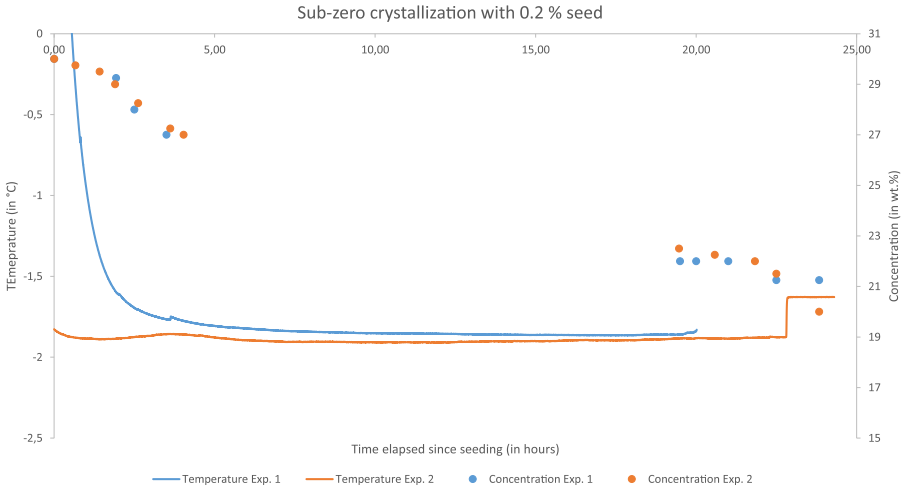

Figure 2C-2 Temperature and concentration profile for sub-zero crystallization with 0.2% seed

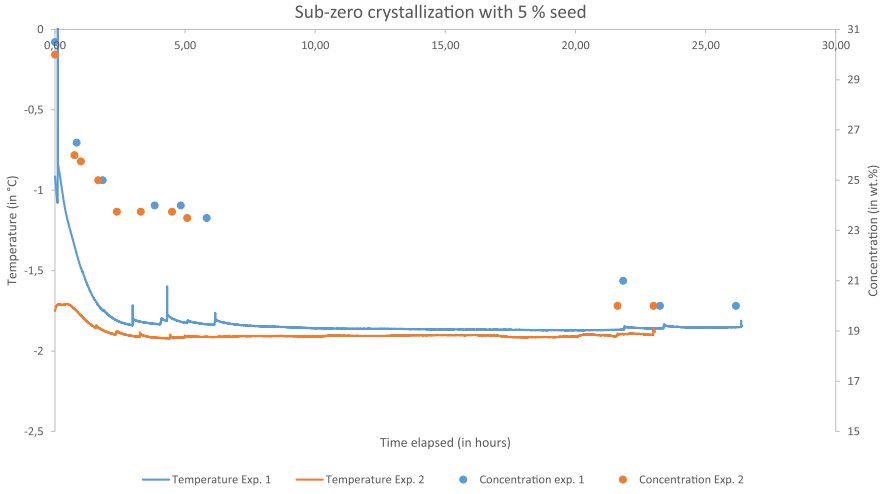

Figure 2C-3 Temperature and concentration profile for sub-zero crystallization with 5% seed

Table 2C-1 Overview of the different sub-zero crystallization experiments

Seed (in %)	Test #	Final concentration (in wt.%)	Recovered (in %)	Time after seeding (h)
0.08	1	22	35	27.1
0.08	2	22.75	26	22.8
0.2	1	21.25	-	23.8
0.2	2	21	35	23.8
5	1	20	50	26.2
5	2	20	45	23.0

Table 2C-2 Overview of particle sizes d10, d50, d90 and the span as function of seed amount

Seed amount (%)	d10 (µm)	d50 (µm)	d90 (µm)	Span (-)
0.08	9.4	33.9	108.8	2.9
0.08	8.3	29.8	100.4	3.1
0.2	4.7	13.7	40.2	2.6
0.2	4.8	13.9	41.3	2.6
5	2.4	6.7	14.0	1.7
5	2.3	6.6	13.7	1.7
5	2.1	6.4	13.4	1.8

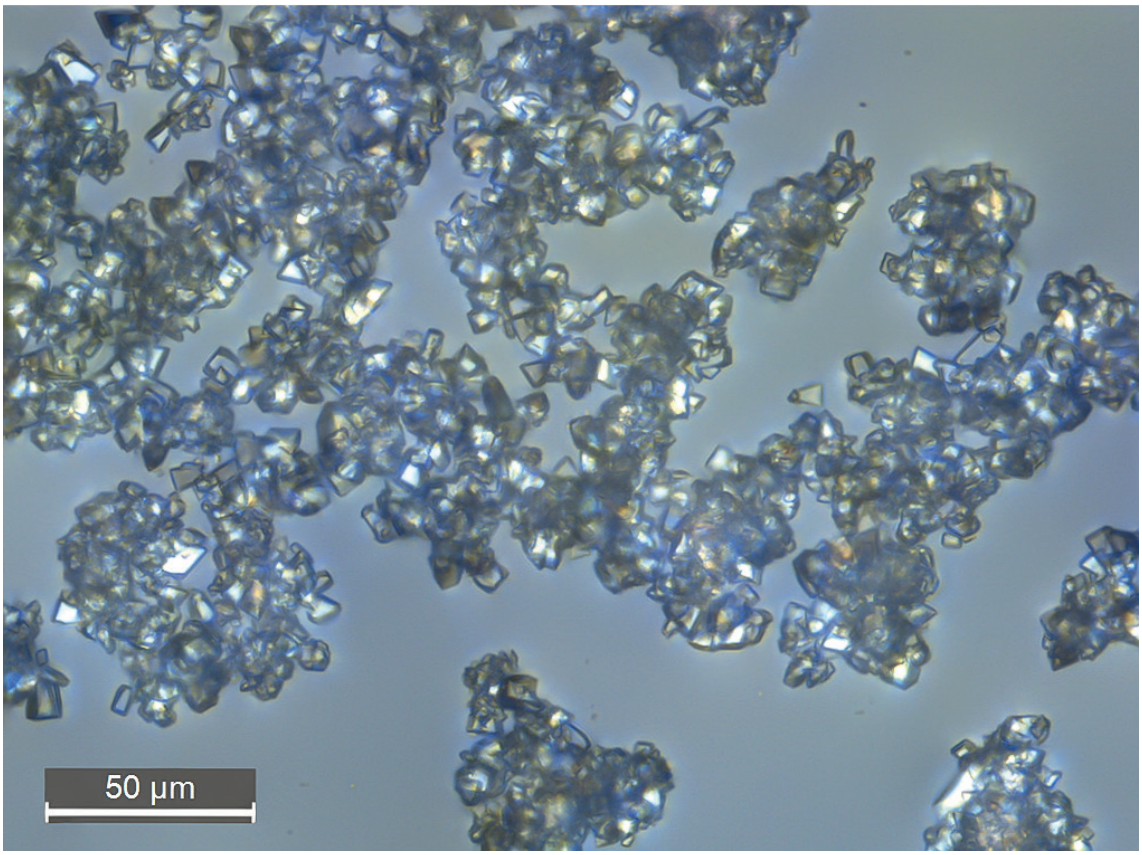

*Lactose crystals after a few hours of growth

Chapter 3

Crystallization kinetics of lactose recovered at sub-zero temperatures

This chapter has been published as:
Halfwerk, R., Yntema, D., Van Spronsen, J., Keesman, K.J., Van der Padt, A., (2023). Crystallization kinetics of lactose recovered at sub-zero temperatures: A population balance model combining mutarotation, nucleation and crystal growth. Journal of Food Engineering

Abstract

Crystallization kinetics of lactose at sub-zero temperatures are modelled in this paper using a population balance model. There are two competing effects on the crystallization kinetics at low temperatures. On the one hand, mass transport and the rate of both mutarotation and nucleation are reduced, reducing the crystallization rate. On the other hand, supersaturation is increased, which increases nucleation and crystal growth and thereby increases the crystallization rate. To explore this phenomenon, the crystal growth of α-lactose monohydrate at sub-zero conditions was modelled, including the effects of mutarotation and nucleation. The model is compared with experiments. It was found that stirring did not have a significant influence, indicating that the process was not limited by mass transfer. Mutarotation had a significant effect; the model showed fast depletion of α-lactose; at high lactose concentrations, the mutarotation of β-lactose could not keep up with this depletion.

3.1 Introduction

Lactose is used in a wide range of applications, like the production of infant formulae or as a carrier compound in the pharmaceutical industry. Industrially lactose is produced by concentrating whey permeate using evaporation followed by a slow cooling crystallization process (Wong and Hartel, 2014). In this article we investigate the use of an alternative method at temperatures below zero: eutectic freeze crystallization (EFC).With this separation technique, both solvent and solute crystallize simultaneously producing ice and crystals(van der Ham et al., 1999).

Extensive research has been done using EFC for separation, proving that it is possible to separate a stream into pure fractions at a low energy demand (Fernández-Torres et al., 2012)(Randall et al., 2011). Hardly any research is known using EFC for organic crystals such as sugars. However, using a low temperature process is potentially beneficial for food applications because there is virtually no product degradation, preserving taste and quality, there is low biological activity, and scaling and corrosion issues are expected to be lower.

In our previous article (Halfwerk et al., 2021), we showed that crystallization and separation of lactose from the solution at sub-zero conditions is possible, producing tomahawk-shaped crystals with an average size of 26 µm. In this article, we focus on the kinetics of crystallization of lactose at sub-zero conditions, which is essential to better understand the process and assess the viability of upscaling. Using temperatures below 0°C has two opposing effects on the crystallization rate: generally, the kinetics are temperature dependent, thus a lower crystallization rate is expected, however, the crystallization rate is also dependent on supersaturation, which increases with decreasing temperature because the solubility is lower (Hartel and Shastry, 1991).

In general, kinetic studies can be divided into single-crystal studies and population balance studies. Population balance studies investigate the development of a group of particles rather than a single crystal or the surface of a crystal. Most population balance studies make use of the power law expression for nucleation and crystal growth (Sections 3.2.3 and 3.2.4). The kinetic rate constants are usually determined by regression, comparing a model with measured results. Population balance modelling for crystallization of lactose has been studied by several authors (Gernigon et al., 2013)(Lifran et al., 2007)(Mimouni et al., 2009)(Shi et al., 1990)(Vu et al., 2005)(Vu et al., 2006) (Wong et al., 2010). All these studies look at the crystallization at temperatures above 20°C and they should be adapted for crystallization at sub-zero temperatures.

In this article, a kinetic model is presented to estimate the lactose crystallization process at sub-zero conditions without ice formation. While the studies above are based on batch experiments, EFC would preferably be a continuous process, removing ice and solute simultaneously. On lab scale, continuous removal appeared to be impossible, therefore, it was decided to use a batch system and to operate just above the freeze point, still describing the low temperature kinetics for lactose but removing the effect of ice. The experimental desaturation profile and crystal size distributions over time are compared with the model. The model entails a population balance model combining mutarotation, nucleation, and crystal growth.

3.2 Theory

In the following sections, the steps of crystallization of lactose and their influence on the population balance model are explained. Crystallization of lactose is an interplay of three processes: (1) mutarotation between α- and β-lactose, (2) initial creation of nuclei (nucleation) and (3) growth of the crystals (Mimouni et al., 2009). Each of these steps can be rate determining depending on the operational conditions such as temperature, concentration, impurities and agitation rate.

3.2.1 Mutarotation

Lactose is a disaccharide and because of a chiral carbon, can exist in two forms: α- and β-lactose (Hunziker and Nissen, 1926)(Wong and Hartel, 2014). When α- or β-lactose is dissolved in water, the molecules form an equilibrium concentration between α- and β-lactose (Visser, 1983). The change from one form of lactose to another is called mutarotation, and it can be followed by measuring the optical rotation of the solution. The equilibrium concentration and mutarotation rate of α- and β-lactose are temperature dependent (Roetman and Buma, 1974).

(Haase and Nickerson, 1966a) investigated the mutarotation equilibrium and the rate of mutarotation. They found that the mutarotation rate could be described by a first order reaction rate; for simulated whey solutions (lactose solution with added salts), they found that the mutarotation rate was doubled (Haase and Nickerson, 1966a). In a second paper by (Haase and Nickerson, 1966b), they compared the mutarotation rate with the crystallization rate of lactose. They investigated mutarotation/crystallization in a temperature range between 0.5°C and 45°C with and without stirring. They found that

mutarotation was relatively fast compared with the crystallization rate for lactose crystallization from water and from whey (Haase and Nickerson, 1966b).

The rate of crystallization of α-lactose is dependent on the supersaturation of α-lactose rather than on the total lactose supersaturation. Therefore, (Visser, 1983) developed a model to determine the relative supersaturation of α-lactose solutions in mutarotation equilibrium below 93.5°C:

$$\Delta c_\alpha = c_\alpha - c_{\alpha s} = \frac{c - c_s + F \cdot K_m (c - c_s)}{1 + K_m} \tag{3-1}$$

where c_α and $c_{\alpha s}$ are the concentration and equilibrium concentration of α-lactose (in kg α-lactose/kg water), c and c_s are the concentration and equilibrium concentration of the total amount of lactose (in kg lactose/kg water), for the equilibrium concentration the eutectic concentration is used (10.75wt.% from (Halfwerk et al., 2021)). K_m is the ratio of β/α lactose in mutarotation equilibrium and T_K is the temperature in degrees Kelvin. F is a temperature dependent compensation factor for the lower solubility of α-lactose as affected by β-lactose. It can be determined from the following equation (Visser, 1982):

$$F = \mathrm{e}^{\left(-\frac{2374.6}{T_K} + 4.5683\right)} \tag{3-2}$$

3.2.2 Effect of mutarotation on the crystallization process

Below 93.5°C, lactose crystallizes as α-lactose monohydrate. When α-lactose is removed from a solution, β-lactose is converted into α-lactose until equilibrium is reached again (Haase and Nickerson, 1966b):

$$\beta\text{-lactose (aq)} \leftrightarrows \alpha\text{-lactose(aq)} \rightarrow \alpha\text{-lactose}_{H_2O}\text{(s)}$$

When lactose crystallizes, it thus decreases the amount of α-lactose in the solution; if β-lactose is not converted fast enough, it could reduce/limit the crystallization rate. (Mimouni et al., 2009) presented a model incorporation the

three main steps of lactose crystallization, i.e. mutarotation, nucleation and crystal growth. They found that mutarotation had a significant influence on the crystallization process even under non-seeded conditions. The production and depletion of α-/β-lactose by mutarotation and crystallization can be described by:

$$\frac{dc_\alpha}{dt} = k_2 \cdot c_\beta - k_1 \cdot c_\alpha - \frac{dm_t}{dt} \quad (3\text{-}3)$$

$$\frac{dc_\beta}{dt} = k_1 \cdot c_\alpha - k_2 \cdot c_\beta \quad (3\text{-}4)$$

Here, c_α, is the alpha lactose concentration (kg α-lactose /kg water), c_β, is the beta lactose concentration (kg β-lactose /kg water), m_t is the suspension density (kg crystal/kg water), e.g. the amount of lactose that has crystallized (see Eqs. (*3-7* and (*3-10*). The rate of conversion of β-lactose to α-lactose, and vice versa, depends on the mutarotation rate constants k_1 and k_2 (1/h). The rate constants are temperature and concentration dependent and are derived from data from (Haase and Nickerson, 1966a) and (Hargreaves, 1995). The values are extrapolated to temperatures below 0°, see Table 3-1 and Appendix 3.A.

*Table 3-1 Overview of constants used in the population balance model. *The eutectic point was used as solubility concentration based on (Halfwerk et al., 2021) Mutarotation rates were extrapolated from Refs. (Haase and Nickerson, 1966a) and (Hargreaves, 1995).*

Parameter	Value
Density lactose (kg/m^3)	1590
Solubility concentration used, eutectic point (wt.%)	10.75
Kinetic rate mutarotation α-lactose k_1 (1/h)	4.89×10^{-2}
Kinetic rate mutarotation β-lactose k_2 (1/h)	2.98×10^{-2}
Equilibrium constant K_m	1.65

3.2.3 Nucleation rate

Nucleation is strongly affected by the type of material (impurities, additives, etc.), supersaturation, temperature, and agitation. The effect of temperature is twofold because in general, supersaturation increases with decreasing temperature due to the lower solubility. However, the nucleation rate is also dependent on the temperature, resulting in an opposing kinetic effect at a lower temperature. Therefore, at a certain temperature, the supersaturation is counter affected by the lower temperature, reducing the nucleation rate (Hartel and Shastry, 1991).

Despite the fact that nucleation is not well understood, a simplified relationship is commonly used to describe the amount of nucleation as a function of supersaturation, suspension density and operating conditions (Wey and Karpinski, 2002). A wide range of nucleation rate relationships for lactose can be found in literature (Agrawal et al., 2015) (Gernigon et al., 2013)(Mimouni et al., 2009) (Shi et al., 1990)(Wong et al., 2010).

The most common relationship used for nucleation is the power law expression:

$$B_0 = k_N \Delta c_\alpha^j m_t^b \tag{3-5}$$

where B_0 is the nucleation rate (in nuclei/h) and k_N is the nucleation rate constant $(\#/\mathrm{h} \cdot (\text{kg α-lactose/kg water})^{-j} (\text{kg crystals/kg water})^{-b})$ which is a factor that is usually dependent on the temperature and agitation rate. The exponent j usually has a value between 0.5 and 2.5, and when secondary nucleation is the predominant mechanism, the value of exponent b is equal to 1 (Wey and Karpinski, 2002).

3.2.4 Crystal growth

Many different steps are involved in crystal growth: transport of molecules towards the surface, back diffusion of non-crystallizing compounds, integration into the crystal lattice and removal of latent heat from the crystal surface (Meenan et al., 2002)(Agrawal et al., 2015). All these steps can be limiting for crystal growth; many relations can be found in the literature describing the growth of crystals or to describe the growth of an individual face of a crystal. In industrial crystallization, a power law-like equation is commonly used depending on the supersaturation to describe the growth of a single crystal. A wide range of power law expressions and kinetic parameters for the crystal growth of lactose can be found in the literature (Gernigon et al., 2013) (Lee et al., 2019)(Lifran et al., 2007)(Mimouni et al., 2009)(Shi et al., 1990)(Wong et al., 2010)(Vu et al., 2006).

The power law expression can be independent or dependent on the crystal size. Size dependency can occur due to (1) differences in the amount of dislocation; larger crystals can have more dislocation so that they grow faster in size; (2) bulk diffusion limitation where large crystals grow faster; (3) a difference in solubility between bigger and smaller particles, something that can occur for particles smaller than 1 μm (Lee et al., 2019). Although there is some evidence of size-dependent growth, research has shown that, in many instances, what is attributed to size-dependent growth is actually growth rate dispersion.

Growth rate dispersion is the effect whereby the same sized crystals under identical conditions still have a difference in growth rate (Lee et al., 2019). In batch -wise crystallization, growth rate dispersion appears as a widening of the crystal size distribution due to accumulation of small slow-growing crystals (Wey and Karpinski, 2002). It can thus be expected that growth rate dispersion will have an impact on the growth of the lactose crystals in our batch

system and will influence the outcome of the population balance model. However, differentiating between growth rate dispersion and length-dependent growth in a population balance is impossible because information about the individual growth of a crystal is not measured. Therefore, the growth rate in the population balance is modelled as a classic power law (Eq. (*3-6*) with length dependency and exponents g and p.

$$G = k_g \cdot \Delta c_\alpha^{\,g} \cdot (1 + \gamma \cdot L)^p \tag{3-6}$$

where G is the growth rate in m/h, k_g is the kinetic rate factor (m/h·(kg lactose/kg solvent)-g), Δc_α is the supersaturation of α-lactose (kg α-lactose/kg solvent) and L is the size of the crystal (m).

3.3 Description of the model

A population balance model in combination with a least squares estimation of the relevant parameters is used to describe the crystallization process. Not only predicting the desaturation profile of α-lactose, using mutarotation, but also considering the crystal size distribution. By dividing the particles into size bins, we can keep track of the crystal size distribution. Assuming that every particle grows according to Eq. (*3-6*), a particle will grow from its class and end up in the next class.

3.3.1 Population balance model

For a perfectly mixed batch reactor, the population balance can be described as (Wey and Karpinski, 2002):

$$\frac{\partial n(L,t)}{\partial t} + \frac{\partial\big(G(L,t)\cdot n(L,t)\big)}{\partial L} = 0 \tag{3-7}$$

This relationship describes the development of a crystal population n as function of size L and time t. The first term is the change in the amount of crystals

over time, the second term describes the flux of particles over a length domain L, which can be seen as the boundary between two neighbouring size classes. The growth rate G is in m/h and is size and time dependent (Eq. (*3-6*)). It is assumed that breakage and agglomeration can be neglected. Nucleation does not appear in Eq. (*3-7*), however it is included as boundary condition, i.e. new crystals $n(0,t)$ produced by nucleation enter the system at the smallest size class:

$$n(0,t) = \frac{B_0(t)}{G(0,t)}$$

Here, B_0 is the nucleation rate in nuclei/h depending on supersaturation and the suspension density (Eq. (*3-5*)). The amount of lactose that crystallized, i.e., the suspension density (m_t), determines the concentration of lactose. Therefore, the population balance is linked to a system of equations describing the mass balances for lactose (Eq. (*3-8*) and (*3-9*)), water (Eq. (*3-10*)) and the suspension density (Eq. (*3-12*)). The amount of lactose that has crystallized can be determined from the population of crystals n as a function of crystal size L.

$$\mathrm{m_{lactose.H2O}(t) = k_v \cdot \rho \cdot \int_0^{\infty} n(L,t) \cdot L^3 dL} \quad (3\text{-}8)$$

$$\mathrm{m_{lactose}(t) = m_{lactose}(t=0) - m_{lactose.H2O}(t) \cdot \frac{M_{lactose}}{M_{lactose.H2O}}} \quad (3\text{-}9)$$

$$m_{water}(t) = m_{water}(t=0) - m_{lactose.H2O}(t) \cdot \frac{M_{H2O}}{M_{lactose.H2O}} \quad (3\text{-}10)$$

$$\mathrm{c_{lactose}(t) = \frac{m_{lactose}(t)}{m_{water}(t)}} \quad (3\text{-}11)$$

$$\mathrm{m_t(t) = \frac{m_{lactose.H2O(t)}}{m_{water}(t)}} \quad (3\text{-}12)$$

With $\mathrm{m_{lactose.H2O}}$ the mass of crystals (in kg), $\mathrm{k_v}$ a volume shape factor ($\frac{\pi}{6}$), ρ is the density of the crystals (kg/m^3), L the crystal size (in m), $\mathrm{m_{lactose}}$ the mass of lactose dissolved (in kg), $\mathrm{M_i}$ is the molar mass in (g/mol), $\mathrm{m_{water}}$

is the amount of water in solution (kg), $c_{lactose}$ is the concentration in (kg/kg water), and m_t the suspension density (in kg/kg water).

3.3.2 Solving the model and parameter estimation

Figure 3-1 shows an overview of the population balance model, a similar scheme is used as described in (Wey and Karpinski, 2002). The initial concentration, the amount of seed and first crystal size distribution are required as input for the model. When seeding is used, the number distribution of the seed can be used as an initial condition, i.e. $n(L,0) = n_{seed}(L)$. A discrete number distribution is calculated from the seed amount and crystal size distribution:

$$n(L,0) = \frac{m_{seed} \cdot V_i}{\rho \cdot k_v \cdot L_i^3} \tag{3-13}$$

where m_{seed} is the mass of the seed (kg) and V_i is the fraction of particles in class size i based on the volume size distribution of the seed and L_i is the size of particle in class size i. When no seed is used, the initial size distribution can be used.

Eq. (*3-7*) is a non-linear partial differential equation that cannot be solved analytically. Therefore, a finite volume, with first order interpolation, scheme was used to discretize the population balance into a set of differential equations(Qamar et al., 2006). The model shown in Figure 3-1was implemented using MATLAB, the integration of the set of equations was done with the ode45 solver. The population balance is solved over a time process span of 5 min, after which a new mass balance is made; the amount of lactose that crystallized is determined and the lactose concentration in the solution is calculated (Eqs. 8, 9, 10 and 11). Subsequently a new growth and nucleation rate is determined for the next iteration. The population after one time step serves as input for the finite volume method for the next time step.

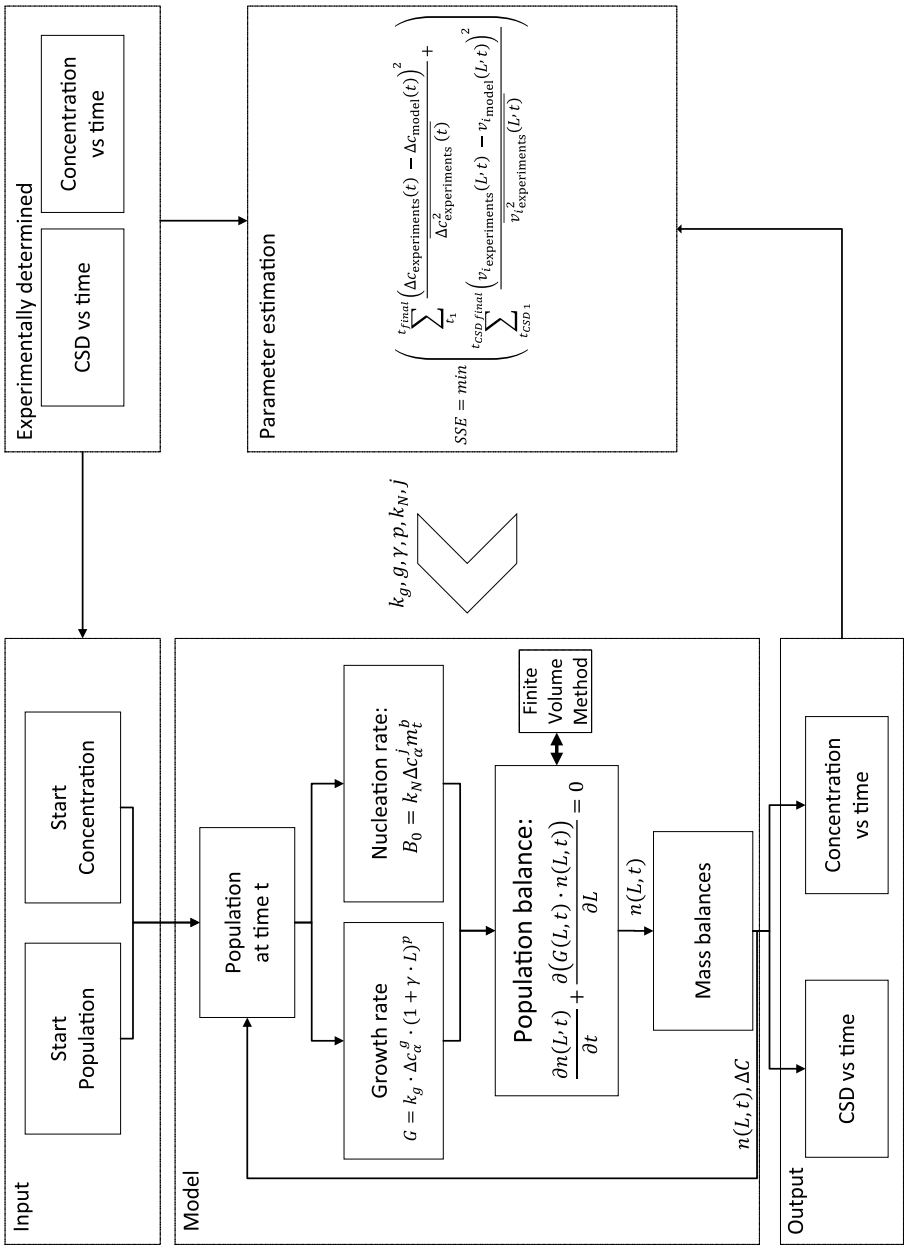

Figure 3-1 Model overview: combined population balance model with mass balances and parameter estimation

From Eqs. ((*3-1*)-(*3-11*)), 6 parameters $(k_g, g, \gamma, p, k_N, j)$ are unknown. The parameters are estimated by minimizing the difference between the model outcome and the experimental results: the desaturation profile and the different cumulative volume distributions determined by laser diffraction measurements for $t = t_1, \dots, t_{\text{final}}$ and $t = t_{CSD\,1}, \dots, t_{\text{CSD final}}$:

$$SE = min\left(\begin{array}{l} \sum_{t_1}^{t_{final}} \frac{\left(\Delta c_{\text{experiments}}(t) - \Delta c_{\text{model}}(t)\right)^2}{\overline{\Delta c^2_{\text{experiments}}(t)}} + \cdots \\ \sum_{t_{CSD\,1}}^{t_{CSD\,final}} \frac{\left(v_{i_{\text{experiments}}}(L,t) - v_{i_{\text{model}}}(L,t)\right)^2}{\overline{v_{i^2_{\text{experiments}}}(L,t)}} \end{array}\right) \qquad (3\text{-}14)$$

The parameter estimation is performed with MATLAB's non-linear optimization function fmincon.

3.3.3 Assumptions

The following assumptions were made:

- All crystals are regarded as spherical particles. Although they are tomahawk-shaped crystals, the crystal size distributions are all determined based on a spherical shape.
- The crystal growth rate and nucleation rate are constant over the integration step (10 min).
- Crystals created by primary and secondary nucleation are added to the smallest size class of the crystal size distributions. (e.g. $n(0,t) = B_0(t)/G(0,t)$).
- A logarithmic size distribution was used in the range of 0.1 to 300 µm, and the number of size bins was set to 100.
- Only lactose crystallizes; there is no ice crystallization. The temperature is chosen such that it is above the freezing point of the solutions.

- Agglomeration is not taken into the system border of the model, it can be expected that agglomeration of crystals will happen, however, prior to the particle size measurements agglomerates were disaggregate by ultrasound treatment. Therefore, the model describes the growth/development of the individual crystals even if agglomeration takes place.

3.3.4 Statistical analysis and model reduction

All six parameters (k_g, g, γ, p, k_N and j) from the growth and nucleation rate equation ($G = k_g \cdot \Delta c_\alpha^{\,g} \cdot (1 + \gamma \cdot L)^p$ and $B_0 = k_N \Delta C_\alpha^{\,j} m_t^b$) were determined by minimization of the sum of squared errors (SSE) between the measured concentrations and crystal size distributions and corresponding predicted values.

To minimize the risk of overfitting, which would result in an incorrect model with very uncertain parameter estimates or end up in local minima, the identifiability of the model and accuracy of the estimates were investigated. A so-called practical or posterior identifiability analysis was performed. The independence of the parameter estimates was investigated using the correlation matrix and an eigenvector analysis of the covariance matrix of the estimates. The 95% confidence intervals of all parameter estimates were determined based on the method described by (Keesman, 2011). See Appendix 3.B and 3.C for a complete overview.

Subsequently, a detailed analysis was performed to determine the kinetic parameters using the following approach:

1. The population balance model was solved as described in Sections 3.1 and 3.2, and the six different parameters in Eqs. (5) and (6) were determined. The accuracies (95% confidence intervals) were determined, and the correlation between the parameters was investigated by analysis of the

correlation matrix and covariance matrix with corresponding eigenvectors (Appendix 3.B and 3.C).

2. The parameters were determined and compared for all operating conditions. If a parameter estimate had a high variation, i.e. the parameter has only limited influence, it was set to its nominal value. Furthermore, it was investigated whether parameters were correlated, and if so, whether one of these parameters could be set to a fixed value.

3. Subsequently, new parameters were determined based on this reduced model; the model was again analysed for correlation and spread of the parameter estimates.

4. Finally, it was investigated if a single set of parameters could represent all the different experimental conditions describing the crystal size and concentration.

3.4 Materials and methods

3.4.1 Experimental setup and procedure

The crystallization rates of α-lactose monohydrate were investigated at subzero temperatures by crystallizing it under different process conditions: varying stirring rates and initial concentrations. All experiments were done in duplicate. Experiments ran for a period of 24–100 h. Lactose solutions (800 mL) were poured into a double-wall crystallizer. The chiller temperature was chosen such that the resulting solution temperature was -1°C±0.5°C. The final temperature was just above the freeze point of the lactose solution used in this system to avoid ice formation during the different crystallization runs. The solutions were cooled within 2 hours to the desired temperature, before seed was added to the system a sample was taken to investigate if any crystals

nucleated. Only for the highest concentration a few crystals were visible at the start but compared to number present ($5.2 \cdot 10^{10}$) in the seed this was neglectable. Previously it was shown that freeze concentration was possible well above the solubility without excessive nucleation(Halfwerk et al., 2021). It can be expected that the conditions at the start are similar. Agitation of the solution was done by an anchor stirrer inside a glass beaker at 75 rpm. The use of an anchor mixer ensures that the area near the wall is well mixed and that a uniform temperature is created. The extent of crystallization was determined using an automatic refractometer (Krüss). Every 20 min, a sample of a few millilitres of solution was automatically taken, measuring the °brix. The °brix was correlated to the concentration of lactose by a calibration curve. The refractometer was cooled to minimize heating of the solution and was rinsed after every measurement. A schematic overview of the experimental setup is shown in Figure 3-2.

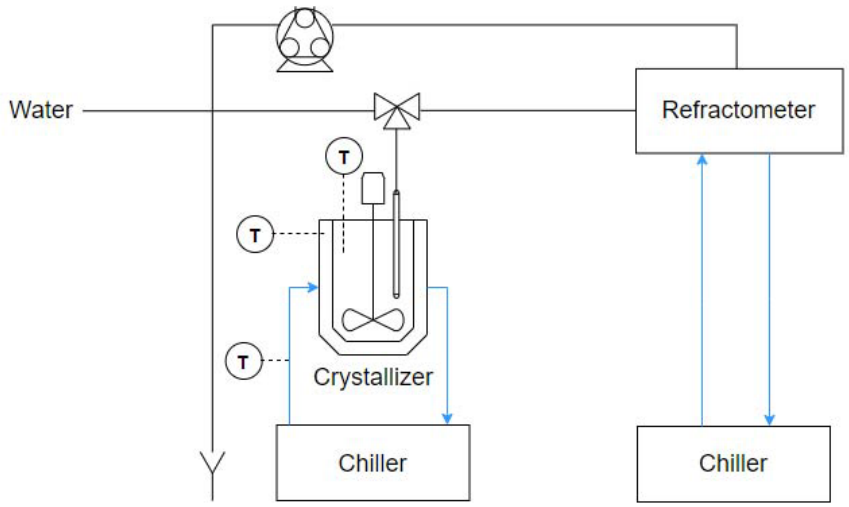

Figure 3-2 Experimental setup, eutectic freeze crystallizer with automatic refractometer.

3.4.2 Materials

The lactose solutions were prepared by dissolving analytical grade lactose monohydrate (≥99% α-lactose) in hot (60°C–80°C) MilliQ water. During dissolution, the solution was stirred with a magnetic stirrer. The concentration of the solution was determined using a manual refractometer (Krüss AR4), and any evaporation was compensated by adding MilliQ water.

Micronized lactose from DFE Pharma (Lactohale 300) was used as seed. Fifty percent of the particles were smaller than 5 µm and 90% of the particles were smaller than 10 µm. The material does not have a defined morphology. The seeds were produced by milling and fractionated by air classification. A seed amount of 250 mg/kg solution was used based on (Halfwerk et al., 2021).

3.4.3 Experimental conditions

Two operating conditions were investigated to determine their effect on crystallization at sub-zero conditions:

- The effect of the stirrer rate was investigated by varying the stirrer rate at 75, 120, 130 and 160 rpm. A seed amount of 250 mg/kg solution was used to initialize the process, and an initial concentration of 40 wt.% lactose was used.
- The effect of the initial concentration was investigated using an initial amount of 25 wt.%, 30 wt.% and 40 wt.% of lactose, 250 mg of seed per kg of solution was used to initialize the process and the stirrer rate was 75 rpm.

For all experiments, the temperature and concentration were monitored over time. Particle size analysis was performed by laser diffraction (Malvern Mastersizer 3000) with a hydro unit (120 ml). Analysis in the particle sizer was performed with saturated lactose solution (18 wt.%), which was continuously

cooled at 12°C. A few millilitres of slurry was taken from the reactor every few hours and added to the particle sizer. The samples were first treated with ultrasound (100%) to break any agglomerates until the particle size was stable (±1200 s), and then three measurements of 1 min were taken to ensure reproducibility Before the particle size measurements some samples were taken and observed by microscopy, only single crystals were visible. All particle size measurements were taken as volume size distributions over a size range of 0.1–500 µm. This analysis could only be done during the day for practical reasons, therefore overnight values are missing.

3.5 Results and discussion

To enable modelling of the lactose crystallization process at sub-zero conditions, batch experiments were carried out to examine whether mass transfer limitation takes place (the effect of the stirrer rate) and the influence of the initial concentration. For each experiment, all six parameters from the growth and nucleation rate equation (k_g, g, γ, p, k_N and j), were determined by minimization of the sum of squared errors (SSE) between the measured concentrations and crystal size distributions and corresponding predicted values. For a full description and overview of the results, see Section 3.3 and Appendices B and C. For all experiments, hold r-squared is >0.8 (Table 3C-3). To consolidate the model, the number of model parameters was reduced to arrive at a 3-parameter model for each experiment. Next, the influence of the stirrer speed and initial concentration are discussed comparing the model results and measurements. Finally, this led to postulation of an extra empirical relationship to describe the crystallization of lactose at sub-zero temperatures.

3.5.1 Reduction of the number of model parameters

Analysis of the parameters and their covariance and correlation show the following effects of the experiments:

- The estimates of growth and nucleation parameters are correlated, which can be explained by the fact that the population balance is determined by both nucleation and growth (Figure 3-1).
- The estimate of γ has a large standard deviation and a high spread, indicating that its value does not significantly influence the outcome of the model. Therefore, it was fixed at a value of 1.
- The estimates of the kinetic parameters (Eq. (*3-5*)) k_n and j are highly correlated. Thus, the estimate of j depends on the estimate of k_n and vice versa. Consequently, the value of j was set to 1.5 which is the average value of all experiments. The value of 1.5 is in agreement with previous studies (Dincer et al., 2009)(Mimouni et al., 2009), which also used a value of 1.5 for nucleation.
- Figure 3-3 shows estimated value of g versus the logarithmic value of k_g. The error bars show the 95% confidence intervals of the estimated parameter g (see Section 3.3). From the figure, there is a correlation between the estimates of g and k_g, therefore g was fixed to the average value of 2.2.

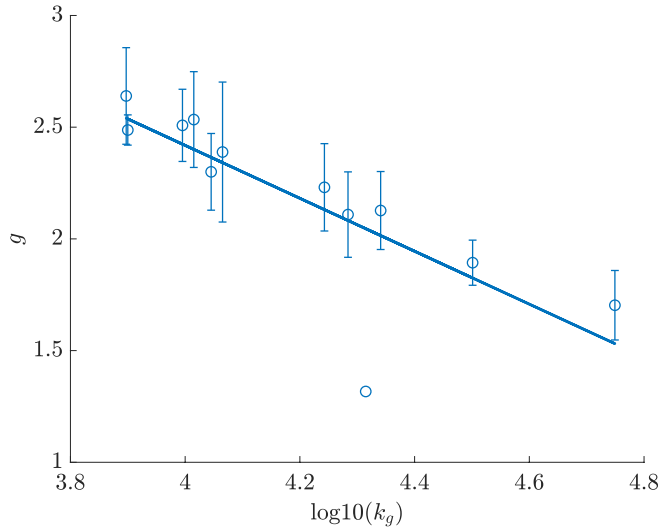

Figure 3-3 Correlation between the parameters kg and g.

Based on the above assumptions, the parameters g, γ and j were fixed. Hence, the nucleation and growth rate were reduced to only being dependent on k_g, p and k_N. Therefore, Eqs. (*3-5*) and (*3-6*) can be reduced to Eqs. (*3-15*) and (*3-16*):

$$G = k_g \Delta c_\alpha^{2.2} (1+L)^p \tag{3-15}$$

$$B_0 = k_N \Delta c_\alpha^{1.5} m_t \tag{3-16}$$

Based on Eqs. (*3-15*) and (*3-16*), a new non-linear parameter estimation was formulated to determine the unknown parameters k_g, p and k_N. It must be noted that the value of the parameters are conditional estimates based on the fixed values of γ, j and g. Table 3-2 shows the 95% confidence intervals of the parameter estimates at varying operating conditions.

There is no straightforward dependency between the operating conditions and the parameters. The k_g values are in the range of 50-70 µm/h·(kg α-lactose/kg

water)$^{-2.2}$, p is in the range of 0.7–1 and k_N is between 1 and $10 \cdot 10^{14}$ #/h·(kg α-lactose/kg water)$^{-1.5}$·(kg crystal/kg water)$^{-1.5}$.

Because there is no straightforward dependency, first the influence of the process settings is evaluated for each series of experiments, next the rate limiting step is explored and finally it is investigated if a single parameter set can fit all the different experimental conditions.

Table 3-2 Overview of the estimates of the three parameters (k_g, p and k_n) determined by the population balance model with their 95% confidence intervals with k_g in µm/h·(kg alpha lactose/kg water)$^{-2.2}$ and k_N in nuclei/h·(kg alpha lactose/kg water)$^{1.5}$·(kg crystal/kg water)$^{-1}$.

Operating condition	Initial concentration (wt.%)	Stirrer rate (rpm)	k_g		p		$k_N \times 10^{14}$	
			Min	Max	Min	Max	Min	Max
1	25	75	49.4	63.8	0.69	0.81	2.4	7.6
1	25	75	57.3	75.2	0.65	0.78	1.9	6.4
1	25	75	45.9	56.9	0.57	0.68	0.3	1.2
2	30	75	48.5	52.5	0.83	0.85	7.0	8.0
2	30	75	60.9	63.0	0.76	0.77	4.7	5.0
3	40	75	48.3	51.8	0.99	1.00	4.1	5.5
3	40	75	62.4	66.2	0.95	0.96	6.7	7.6
4	40	120	69.9	77.0	0.99	1.00	0.0	0.0
4	40	120	110.9	234.7	0.94	0.96	5.9	16.9
5	40	130	67.6	72.8	0.92	0.93	2.1	3.3
5	40	130	68.9	74.1	0.89	0.89	6.0	6.9
6	40	160	54.5	63.4	0.98	1.00	0.8	4.5

3.5.2 Effect of the stirring rate

If there is mass transfer limitation towards the crystal or when a large amount of breakage of crystals occurs, the rate of crystallization is dependent on stirring. For this purpose, four stirrer rates were tested at 40 wt.% lactose, and 250 mg/kg solution of seed was added when the temperature dropped below −0.5°C (operation conditions 3, 4, 5 and 6).

Table 3-2 shows that the growth rate parameters k_g and p are similar for the different stirrer rates, with k_g in the range of 50–75 µm/h·(kg alpha lactose/kg water)$^{-2.2}$ and p between 0.9 and 1. Whereas k_N, the nucleation rate parameters, are in the range of 1–17·10^{14} with an average value of 4·10^{14} nuclei/h·(kg alpha lactose/kg water)$^{-1.5}$·(kg crystals/kg water)$^{-1}$. The parameters of 120 rpm, 40wt.% in both experiments deviate from the rest of the experiments. No explanation could be given for this and therefor left out of the further analysis. Due to their low mass with respect to large crystals, small (nucleating) particles have hardly any impact on the desaturation curve and volume size distribution, therefore, the nucleation constant has the highest variation. Table 3-2 shows there is no clear relationship between stirring and nucleation, therefore it is considered to be constant. The growth constant (k_g) seems to increase from 75 to 130 rpm, however, the growth rate is not only determined by k_g but also by exponent p. Analysing the growth rate at different time intervals show no convincing relation between stirrer speed and growth rate. These observations cancel out the influence of the stirrer speed and the data from Table 3-2 can be averaged for the different initial concentrations (Table 3-3).

Table 3-3 . Overview of the average values of the estimates of the three parameters (k_g, p and k_n) determined by the population balance model with µm/h·(kg alpha lactose/kg water)$^{-2.2}$ and k_N in nuclei/h·(kg alpha lactose/kg water)$^{1.5}$·(kg crystal/kg water)$^{-1}$. For 40 wt.%, the values of 120 rpm have been removed because they had a large deviation from the rest of the values.

$w_{\text{lactose}}(t=0)$ (wt.%)	k_g	p (-)	$k_n \times 10^{14}$
25	50.9	0.75	3.2
30	55.9	0.80	6.0
40	62.4	0.95	4.1

Figure 3-4 shows the desaturation curves at varying stirrer speeds; the line represents the fit on the averaged parameters given in Table 3-3. The difference between the desaturation curves of the experiments can be explained by the stochastic nature of a crystallization process; even under the same conditions, slight differences occur.

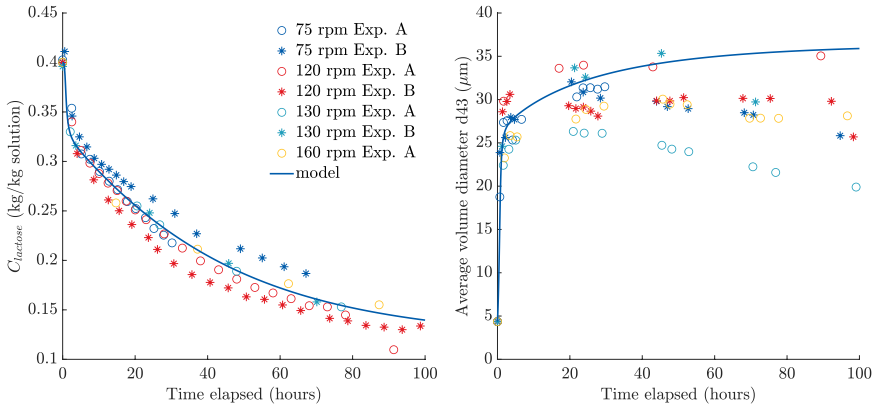

Figure 3-4 Effect of the stirrer rate on the desaturation curve (left) and average volume diameter d43 (right).

The crystal size distribution is modelled beside the desaturation curves. Figure 3-4 (right) shows the average volume diameter over time (d43). It is notable that for all experiments, there is a fast increase in particle size in the first 4 h after which the particle size slowly increases, thus showing two

distinguishable time scales. In some experiments, even a slight decrease is detected; this is probably due to a small amount of abrasion/attrition of the crystals generating small new crystals. This is confirmed by the image shown in Figure 3-8 (right), where different artefacts on the surface of the crystals are visible. Although there is still lactose available for growth, the average size does not seem to change very much ±4 h after seeding. It appears that a steady state is reached between the generation of new particles from attrition and the crystallization rate.

Based on the results shown in Figure 3-4 and the estimated model parameters in Table 3-2, there is no noticeable effect of stirring on the process. This shows that it is not governed by a convection/diffusion process but by surface growth or mutarotation. Hence, for the subsequent experiments, a stirring rate of 75 rpm was used. Furthermore, from Figure 3-4 and Table 3-3, two effects are observed. Two time-dependent effects are distinguishable, one fast and another slower, and the growth rate constants seem to increase with the initial concentration. The following sections explore these effects further.

3.5.3 Effect of mutarotation

For the experiments with the highest concentration (40 wt.%), two-time scales can be seen (from 0 to ±4 h and from ±4 h to end) (Figure 3-4). After the initial fast depletion of lactose, the depletion of supersaturation levels off and becomes more gradual. The same behaviour is seen in the average volume diameter; after the fast initial growth, the increase in size levels off.

This is an indication that mutarotation from β-lactose to α-lactose is influencing the crystallization process (Section 2.1). Figure 3-5 shows the desaturation curve and the α- and β-lactose concentration over time for an initial concentration of 25 wt.% (left figure), and 40 wt.% (right figure). For an initial concentration of 40%, the initial α-lactose decay, and thus the total lactose

concentration decay, is very fast. The decay then slows, and the β-lactose is not converted fast enough to supplement α-lactose to maintain the same rate. For an initial concentration of 25 wt.%, the supersaturation is lower hence the crystallization rate is also lower. Therefore, the depletion of α-lactose is more gradual over time giving mutarotation sufficient time to produce more α-lactose. This implies that at sub-zero conditions, mutarotation controls the crystallization when the crystallization rate is high.

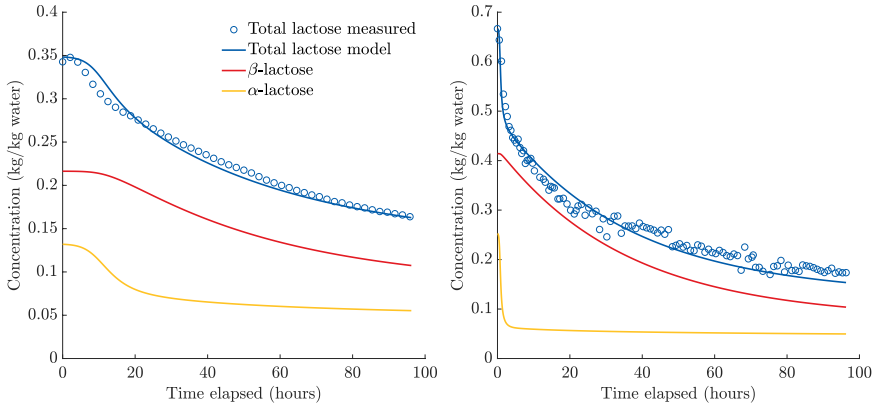

Figure 3-5 Total, α- and β-lactose concentration with 25 wt.% (left) and with 40 wt.% (right) of total lactose at the start

3.5.4 Effect of the initial concentration

In Section 5.2, it was observed that crystal growth seems to increase with a higher initial concentration and size of the crystal (Table 3-3). The growth and nucleation rate (Eqs. 5 and 6) are dependent on the supersaturation; one would therefore expect that the parameter values will be equal or at least close to each other. Therefore, a more detailed evaluation was carried out looking into the effect of the initial concentration. Batch experiments at different initial concentrations were done at 25 wt.%, 30 wt.% and 40 wt.%. All experiments were performed with 800 ml of lactose solution in duplicate; when the temperature dropped below −0.5°C, 250 mg/kg solution of seed was added.

Figure 3-6 shows the desaturation curve from the isothermal batch experiments. It can be clearly seen that the rate of supersaturation decay is steeper for the experiment with higher initial concentration. Furthermore, a higher initial concentration has a large impact on the final crystal size, resulting in the largest crystals at 40 wt.%. Three phenomena are playing a role here: the higher supersaturation, the kinetics of mutarotation at sub-zero temperatures (see Section 5.3) and, as discussed in Section 2.4, the growth rate can depend on the crystal size.

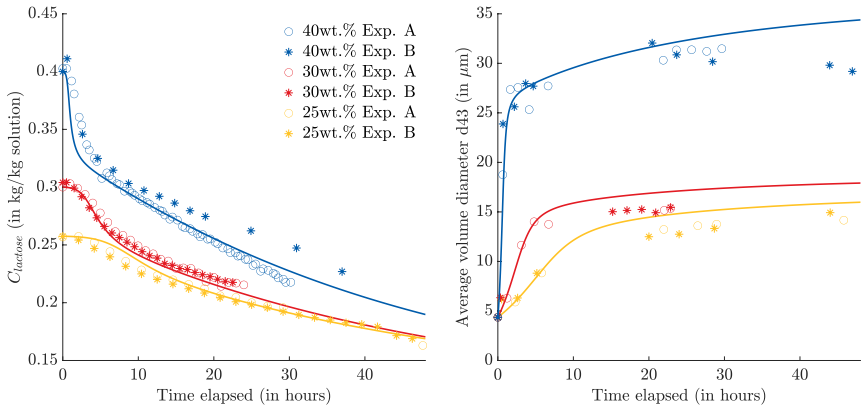

Figure 3-6 Effect of the initial concentration on the desaturation curves (left) and average volume diameter d43 (right).

To explore the effect of the crystal size on growth, crystals were observed by microscopy and scanning electron microscopy. Initially, the seed does not have a defined shape, however after 10 min, crystals with a rhomboid morphology and truncated pyramids are visible (Figure 3-7 left). After 1.5 h, clusters formed with truncated pyramids (Figure 3-7 middle). After that, the crystals seem to grow mainly in the length (010) direction. After 22 h, the main morphology was pyramids/tomahawk crystals with a wide range of sizes (Figure 3-7 right). Figure 3-7 shows the development of crystals for an initial concentration of 40 wt.%, however, a similar development is observed for 30

wt.% at a slower rate, although the final crystals were much smaller for 30 wt.%.

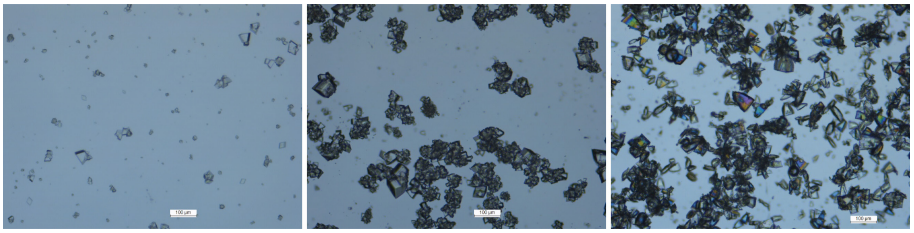

Figure 3-7 Growth of lactose crystals over time, from left to right: crystals after 10 min, 1.5 h and 22 h after seeding at an initial concentration of 40 wt.%.

Figure 3-8 shows two scanning electron images of lactose after ±24 h for an initial concentration of 30 wt.% and 40 wt.%, respectively. Although the morphologies of the crystals are similar, it appears that crystals produced at a higher initial concentration have a more developed body. As confirmed by particle size analysis, there is a large difference in size between an initial concentration of 30 wt.% and 40 wt.%. In both materials, tomahawk-shaped crystals are visible.

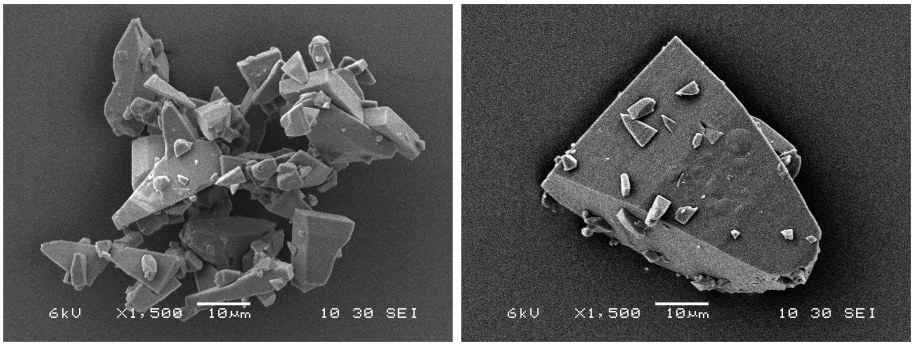

Figure 3-8 Crystal after 24 h produced from 250 mg/kg solution seed with an initial concentration of 30 wt.% (left) and 40 wt.% (right).

With one value for k_g and p, the model is not able to cope with the large difference in crystal size distribution for the different initial concentrations. The length-dependent parameter p has a big impact on the final estimated crystal size distribution, and its value increases slightly with a higher initial concentration (Figure 3-9).

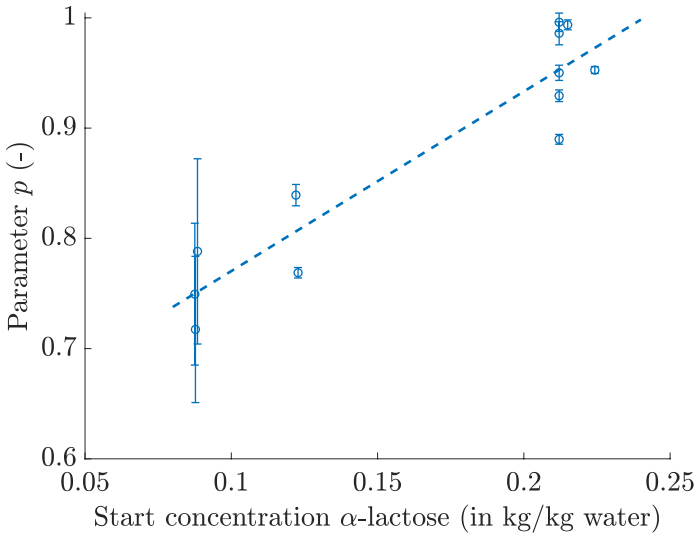

Figure 3-9 Parameter p versus the α-lactose concentration at the start, here p=2.4·c_a (t=0)+0.4. The error bars are the 95% confidence intervals of the estimated parameter.

As indicated in Section 2.4, what appears to be size dependency is probably caused by growth dispersion, which is observed more often in crystallization of lactose and sugars in general(Hartel and Shastry, 1991)(Liang et al., 1987). Although the mechanism of growth rate dispersion is still not fully understood, it occurs mainly at surface integration-controlled growth. It appears that for lactose crystals produced at sub-zero conditions, growth rate dispersion increases with an increase in (initial) concentration. This is confirmed in studies by (Dincer et al., 2009), (Liang et al., 1987) and (Shi et al., 1989). They showed the existence of growth rate dispersion but also found that the

dispersion increased with increased growth conditions (temperature and supersaturation). Furthermore, Dincer et al. studied the combination for growth rate dispersion and the effect of growth on the morphology (Dincer et al., 2009)(Dincer et al., 2014a). They found that the growth rate of the different faces of lactose differed for fast- and slow-growing crystals, resulting in a difference in morphology.

Growth rate dispersion results in a population with faster, larger growing crystals and smaller, slower growing crystals. Although the growth of crystals is not modelled as growth rate dispersion, the resulting population can be accurately described as size-dependent growth. The parameter p in the growth equation ($G = k_g \Delta c^{2.2}(1+L)^p$) combines the effect of growth rate dispersion and the change in morphology of the crystal over time. Surprisingly, the value of p increases only with the initial concentration rather than with the actual concentration. Apparently, the development of crystals is determined at the start of growth of the crystals. The theory of Burton Frank and Cabrera (BCF) is often used to explain growth rate dispersion. According to their theory, the growth rate is dependent on the number and location of screw dislocation at the surface of the crystal(Burton et al., 1951)(Dincer et al., 2014a). The growth of an individual crystal at sub-zero temperature is not measured in this study. However, a possible hypothesis would be that at sub-zero conditions, the creation of dislocations is highest at the start due to the high initial supersaturation, determining the growth behaviour for the rest of the time span. More research is needed to explain this effect. However, Figure 3-9 shows the possibility to extend the growth model using the empirical relationship for p depending on the initial concentration.

3.6 Modified empirical relationships

Initially, all experimental results, e.g. desaturation curves and particles size distribution at different experimental conditions, were used to investigate a single parameter model. This gave a good fit for the different desaturation curves at different initial concentrations. However, for d43, there was a large deviation between an initial concentration of 40 wt.% and the d43 of 25/30 wt.%. The model is unable to cope with the large increase in d43 at 40 wt.%. As described in Section 5.3, it was found that length dependency increases with concentration. This is probably caused by growth rate dispersion and the change in morphology over time. Although the phenomena are not completely understood, an empirical model was developed to accurately describe the growth of crystals over time. The exponent p is made dependent on the initial concentration $c_a\ (t = 0)$ (Figure 3-9). The parameters were again estimated by minimizing the SSE between the model outcome and experimental results; a summation was done for all experimental conditions m:

$$SSE = min \sum_1^m \left(\begin{array}{l} \sum_{t_1}^{t_{final}} \frac{\left(\Delta c_{\text{experiments}}(t) - \Delta c_{\text{model}}(t)\right)^2}{\overline{\Delta c^2_{\text{experiments}}\,(t)}} + \cdots \\ \sum_{t_{CSD\,1}}^{t_{CSD\,final}} \frac{\left(v_{i_{\text{experiments}}}(L,t) - v_{i_{\text{model}}}(L,t)\right)^2}{\overline{v^2_{i_{\text{experiments}}}(L,t)}} \end{array} \right) \tag{3-17}$$

The following relationships were found by minimizing the SSE for all experimental conditions:

$$G = 62.6 \cdot \Delta c^{2.2}(1 + L)^p \tag{3-18}$$

With

$$p = 2.4 \cdot c_a(t = 0) + 0.4 \tag{3-19}$$

$$B_0 = 2.2 \cdot 10^{14} \Delta c^{1.5} m_t \tag{3-20}$$

where G is the growth rate in μm/h and B_0 is the amount of nucleation in nuclei/h. The model was able to closely predict the particle size distribution and the concentration profile over time for the seeded experiments. Figure 3-10 shows the desaturation curve and particle sizes over time for different initial concentrations; the symbols are the measured values, and the line is the output of a model with a single parameter set, based on Eqs. ((*3-18*)-(*3-20*)). The model gives a good prediction of the measurements. The full population balance is modelled over time; thus, the full crystal size distribution can be calculated as well. Figure 3-11 shows the cumulative crystal size distribution at different time intervals for 25wt.% (left figure) and 40wt.% (right figure). The modelled size distributions are close to the measured size distributions by laser diffraction.

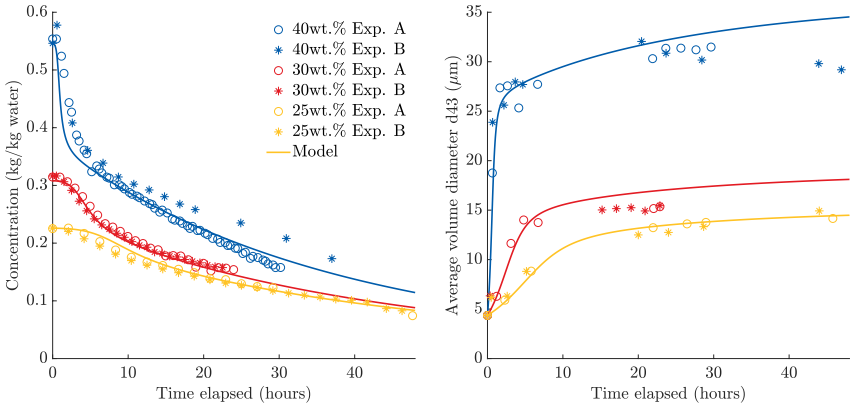

Figure 3-10 Effect of the initial concentration based on the single parameter model (Eqs. 18–20), desaturation curve (left) and average volume diameter (right).

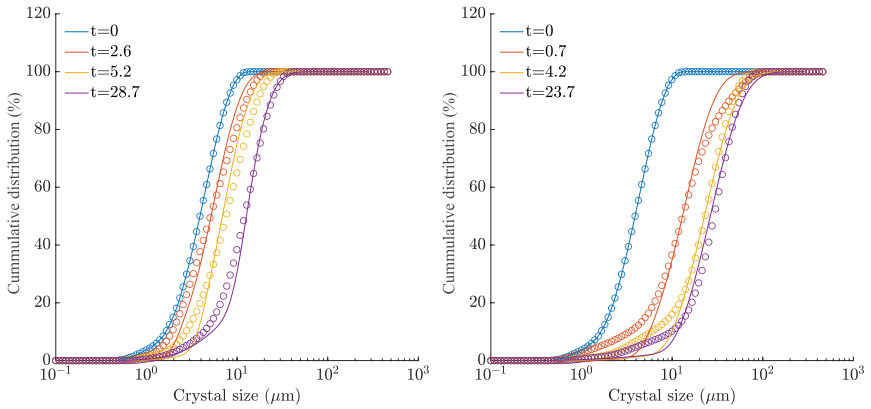

Figure 3-11 Cumulative crystal size distribution at different time intervals for 25wt.% (left figure) and 40wt.% (right figure)

3.7 Conclusions

A kinetic model describing mutarotation, nucleation, and crystal growth for the crystallization of α-lactose monohydrate at sub-zero conditions was developed. The individual kinetic rate constants were determined and compared for experimental conditions with varying stirrer rate and initial concentration.

Changing the stirring rate had no significant effect, indicating that the process was not limited by mass transfer to the crystal. At the highest concentration, the process showed two distinct time scales: fast desaturation in the first few hours and subsequently a slower decay of supersaturation. At the lower initial concentration, the supersaturation decay was more gradual over time. It was discovered that mutarotation was the cause of this; at high crystallization rates, the conversion of β-lactose was not fast enough to replenish the depleted α-lactose fraction. At temperatures below zero, the conversion of β-lactose to α-lactose became rate limiting, reducing both the nucleation rate and the crystal growth rate.

An empirical model was developed describing the population of crystals over time at different conditions, taken into account the effect of initial concentration and size dependency of the crystal growth rate. The model can predict particle size distributions over time and gives a good fit of the desaturation curves.

Nomenclature

b	Nucleation exponent (-)
B_0	Nucleation rate, nuclei/h
c	Lactose concentration, kg lactose in solution/kg water
c_α	α-lactose concentration, kg α-lactose/kg water
c_β	β-lactose concentration, kg β-lactose/kg water
c_s	Lactose solubility, kg lactose in solution/kg water
Δc_α	α-lactose supersaturation, kg α-lactose/kg water
F	Temperature depression factor, -
G	Growth rate, m/h
j	Nucleation exponent (-)
J	Sensitivity matrix, -
k_1	Reaction rate constant α-lactose, 1/h
k_2	Reaction rate constant β-lactose, 1/h
k_g	Growth rate constant, $\mathrm{m/h} \cdot (\text{kg α-lactose/kg water})^{-g}$
K_m	Mutarotation equilibrium constant (-)
k_N	Nucleation rate constant, $\#/\mathrm{h} \cdot (\text{kg α-lactose/kg water})^{-j} (\text{kg crystals/kg water})^{-b}$
k_v	Volume shape factor, $\frac{\pi}{6}$
L_i	Average size of the crystal in class i, m
$m_{lactose}$	Mass of dissolved lactose, kg

$m_{lactose.H2O}$	Mass of lactose monohydrate crystals, kg
m_{seed}	Mass of seed, kg
m_t	Suspension density, kg lactose crystal/kg water
m_{water}	Mass of water in solution, kg
M_x	Molar mass, g/mol
$n(L,t)$	Population of crystals as a function of particle diameter L and time t
p	Length dependency power in growth rate equation, -
T_K	Temperature, Kelvin
t	Time in hours
$t_{0.95}$	t value, -
V_i	Volume fractions from particle size, -
$v_{i\,\text{experiments}}$	Cumulative volume distribution from particle size, -
ϵ	Error between model and measured values, -
γ	Length dependency constant in growth rate equation, 1/m
ρ	Density of lactose crystals, kg/m3
$\hat{\sigma}^2$	Estimated variance of errors

3.8 Acknowledgements

This work was performed in the cooperation framework of Wetsus, European Centre of Excellence for Sustainable Water Technology (www.wetsus.eu). Wetsus is co-funded by the Dutch Ministry of Economic Affairs and Ministry of Infrastructure and Environment, the European Union Regional Development Fund, the Province of Fryslân, and the Northern Netherlands Provinces. The authors would like to thank the participants of the research theme Dehydration for fruitful discussions and financial support. Furthermore, the authors

would like to thank Louise Verdonk and Ignatius Surya Ariffin for carrying out the experimental work.

3.A Appendix Mutarotation constants at sub-zero conditions

The production and depletion of α-/β-lactose by mutarotation and crystallization can be described by:

$$\frac{dc_\alpha}{dt} = k_2 \cdot c_\beta - k_1 \cdot c_\alpha - \frac{dm_t}{dt} \qquad 3.A\text{-}1$$

$$\frac{dc_\beta}{dt} = k_1 \cdot c_\alpha - k_2 \cdot c_\beta \qquad 3.A\text{-}2$$

Here, m_t is the suspension density (kg/kg water), e.g. the amount of lactose that has crystallized (see Eqs. 12). The rate of conversion of β-lactose to α-lactose, and vice versa, depends on the mutarotation rate constants k_1 and k_2 (h^{-1}). The rate constants are temperature and concentration dependent and are derived from data from (Haase and Nickerson, 1966a) and (Hargreaves, 1995). Haase and Nickerson measured the kinetic constants between 0.5-55°C, (Hargreaves between 20-50°C. Figure 3A-1 shows the Arrhenius plots of the two data sets, the values found by the two authors are close to each other. The data of Haase and Nickerson was used to extrapolated to temperatures below zero as the measured values was close to our operating regime.

As it is an equilibrium reaction, k_1 and k_2 can be determined from the equilibrium ratio:

$$K_m = \frac{k_1}{k_2} \qquad 3.A\text{-}3$$

The equilibrium constant were determined from (Roetman and Buma, 1974). They determined the equilibrium constant in a temperature range of 10-35°C (Roetman and Buma, 1974). The values were extrapolated to temperature below zero, an equilibrium constant of 1.64 was found, see Figure 3A-2. The kinetic constant at -1°C are: $k_1 = 1.4 \cdot 10^{-5} \frac{1}{s}$ and $k_2 = 8.3 \cdot 10^{-6} \frac{1}{s}$.

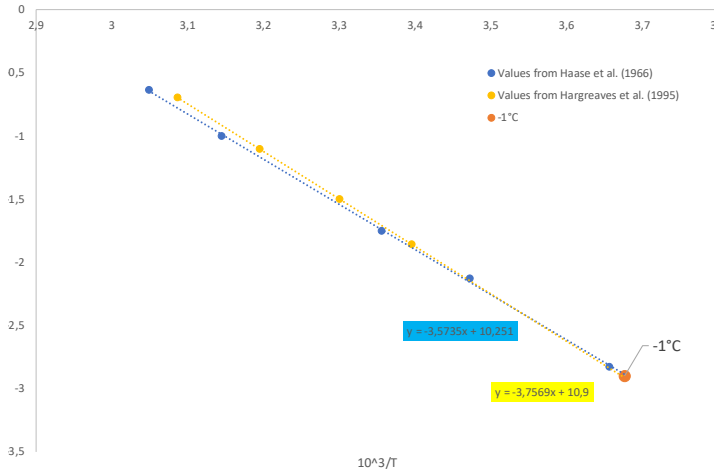

Figure 3A-1 Arrhenius plot of kinetic rate of mutarotation between alpha and beta-lactose

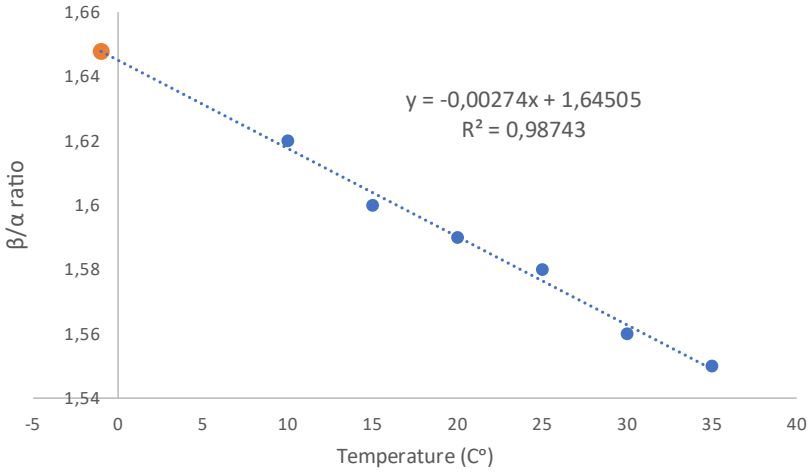

Figure 3A-2 Equilibrium ratio of alpha/beta lactose from Roetman and Buma, 1974

3.B Appendix Statistical analysis

The model has 6 unknown parameters which are determined through minimization of the sum of squared errors. To minimize the risk of overfitting, resulting in an incorrect model with very uncertain estimated parameters, and the risk of finding a local minimum, the accuracy and robustness of the model was investigated. The 95% confidence intervals of all parameters were determined based on the method described by (Keesman, 2011). The 95% confidence interval of any parameter θ is given by:

$$\theta_i \in [\widehat{\theta_i} \pm t_{0.95} \cdot \sqrt{var(\theta_i)}] \qquad \text{with } i = k_g, \dots, p \qquad \textit{3.B-1}$$

Here θ are the parameters determined as described in chapter 3.1 of the manuscript with $\widehat{\theta_i}$ the least squares estimate. The variances are determined from the covariance matrix F which can be determined from the sensitivity matrix J and the variances of the residuals $\hat{\sigma}^2$:

$$F = \hat{\sigma}^2 (J^T J)^{-1} \rightarrow \qquad \textit{3.B-2}$$

$$F = \begin{bmatrix} var(\widehat{k_g}) & cov(\widehat{k_g}, \hat{g}) & . & . & . & cov(\widehat{k_g}, \hat{\jmath}) \\ cov(\hat{g}, \widehat{k_g}) & var(\hat{g}) & & . & . & . \\ . & . & var(\hat{\gamma}) & . & . & . \\ . & . & . & var(\hat{p}) & . & . \\ . & . & . & . & var(\widehat{k_N}) & . \\ cov(\hat{\jmath}, \widehat{k_g}) & . & . & . & . & var(\hat{\jmath}) \end{bmatrix}$$

The sensitivity (or Jacobian) matrix was determined numerically based on a central (±2%) difference scheme:

$$J = \begin{bmatrix} \frac{\Delta c(t=t1)}{\Delta k_g} & \frac{\Delta c(t=t1)}{\Delta g} & \frac{\Delta c(t=t1)}{\Delta \gamma} & \frac{\Delta c(t=t1)}{p} & \frac{\Delta c(t=t1)}{k_N} & \frac{\Delta c(t=t1)}{\Delta j} \\ \vdots & \vdots & \vdots & \vdots & \vdots & \vdots \\ \frac{\Delta c(t=t_{final})}{\Delta k_g} & \frac{\Delta c(t=t_{final})}{\Delta g} & \frac{\Delta c(t=t_{final})}{\Delta \gamma} & \frac{\Delta c(t=t_{final})}{\Delta p} & \frac{\Delta c(t=t_{final})}{\Delta k_N} & \frac{\Delta c(t=t_{final})}{\Delta j} \\ \frac{\Delta v\%(L_1 \text{ at } t_x)}{\Delta k_g} & \frac{\Delta v\%(L_1 \text{ at } t_x)}{\Delta g} & \frac{\Delta v\%(L_1 \text{ at } t_x)}{\Delta \gamma} & \frac{\Delta v\%(L_1 \text{ at } t_x)}{\Delta p} & \frac{\Delta v\%(L_1 \text{ at } t_x)}{\Delta k_N} & \frac{\Delta v\%(L_1 \text{ at } t_x)}{\Delta j} \\ \vdots & \vdots & \vdots & \vdots & \vdots & \vdots \\ \frac{\Delta v\%(L_N \text{ at } t_x)}{\Delta k_g} & \frac{\Delta v\%(L_N \text{ at } t_x)}{\Delta g} & \frac{\Delta v\%(L_N \text{ at } t_x)}{\Delta \gamma} & \frac{\Delta v\%(L_N \text{ at } t_x)}{\Delta p} & \frac{\Delta v\%(L_N \text{ at } t_x)}{\Delta k_N} & \frac{\Delta v\%(L_N \text{ at } t_x)}{\Delta j} \end{bmatrix} \quad \textit{3.B-3}$$

The variance of the residuals was determined from:

$$\hat{\sigma}^2 = \frac{1}{N-P} \epsilon^T \epsilon \quad \textit{3.B-4}$$

N is the number of measured values and P is the number of parameters, and ϵ the error between the model and measured value normalised by the mean of the measured values:

$$\epsilon = \frac{x_{experiments} - x_{model}}{\overline{x_{experiments}}} \quad \textit{3.B-5}$$

The independence of the different variable was investigated by use of the correlation matrix and an eigenvector analysis of the covariance matrix.

Nomenclature

F	Covariance matrix
J	Jacobian matrix
N	Number of measured values
P	Number of parameters
$t_{0.95}$	t-value
$x_{experiments}$	Measured value (e.g. concentration/particle size)
x_{model}	Modelled value (e.g. concentration/particle size)
ϵ	Error between measured and modelled value
θ_i	Different parameters as described in chapter 3.1
$\widehat{\theta_i}$	The least squares estimate of the parameter

3.C Appendix Reducing the amount of parameters of the model

Determination of all parameters

The population balance model is mainly determined by the growth and nucleation rate which are here described by:

$$G = k_g \cdot \Delta c_\alpha^g \cdot (1 + \gamma \cdot L)^p \qquad 3.C\text{-}1$$

$$B_0 = k_N \Delta c_\alpha^j m_T^1 \qquad 3.C\text{-}2$$

With $k_g = 10^{-a}$ and $k_N = 10^b$ to prevent numerical issues to a large extent. All six parameters, k_g, g, γ, p, k_n *and* j, were determined by minimization of the sum of squared errors (SSE) between the measured concentration and particles size distributions. Table 3.C-1 shows the values for all experimental conditions: stirrer rate, initial concentration, and different amount of seed.

For all experimental conditions the covariance matrix was determined to investigate the correlation between the different parameter estimates and their effect on the model outcome. From the covariance matrix the eigenvalues and eigenvectors can be determined. The two largest eigenvalues were investigated further by analysing the two corresponding eigenvectors, representing the two most uncertain parameter combinations. Each element of an eigenvector shows the weight of the corresponding parameter in the parameter combination. Furthermore, eigenvectors of a covariance matrix define orthogonal directions in the parameter space (Keesman, 2011). Thus, from eigenvalue/eigenvector analysis of a covariance matrix, also known as principal component analysis, it can be determined which parameters contribute to the largest or smallest (after selecting the smallest eigenvalues) spread. In the following, the results of an eigenvector analysis for the determination of the most uncertain

parameters, for an initial concentration for 40 wt.%, 120 rpm and 250 mg of seed, are given by:

$$\lambda_1 = 420.6 \quad v_1 = \begin{pmatrix} 0 \\ 0 \\ 1 \\ 0 \\ 0 \\ 0 \end{pmatrix} \text{ and } \lambda_2 = 1.2 \quad v_2 = \begin{pmatrix} 0 \\ 0 \\ 0 \\ 0 \\ -0.88 \\ -0.47 \end{pmatrix}$$

From this example it is clear that the first eigenvector is mainly determined by the third value, i.e. γ has a high spread and thus a limit influence on the model outcome. For the second eigenvector the last two terms in the vector (i.e. k_N and j) are high. Meaning that they both contribute to the large spread in the corresponding direction and as both values are high they are correlated with each other.

From Table 3C-1 and the eigenvector analysis the following effects are seen for the experiments:

There is a high spread in the estimated value of γ indicating that its value does not significantly influence the outcome from in the model.

The estimates of the kinetic constants (eq. B.5) k_N and j are highly correlated, i.e.. j depends on the value of k_N and vice versa.

W	(t 0)	Seed (in gram)	RPM	a	g	γ	p	b	j	R
26		250	75	4.3 ± 0.24	2.1 ± 0.05	0.9 ± 1.11	0.75 ± 0.14	14.0 ± 0.52	1.0 ± 0.37	0.97
26		250	75	4.2 ± 0.45	2.1 ± 0.05	1.0 ± 2.49	0.68 ± 0.26	13.2 ± 0.69	0.5 ± 0.40	0.88
26		250	75	3.9 ± 0.18	2.6 ± 0.04	0.6 ± 0.57	0.84 ± 0.15	13.1 ± 0.57	0.5 ± 0.38	0.89
30		250	75	4.2 ± 0.44	2.5 ± 0.28	2.5 ± 2.82	0.77 ± 0.07	16.0 ± 1.05	2.5 ± 1.02	0.96
30		250	75	3.8 ± 0.65	3.0 ± 0.17	10.0 ± 23.0	0.67 ± 0.04	16.0 ± 0.48	2.5 ± 0.46	0.95
40		250	75	5.0 ± 0.89	2.2 ± 0.24	10.0 ± 24.0	0.89 ± 0.04	15.9 ± 1.53	2.5 ± 2.01	0.90
40		250	75	4.6 ± 0.98	2.7 ± 0.30	10.0 ± 27.4	0.85 ± 0.04	15.7 ± 0.58	2.2 ± 0.55	0.92
40		250	120	5.5 ± 0.83	1.7 ± 0.19	10.0 ± 21.6	0.89 ± 0.03	8.4 ± inf	1.5 ± inf	0.89
40		250	120	4.8 ±	1.2 ±	8.7 ±	0.85 ±	15.9 ±	1.3 ±	0.93
40		250	130	5.2 ± 0.87	1.9 ± 0.15	10.0 ± 24.1	0.82 ± 0.04	14.2 ± 0.65	1.0 ± 0.49	0.75
40		250	130	5.0 ± 1.53	2.0 ± 0.35	10.0 ± 46.2	0.78 ± 0.07	14.5 ± 0.47	1.0 ± 0.31	0.96
40		250	160	5.0 ± 1.48	2.3 ± 0.45	10.0 ± 40.5	0.88 ± 0.06	13.4 ± 2.33	0.5 ± 1.22	0.78

Table 3C-1 Parameter estimates and 95% confidence intervals for the 6 parameter model as function of initial concentration, seed amount and stirrer rate (With $G = 10^{-a} \cdot \Delta c_\alpha^g \cdot (1 + \gamma \cdot L)^p$*) and* $B_0 = 10^b \Delta c_\alpha^j m_T^1$*)*

Reduction of parameters

In order to better explain the data, the following simplifications of the model were made:

- As γ had a limited effect on the outcome of the model it was removed from the model, the growth rate equation (eq. B.1) was thus reduced to:

$$G = k_g \Delta c^g (1 + L)^p \qquad 3.C\text{-}3$$

- As the k_N and j are correlated it was decided to fix j to an average value of 1.5 which was the average value of j found in previous paragraph. The values of 1.5 is in agreement with (Agrawal et al., 2015)(Liang et al., 1991)(Mimouni et al., 2009) which also used a value of 1.5 for nucleation. Consequently, the nucleation rate becomes:

$$B_0 = k_N \Delta c^{1.5} m_t \qquad 3.C\text{-}4$$

Solving with new parameters and further reduction

Table 3C-2 shows the estimates of the kinetic constants $k_g, g, p \; and \; k_N$. From Table 3C-2 and the eigenvector analysis it appears that there is a correlation between the value of a and g. Figure 3C-1 shows a vs g, a linear line could be drawn through the points.

As the values of $k_g$and g are related an average value of 2.2 for g is determined from all experimental values. The growth rate becomes then:

$$G = k_g \Delta c^{2.2} L^p \qquad 3.C\text{-}5$$

Table 3C-2 Parameter estimates and 95% confidence intervals for the 4 parameter model as function of initial concentration, seed amount and stirrer rate (With $G = 10^{-a} \cdot \Delta c_\alpha^g \cdot (1 + \gamma \cdot L)^p$*) and* $B_0 = 10^b \Delta c_\alpha^j m_T^1$*)*

W (t 0)	Seed (in gram)	RPM	a	g	p	b	R
25	250	75	4.3 ± 0.14	2.1 ± 0.17	0.7 ± 0.07	14.6 ± 1.12	0.97
25	250	75	4.3 ± 0.15	2.1 ± 0.19	0.7 ± 0.07	14.5 ± 1.40	0.90
25	250	75	4.0 ± 0.18	2.5 ± 0.21	0.8 ± 0.06	14.4 ± 1.53	0.90
30	250	75	4.0 ± 0.15	2.5 ± 0.16	0.8 ± 0.01	14.9 ± 0.03	0.96
30	250	75	3.9 ± 0.06	2.5 ± 0.07	0.8 ± 0.00	14.8 ± 0.02	0.96
40	250	75	4.2 ± 0.13	2.2 ± 0.20	1.0 ± 0.01	14.8 ± 0.07	0.86
40	250	75	3.9 ± 0.14	2.6 ± 0.22	1.0 ± 0.00	14.8 ± 0.05	0.87
40	250	120	4.7 ± 0.11	1.7 ± 0.16	1.0 ± 0.01	3.3 ± inf	0.86
40	250	120	4.3 ±	1.3 ±	1.0 ±	10.0 ±	0.89
40	250	130	4.5 ± 0.07	1.9 ± 0.10	0.9 ± 0.00	14.4 ± 0.08	0.81
40	250	130	4.0 ± 0.12	2.3 ± 0.17	0.9 ± 0.01	9.8 ± 0.04	0.94
40	250	160	4.1 ± 0.21	2.4 ± 0.31	1.0 ± 0.01	14.4 ± 0.29	0.76

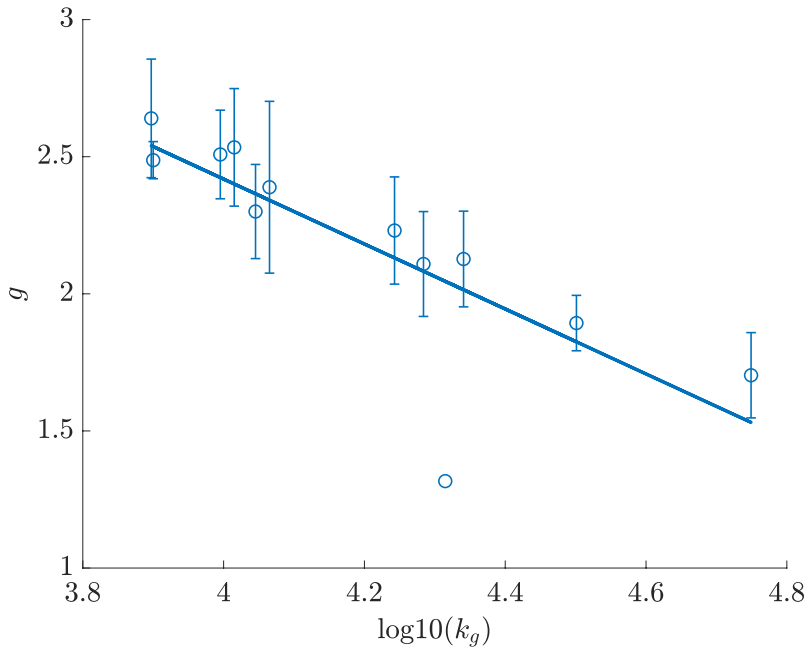

Figure 3C-1 Correlation between g and for the 4-parameter model

Regression with parameters: k_g, p and k_N

Next a new regression of the parameters is made for all experimental conditions, determining k_g, p, k_n. For an overview of three parameters with their 95% confidence intervals see Table 3C-3. See Table 3C-4 for the average values used at different operating conditions.

Table 3C-3 Parameters and 95% confidence intervals for the 3 parameter model as function of initial concentration, seed amount and stirrer rate

$w_{lactose}$ $(t=0)$ (wt.%)	Seed amount (mg)	Stirrer rate (rpm)	k_g		p		$k_n \cdot 10^{14}$		R^2
			min	max	min	max	min	max	
25	250	75	49.4	63.8	0.69	0.81	2.4	7.6	0,97
25	250	75	57.3	75.2	0.65	0.78	1.9	6.4	0,91
25	250	75	45.9	56.9	0.57	0.68	0.3	1.2	0,90
30	250	75	48.5	52.5	0.83	0.85	7.0	8.0	0,95
30	250	75	60.9	63.0	0.76	0.77	4.7	5.0	0,95
40	250	75	48.3	51.8	0.99	1.00	4.1	5.5	0,88
40	250	75	62.4	66.2	0.95	0.96	6.7	7.6	0,88
40	250	120	69.9	77.0	0.99	1.00	0.0	0.0	0,84
40	250	120	110.9	234.7	0.94	0.96	5.9	16.9	0,90
40	250	130	67.6	72.8	0.92	0.93	2.1	3.3	0,83
40	250	130	68.9	74.1	0.89	0.89	6.0	6.9	0,95
40	250	160	54.5	63.4	0.98	1.00	0.8	4.5	0,77

Table 3C-4 Average parameters and 95% confidence intervals as function of initial concentration, seed amount and stirrer rate: Growth rate $\frac{\mu m}{h\left(\frac{kg\ alpha\ lactose}{kg\ water}\right)^{2.2}}$*, power for length dependency p(-) and nucleation rate* k_n ($\frac{\#}{h\cdot\left(\frac{kg_{alpha}}{kg_{water}}\right)^{1.5}\cdot\left(\frac{kg_{crystals}}{kg_{water}}\right)}$).

$w_{lactose}(t=0)$ (wt.%)	Seed amount (in mg)	Stirrer rate (RPM)	k_g	P (-)	$k_n \cdot 10^{-14}$
25	250	75	50.9	0.75	3.2
30	250	75	55.9	0.80	6.0
40,0	250	75	62.4	0.95	4.1

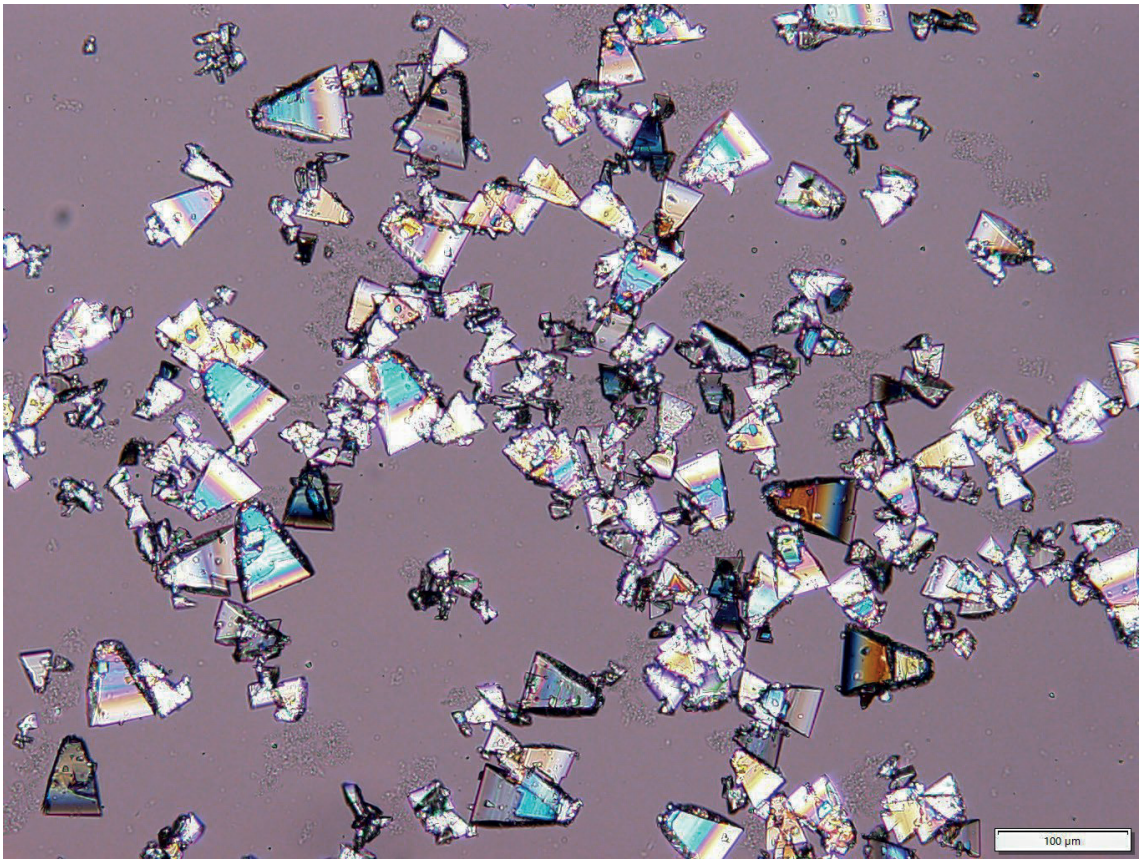

*Lactose crystals produced from delactosed whey permeate at sub-zero temperatures

Chapter 4

Recovery of lactose from simulated delactosed whey permeate

This chapter has been accepted for publication as:
Halfwerk, R., Yntema, D., Van Spronsen, J., Van der Padt, A., (2023). Recovery of lactose from simulated delactosed whey permeate by a low-temperature crystallization process. Journal of Dairy Science

Abstract

Delactosed whey permeate is the mother liquor/by-product of lactose manufacture, but it still contains around 20 wt% lactose. The high mineral content, stickiness, and hygroscopic behaviour prevent further recovery of lactose in the manufacturing process. Therefore, its use is currently limited to low-value applications such as cattle feed, and more often it is seen as waste. This study investigates a new separation technique operating at sub-zero conditions. At low temperature, precipitation of calcium phosphate is expected to be reduced and the lower solubility at sub-zero temperature makes it possible to recover a large portion of the lactose. We found that lactose could be crystallized at sub-zero conditions. The crystals had a tomahawk morphology and an average size of 23 µm and 31 µm. In the first 24 h, the amount of calcium phosphate precipitated was limited, while the lactose concentration was already close to saturation. The overall rate of crystallization was increased compared with the crystals recovered from a pure lactose solution. Mutarotation was rate limiting in the pure system but it did not limit the crystallization of lactose from delactosed whey permeate. This resulted in faster crystallization; after 24 h the yield was 85%.

4.1 Introduction

Delactosed whey permeate (DLP) is the mother liquor/ by-product of crystallization of lactose from cheese whey permeate. It is composed of milk minerals, acids, residual proteins, sugars, and water. The use of DLP is currently limited to low-value applications such as animal feed and fertilizer (Durham, 2009;(Oliveira et al., 2019). More often it is disposed of as an effluent stream and is therefore viewed as an economic burden by lactose manufacturers (Oliveira et al., 2019). However, DLP still contains ±20 wt% lactose, which is not recovered during the lactose crystallization step. Recovery of the remaining lactose could increase the profitability of the process and at same time decrease the environmental burden. Annual milk production in the Netherlands is 13.8 M ton and 58% of that was used to produce cheese (Source: Zuivel in cijfers 2023 ZuivelNL). For every kilogram of milk used for cheese manufacturing ±0.05 kg of DLP is produced. Thus, there is high potential for valorization of lactose from DLP.

The reason why lactose is not further recovered by the manufacturers is because DLP is sticky, has a high mineral content, and has hygroscopic behavior (Oliveira et al., 2019). In addition, the high water content of DLP makes it difficult to use in food applications without further modification (Liang et al., 2009). Removal of water, for example, by spray drying, is difficult because of the sticky and hygroscopic nature of DLP. The reason for the stickiness is unclear, however, the presence of organic acids and minerals are thought to be responsible for drying problems and post-drying instability (Liang et al., 2009). Furthermore, DLP has a high concentration of calcium and phosphate and is already supersaturated with regard to the solubility of the various calcium phosphate precipitates. Calcium precipitation is favoured by concentration, increased temperatures, and alkaline ph. During the manufacture of

lactose, calcium phosphate precipitation is inevitable during heating and concentrating, forming a hard, shell-like material on the heating surfaces of the evaporator. The high mineral and organic content of DLP makes it unstable and perishable. For these reasons, the usage/disposal of DLP is a major challenge for lactose manufacturers (Durham, 2009).

Further recovery of lactose from DLP has been suggested by different researchers. Cloidt and Lehmann (2006) described a method whereby the mother liquid after lactose crystallization was treated to remove minerals by membrane separation or electrodialysis and then recirculated into the process. Alexander et al. (2016) described a similar method in which DLP is fractionated by membranes into a salt-rich permeate and lactose-rich retentate. The salt-rich stream can be used as a salt replacer in food applications, and the lactose-rich stream can be recycled into the lactose crystallization process. Other studies have focused on using DLP as a salt substitute or as a source of oligosaccharides (Oliveira et al., 2019).

An alternative route for further recovery of lactose from DLP could be eutectic freeze crystallization (**EFC**). With this separation technique, both the solvent and the solute are crystallized simultaneously, producing ice and crystals (van der Ham et al., 1999). Using a low-temperature process can be valuable because there is a low level of biological activity and scaling, and corrosion issues are expected to be lower. Furthermore, fouling is expected to be less because the main fouling component (calcium phosphates) has reversed solubility (Durham, 2009), e.g., precipitation will occur more easily at higher temperatures. Previous research on EFC has focused on the separation of brine streams (Van Der Ham et al., 1998; Lewis et al., 2010; Randall and Nathoo, 2015). Previously, we have shown that crystallization and separation of lactose in sub-zero conditions is possible, producing tomahawk-shaped crystals

with an average size of 26 µm (Halfwerk et al., 2021). We found no research on the recovery of lactose from DLP at sub-zero temperatures.

Crystallization of lactose is an interplay of three processes: mutarotation between α- and β-lactose, initial creation of nuclei (nucleation), and growth of the crystals (Mimouni et al., 2009). Each of these steps can influence the rate of the process and the final morphology and size of the crystals. Furthermore, they are affected by the operating conditions (temperature, concentration, impurities, and agitation rate). Impurities can catalyse or slow down the crystallization process. DLP has a high content of minerals, acids, and organics, which can be expected to have an impact on the process and the final crystals. The effect of different additives on the growth of lactose crystals has been studied by different authors, and an overview was given by Wong and Hartel (2014). However, in these studies, only the effect of one individual compound was investigated rather than a mixture as present in DLP.

This study investigates the further recovery of lactose from DLP using a sub-zero crystallization process. Furthermore, a population balance model is used to analyse the kinetics of mutarotation, nucleation, and crystal growth. The yield, final crystal size distribution, and crystallization rate of a pure lactose solution (Halfwerk et al., 2023a) and DLP are compared.

4.2 Materials and methods

4.2.1 Development of simulated DLP

The exact composition of DLP depends on the source, operating conditions, and the various processing steps that whey undergoes. There is no standard for the composition of DLP known by the authors. Furthermore, DLP in liquid form is not readily available. For this reason, a simulated DLP was developed based on the average composition reported by Dairy company FrieslandCampina (Table 4-1) , with values in the same range as the average values reported by Liang et al. (2009).

Table 4-1 Composition of delactosed whey permeate as reported by FrieslandCampina and the average calculated from values reported by Liang et al. (2009)

Composition (in % dry mass)	FrieslandCampina	Liang et al.
Calcium	0.8	0.9
Magnesium	0.3	0.3
Phosphorus	1.7	2.0
Potassium	7.9	6.4
Sodium	2.2	2.0
Chloride	6.6	4.0
Citrate	4.8	4.7
Protein	8.2	2.0
Lactose	58.2	53.6

A method similar to that used for the production of simulated milk ultra-filtrate developed by (Jennes, R.; Koops, 1962) was used for the development of simulated DLP. Three stock solutions were used with different salt concentrations (Table 4-2). For stock 3, the procedure described by Jannis and Koops was slightly modified by adding a third salt (NaCl) to compensate for the higher sodium concentration. Analytical grade lactose monohydrate (≥99% α-lactose) was first dissolved in stock 1 and 2 and MilliQ water. Subsequently,

the solution was heated to ±65°C to dissolve all the lactose. Next, the solution was cooled to 5°C without stirring, and the third stock solution was added.

Adding stock 3 before the temperature of the solution was sufficiently low led to precipitation of calcium phosphate. When a precipitate was present, it did not dissolve during further processing, because calcium phosphate was already supersaturated. The amount of lactose and stock solutions depends on the desired concentration. For a solution with a lactose concentration of 30 wt%, 315.8 g of α-lactose monohydrate, 260 g of stock 1, 200 g of stock 2, and 120 g of stock 3 are needed, with MilliQ water added to make 1000 g of solution. For higher concentrations, the amount of stock solution must be adapted in the same ratio as the amount of lactose.

Table 4-2 Stock solutions for production of simulated delactosed whey permeate

	Component	Concentration (in g/kg solution)
Stock 1	KH_2PO_4	157.7
	K_3-citrate.H_2O	66.9
	Na_3-citrate.$2H_2O$	99.8
	K_2SO_4	41.8
Stock 2	K_2CO_3	41.8
	KCl	148.8
Stock 3	$CaCl_2 \cdot 2H_2O$	132.4
	$MgCl_2 \cdot 6H_2O$	91.7
	NaCl	115.9

During the addition of stock 3, a small amount of precipitation formed; the particles were small and they were only visible with phase contrast microscopy. The concentration of phosphate was 5-10% lower and calcium was reduced by 40-50%. Raman spectroscopy of this precipitate showed that the precipitate was a form of calcium phosphate. Therefore, after adding stock 3, the solution was centrifuged for 15 min at 10,000 rpm to remove any precipitates.

Subsequently, the ion composition, carbon content, and citric acid content were determined using ion chromatography (Metrohm 930 Compact IC flex), HPLC (Thermo Scientific Dionex), and total organic carbon analysis (Shimadzu TOC-L). The lactose concentration was calculated from the difference between the total organic carbon and carbon derived from citric acid. In the simulated DLP, the only organic carbon sources are derived from lactose and citric acid.

4.2.2 Experimental Setup

Crystallization experiments were caried out in a 1-L double-wall reactor, which was cooled by chiller. A chiller temperature of −3°C was used, resulting in a solution temperature of −2°C±0.2°C. An anchor stirred was used to agitate the solution at a rate of 125 rpm. The use of an anchor mixer ensures that the area near the wall is well mixed, preventing ice formation, and that a uniform temperature is created. Figure 4-1 shows a schematic overview of the setup; for a full description of the setup, refer to our previous publication (Halfwerk et al., 2021).

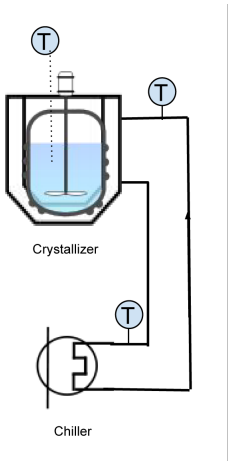

Figure 4-1 Experimental setup in a 1-L batch crystallizer.

The temperature inside the glass crystallizer beaker was measured using a precision temperature sensor (Tempcontrol PT 6180 with ASL F200 indicator), which has (calibrated) accuracy of 0.02K. Data acquisition and equipment control was done using Python.

4.2.3 Experimental Procedure

A concentrated DLP solution with 30 wt.% lactose was used to investigate the crystallization of lactose at sub-zero conditions, the experiments were done in duplicate. The solution was cooled immediately after preparation. The temperature of the chiller was set to −3°C, resulting in a final solution temperature of −2°C±0.1°C. The solution was not seeded because there was spontaneous nucleation during cooling below 0°C. The temperature of the chiller was kept stable for 100 h.

After 24 h, a small part of the crystallized slurry (±100 mL) was filtered over a sintered glass filter with pore size 16–40 µm to analyse the solid product. The filtrate was subsequently washed with ±100 mL of 2-propanol to lower the water content. The lactose crystals were dried in an incubator at 45°C until constant weight to remove any remaining water. A sample of the lactose was dissolved to determine the purity/mineral fraction. The overall mass balance was evaluated by determining the final concentration and the amount of lactose recovered.

Throughout the crystallization experiment (100 h), samples were taken every few hours to determine the lactose concentration, ion concentration, and particle size. The analysis could only be performed during the day, therefore there are no overnight values. The extent of crystallization was determined by sampling a few millilitres of solution and measuring the °brix with a refractometer (Kruss). The ion composition, citric acid content, total organic carbon were

measured and the lactose concentration was again calculated as described in previous section.

The lactose crystals were investigated under a microscope (Leica dm 750 with polarized light) to determine the morphology and to determine if any precipitates besides lactose were present. Particle size was analysed by laser diffraction (Malvern Mastersizer3000) with a hydro unit (120 mL). The analyses in the particle sizer were performed with saturated lactose solution (18 wt%), which was continuously cooled at 12°C. A few millilitres of slurry from the reactor were taken every few hours and added to the particle sizer. The samples were first treated for 1200 s with ultrasound (100%) to break any agglomerates.

4.2.4 Modelling of Crystallization Kinetics

The kinetics of the crystallization process is commonly described by a balance model, which describes the development of a group of crystals. In our previous study, we developed a population balance model for lactose crystallized from a pure solution at sub-zero temperatures. The model combined the effect of mutarotation, nucleation, and crystal growth for a sub-zero crystallization process(Halfwerk et al., 2023a). For pure lactose, the model accurately described the growth of crystals, however, the minerals and acids present do affect the kinetics of the process. Therefore, the crystallization kinetics were modelled using the population balance model coupled with a set of mass balances. For a perfectly mixed batch reactor, the population balance can be described as (Wey and Karpinski, 2002):

$$\frac{\partial n(L,t)}{\partial t} + \frac{\partial\left(G(L,t)\cdot n(L,t)\right)}{\partial L} = 0 \qquad (4\text{-}1)$$

This relationship describes the development of a crystal population n as a function of size L and time t. The first term is the change of crystals over time,

and the second term describes the flux of particles over a length domain L, which can be seen as the boundary between two neighbouring size classes. The population balance is linked to a set of mass balances for lactose and water. The model not only predicts the desaturation profile of α-lactose, considering mutarotation, but also predicts the crystal size distribution.

The model describes the development of crystals based on the kinetics for mutarotation, growth, and nucleation. The production and depletion of α-/β-lactose by mutarotation and crystallization can be described by:

$$\frac{dc_\alpha}{dt} = k_2 \cdot c_\beta - k1 \cdot c_\alpha - \frac{dm_t}{dt} \tag{4-2}$$

$$\frac{dc_\beta}{dt} = k_1 \cdot c_\alpha - k_2 \cdot c_\beta \tag{4-3}$$

where m_t is the suspension density, e.g., the amount of lactose that has crystallized. The rate of conversion of β-lactose to α-lactose, and vice versa, depends on the mutarotation rate constants k_1 and k_2. For pure lactose, the mutarotation rate is known from the literature (Haase and Nickerson, 1966a) (Hargreaves, 1995), however, no data are available for DLP.

In our previous study, we found that a power law expression for nucleation and the classic power law for growth could best describe the crystallization:

$$G = k_g \Delta c_\alpha^{2.2} (1 + L)^p \tag{4-4}$$

$$B_0 = k_n \Delta c_\alpha^{1.5} m_t \tag{4-5}$$

where G is the growth rate (in µm/h depending on the supersaturation (Δc_α), and size of the crystal L. B_0 is the nucleation rate, which describes the generation of newly produced crystals depending on the supersaturation and suspension density (m_t).

The different kinetic rate constants ($k_g, p, k_N, k_1 + k_2$) in Eqs. 2–5 were determined by non-linear regression between the predicted values and the

measured concentration profiles and crystal size distribution. The 95% confidence intervals of the estimated parameters were determined to ensure accurate values. For a detailed overview of the model, we refer to our previous article (Halfwerk et al., 2023a).

4.3 Results and discussions

4.3.1 Crystallization of Lactose from DLP

The further recovery of lactose from DLP by a crystallization process at a temperature below zero was investigated. A simulated DLP solution was specifically developed for this purpose. A solution containing 30 wt% lactose was cooled to a temperature of −2°C; no ice crystallized because the freeze point is lower due to the presence of lactose and minerals. Under these conditions, the solution is already supersaturated with respect to lactose; nucleation occurred spontaneously, hence no seed was required. The start of the experiment was assumed when the temperature dropped below −1.85°C.

Figure 4-2 shows the lactose concentration over time; the experiments were done in duplicate, indicated by experiments A and B. Although the system was not seeded, the desaturation profiles are similar. After 24 h, the final lactose concentration of the liquid was found to be 14.2 wt% and 13.7 wt%, close to the value of the eutectic concentration of a pure lactose solution (10.75 wt%). This resulted in a yield of 82% and 85% for experiments A and B, respectively, based on the maximum crystallizable amount (C(0)-C(t))/(C(0)-C(∞)). If the crystallization was prolonged (100h), the final concentration reached a value of 11 wt%.

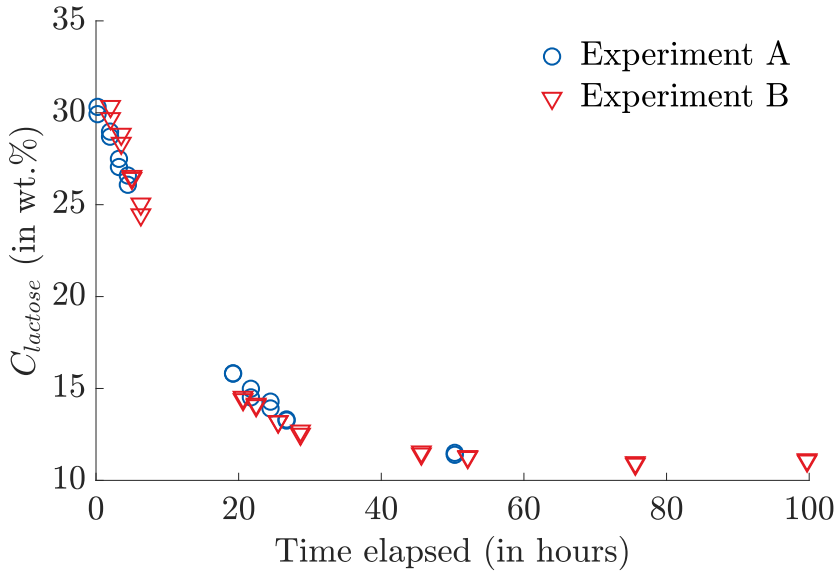

Figure 4-2 Concentration of lactose in mother liquid delactosed whey permeate over time in duplicate.

In addition to the concentration, the size of the crystal was monitored to gain a better understanding of the growth of crystals. Figure 4-3 shows the average volume diameter (d43) over time. The d43 increases quickly initially; after 24 h, the average size levels off and then starts to decrease. As the slurry density increases, there are more collisions between the particles, resulting in more abrasion/attrition of the crystals. Hence, the optimum between crystallization and attrition is around 24 h, resulting in the biggest crystals. Despite the operating conditions and concentrations are similar for both experiments, the average volume diameter after 24h for experiment A is larger than for experiment B. In the next section the crystals size and shape are further investigated.

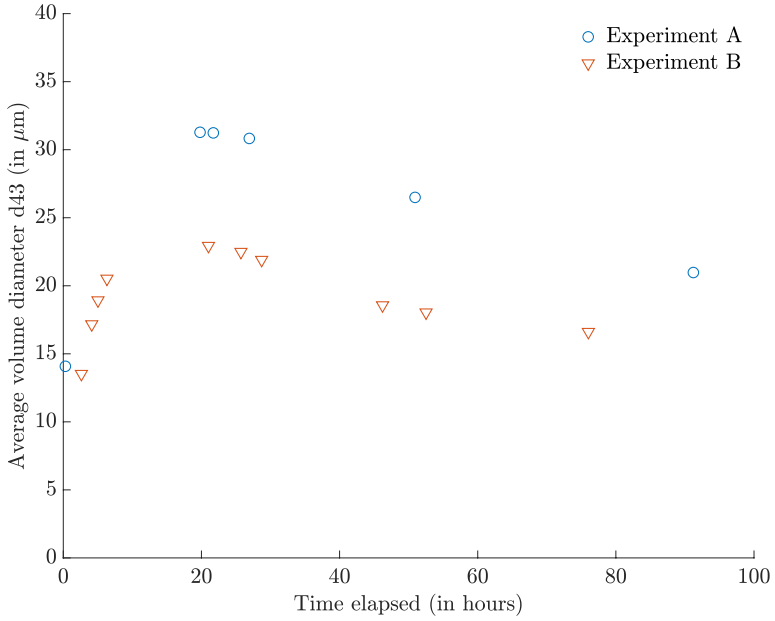

Figure 4-3 Average volume diameter (d43)over time.

4.3.2 Size and Shape of the Crystals

The main crystallization occurs within 20–30 h and the largest crystals were produced around 24 h. To investigate this further, some of the slurry (±100 mL) was taken after 1 day, centrifuged, washed with 2-propanol to remove any remaining moisture and then dried to investigate the crystal properties at this point. The crystals were analysed for morphology and size (Figure 4-4 and Figure 4-5).The crystals have a clear tomahawk morphology with an average volume diameter (d43) of 31 µm and 23 µm for experiments A and B, respectively.

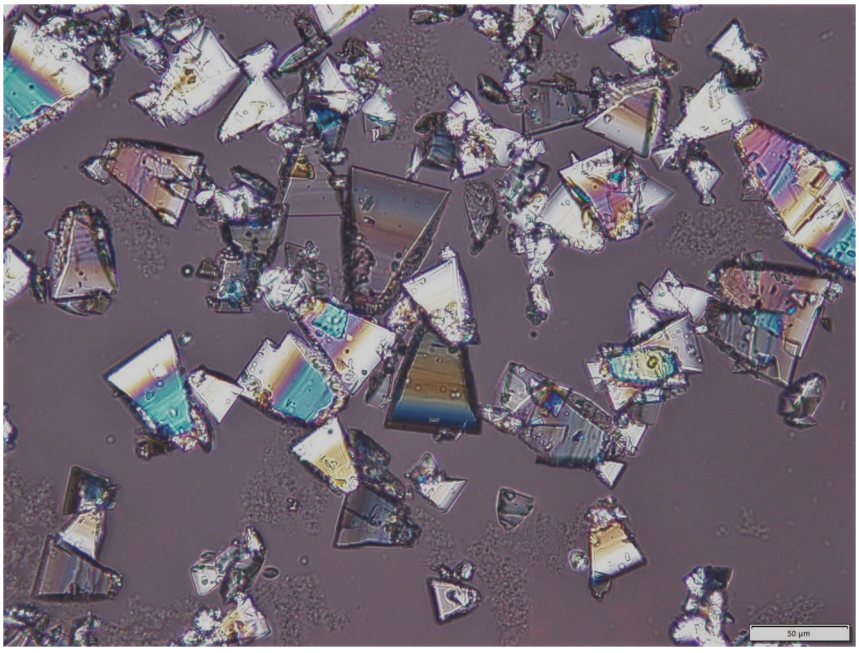

Figure 4-4 Crystals produced from delactosed whey permeate after 24 h just before filtration.

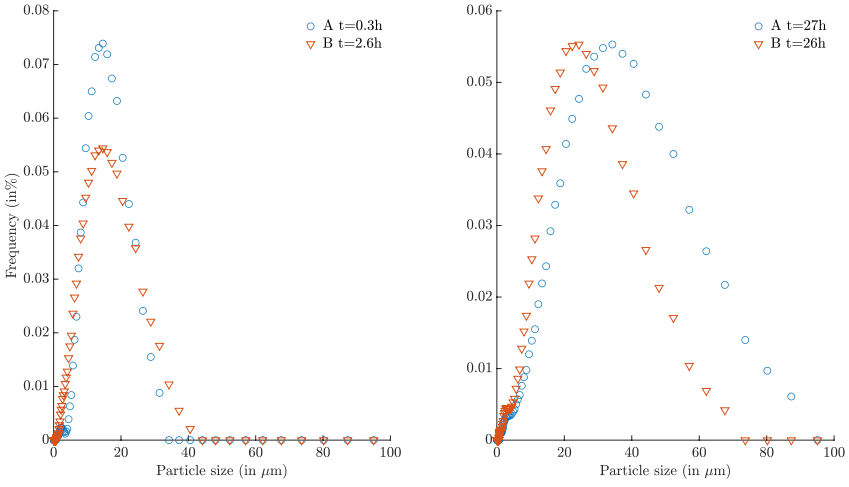

Figure 4-5 Crystals size distribution: initial distribution and distribution after 26/27 h.

At the start, the crystal size distributions (CSD) are similar (Figure 4-5), although the peak around 15 µm is slightly higher for the first experiment. No seed was added because nucleation occurred spontaneously. It appears that fewer particles nucleated in experiment A, giving them more scope for growth because the amount of available molecules is divided among less crystals. Apparently, the stochastic nature of nucleation determines the growth of the crystals for the rest of the process.

4.3.3 Mineral Content

DLP contains, besides lactose, a large amount of milk minerals, including calcium, citrate, chloride, magnesium, and phosphate. Calcium and phosphate are supersaturated with respect to the solubility of the various calcium phosphate precipitates and thus there is a risk for precipitation of these compounds. This is undesirable, because it will result in scaling of the equipment; in an industrial process, this is one of the main reasons why DLP is not further processed.

Figure 4-6 shows the concentration of calcium, magnesium, phosphate, and potassium. Magnesium and potassium serve as controls because they are not expected to form a precipitate. Lactose crystallizes as α-lactose monohydrate, removing a small amount of water from the solution as the crystallization progresses. From Figure 4-6 a clear decreasing trend can be observed for the concentration of calcium and phosphate, whereas magnesium and potassium remain constant, which is an indication that calcium phosphate is formed.

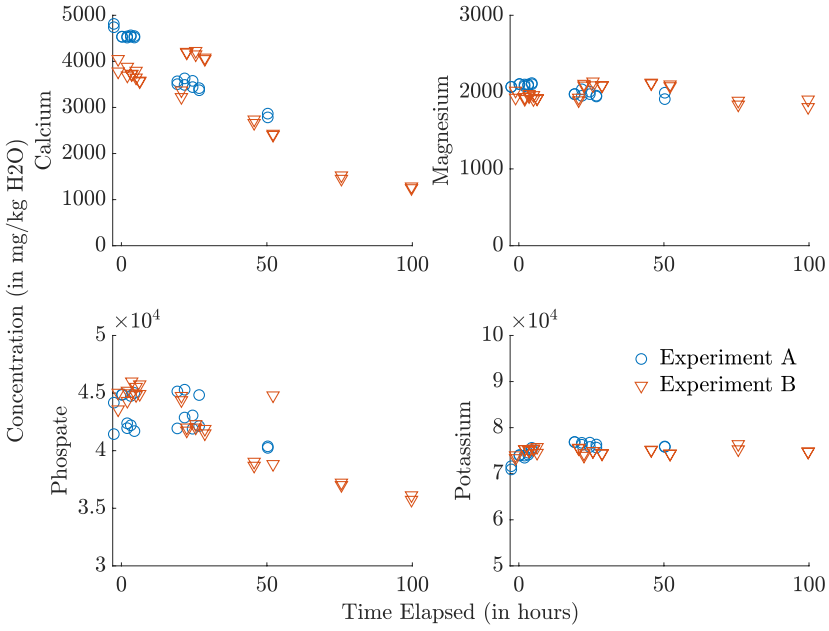

Figure 4-6 Mineral content of the mother liquid over time, please note that the value for phosphate after 50 hours, experiment B, is an outlier, probably a measurement error

Although calcium phosphate is formed over time, the amount in the first 24 h is negligible. After 24 h, a part of the crystals were separated, washed, and analysed for mineral composition (Figure 4-7) and lactose fraction. For experiments A and B, 85 wt% and 97 wt% is lactose monohydrate, respectively; the remainder is left over mother liquid or precipitate. In the first experiment, some minerals remained, whereas nearly all minerals were removed in the second experiment. This is due to the washing step; in the second experiment, the washing step was more effective because the sample had better filtration properties. Based on Figure 4-6 and Figure 4-7 the amount of precipitation is limited in the first 24 h and, if good separation is achieved, high quality crystals can be obtained.

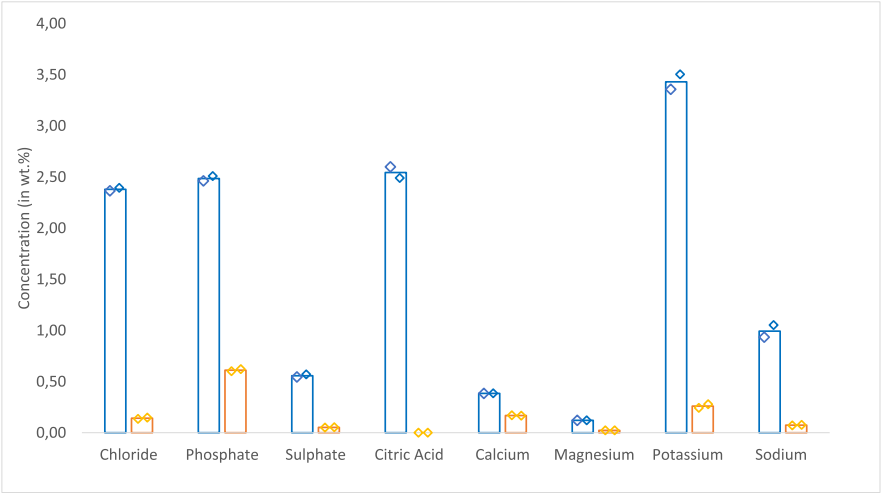

Figure 4-7 Composition of the filtered solid recovered from simulated delactosed whey permeate at sub-zero temperatures after 24 h.

4.3.4 Crystallization Kinetics of DLP versus Pure Lactose

The crystallization kinetics were investigated for DLP and compared with the kinetics for pure lactose. A population balance model was used, combining the effect of mutarotation, nucleation, and crystal growth. The nucleation and crystal growth parameters (k_n, k_g and p) were determined by minimizing the sum of squared errors between the measured and modelled concentration profile and crystal size distribution.

Figure 4-8 shows the desaturation curve and model predications of the population balance model for the two experiments. Initially, the mutarotation rate was fixed to the value for pure lactose extrapolated from Haase and Nickerson (1966). However, as α-lactose was depleted, β-lactose was not converted fast enough according to the model, resulting in an incorrect concentration profile. As indicated earlier, it can be expected that salt increases the mutarotation rate, however its value for DLP is not readily available in the literature. Therefore, the mutarotation rate ($k_1 + k_2$) constant was added as a model parameter.

Values ($k_1 + k_2$) of 0.26 and 0.31 were estimated for experiments A and B respectively. This is a 3-fold increase compared with the mutarotation rate of pure lactose. Apparently, the minerals present in DLP increase the mutarotation rate, consequently increasing the overall crystallization rate. This agrees with findings of Haase and Nickerson (1966) who found that the mutarotation rate was doubled for simulated whey solutions. In contrast to the pure lactose system studied previously(Halfwerk et al., 2023a), the mutarotation was not rate limiting for the DLP system. Therefore, it is not possible to fit the mutarotation accurately, and this is reflected in the large confidence intervals (Table 4-3). However, the fit by the model is good, giving an accurate prediction of the concentration profile (Figure 4-8).

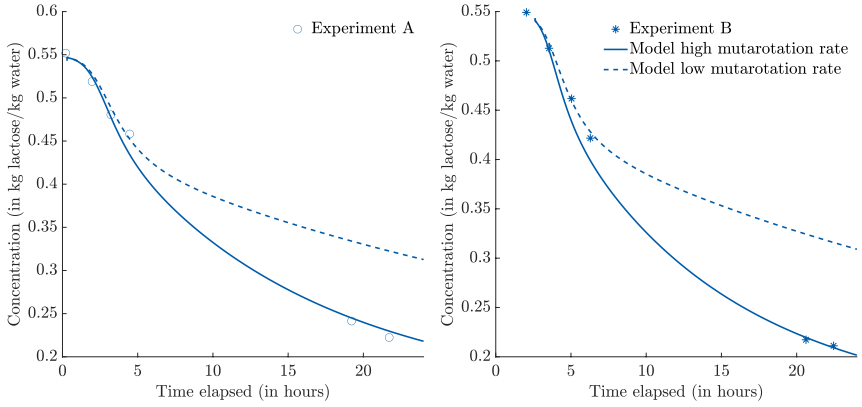

Figure 4-8 Concentration profiles over time with the model predictions.

The growth rate and nucleation constant of pure lactose is higher than for DLP, whereas the length-dependent parameter p is similar (Table 4-3). Although the kinetic constants are lower, the crystallization of lactose from DLP is faster due to the higher mutarotation rate. The model predictions of the desaturation curves of DLP are compared with pure lactose in Figure 4-9. The same initial population and initial concentration (0.55 kg/kg water) were used to make a fair comparison. The initial crystallization is faster for the pure system,

however after ±4 h, it is hindered by the low mutarotation rate, whereas DLP is not limited, resulting in overall faster depletion. After 24 h, the lactose concentration is 14 wt% for DLP (0.22 kg/kg water) versus 22 wt% for the pure system (0.28 kg/kg water), resulting in an estimated yield of 85% versus 70%.

Table 4-3 Overview of the kinetic parameters with 95% confidence intervals

	Pure lactose	Experiment A		Experiment B	
		Min	Max	Min	Max
k_g	62.56	25.31	37.42	18.61	41.5
$k_n \times 10^{14}$	2.24	0.02	0.46	0.18	1.37
p	0.83	0.77	0.85	0.81	0.89
$k_1 + k_2$	0.08	0	0.54	0	0.82

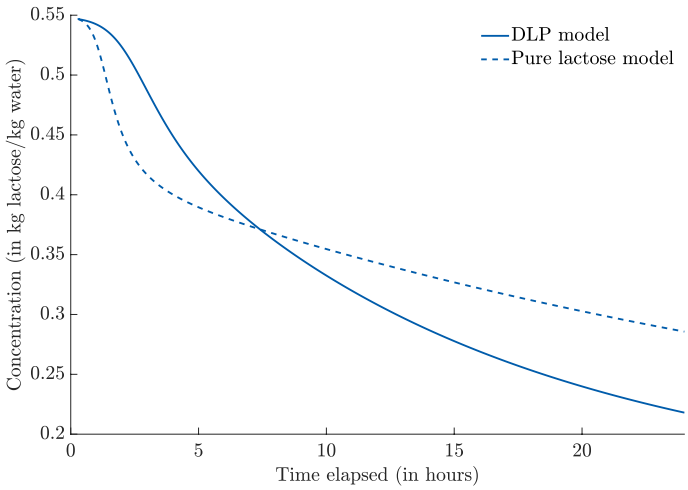

Figure 4-9 Concentration profile model for lactose recovered from delactosed whey permeate (DLP) and a pure lactose solution.

4.4 Conclusions

The further recovery of lactose by a crystallization process operating at temperatures below 0°C was investigated. A simulated DLP solution was specifically developed for this purpose. It was shown that a large portion could still be recovered. The main crystallization occurred in the first 24 h, yielding more than 85% of lactose crystals at a lactose concentration of 14.1 wt% which was close the eutectic point of 11 wt%. The crystals had a tomahawk morphology with average volume diameter of 31 and 23 µm. It appears that mineral deposition was limited in the first 24 h; the resulting powder had a lactose content up to 97 wt%. The kinetic rate of the process was analysed by a population balance model combining mutarotation, nucleation, and crystal growth. It was shown that although the growth and nucleation rate constants were lower for DLP compared with lactose recovered from a pure solution, the overall crystallization rate was increased. Although mutarotation was rate limiting in the pure system, it did not limit the crystallization process for the crystallization of lactose from DLP. The model calculations showed faster crystallization; after 24 h, the yield was estimated to be 85% for the DLP system and 70% for pure lactose.

4.5 Acknowledgments

This work was performed within the cooperation framework of Wetsus, the European Centre of Excellence for Sustainable Water Technology (www.wetsus.eu). Wetsus is co-funded by the Dutch Ministry of Economic Affairs and Ministry of Infrastructure and Environment, the European Union Regional Development Fund, the Province of Fryslân, and the Northern Netherlands Provinces. The authors would like to thank the participants of the research theme Dehydration for fruitful discussions and financial support.

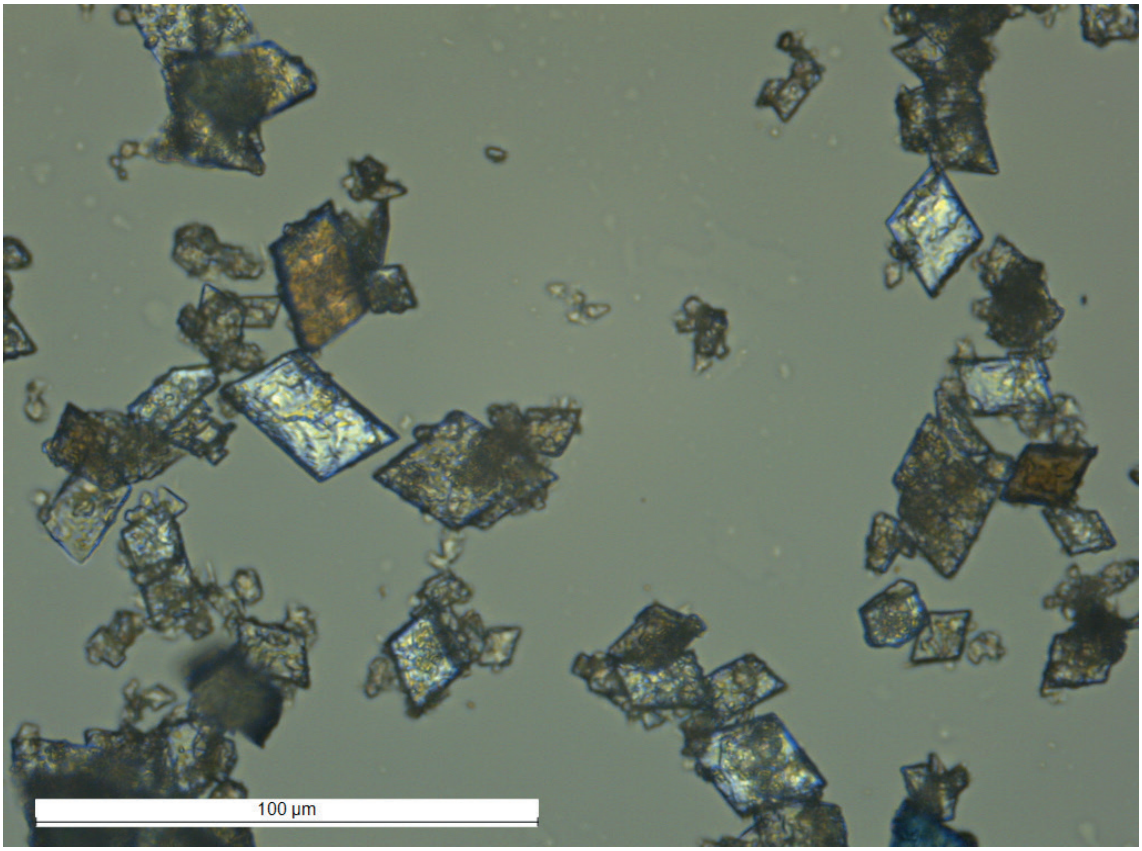

*Parallelogram shaped lactose crystals produced from whey permeate

Chapter 5

A pilot plant study at sub-zero temperatures

This chapter is part of a publication published as:
Halfwerk, R., Verdonk, L., Yntema, D., Van Spronsen, J., Van der Padt, A., (2023). Scaling up continuous eutectic freeze crystallization of lactose from whey permeate: A pilot plant study at sub-zero temperatures. Food Research International.

Abstract

Eutectic freeze crystallization is explored as an alternative to the state-of-the-art evaporation process for the recovery of lactose from whey permeate. At the so-called eutectic freezing point, both water (the solvent) and lactose (the solute) crystallize and can be removed continuously while continuously feeding whey permeate. This continuous process is demonstrated on a pilot scale at sub-zero temperatures. In the first instance, only freeze concentration of whey permeate took place at −4°C. It was possible to reach a lactose concentration of 30 wt.% and hardly any nucleation was observed. The resulting ice had high purity, with a lactose concentration of ±2wt%. Next, the eutectic phase was reached, and lactose and ice crystallized simultaneously and were continuously removed from the system, the resulting crystals had parallelogram morphology with an average size of 10 µm. Ice was recovered at a rate of 60 kg/h and lactose was recovered at a rate of 16 kg/h, yielding over 80% of the feed lactose.

5.1 Introduction

Eutectic freeze crystallization (EFC) is a separation technology whereby the concentration and crystallization steps are combined at sub-zero temperatures. The concentration and temperature of the solution are chosen such that both the solvent and the solute crystallize simultaneously at the eutectic point(van der Ham et al., 1998). In theory, a solution can be converted into ice and salt. In practice, in a batch system ice formation will fill the system over the maximal packed density and the process will stop. Therefore, EFC is operated in continuous mode, adding continuously new solution, and removing ice and crystals. Separation, between ice/liquid and salt, is achieved by the density difference; the lighter ice floats to the top of the separator and the heavier solute sinks (van der Ham et al., 1999). Previous research has mainly focused on the recovery of salts from brine streams (Lewis et al., 2010) (Randall et al., 2011) (Randall and Nathoo, 2015) (van der Ham et al., 1999) (Van Spronsen et al., 2010). Furthermore a lot of attention has been given to the development of different types of crystallizer for EFC (Genceli et al., 2005)(Rodriguez Pascual et al., 2010) (Vaessen et al., 2004) (van der Ham et al., 2004).

Although previously mainly brine streams have been investigated, in theory, the method can also be applied to other crystalline products in the food and agricultural industry such as sugars. Using low temperatures for food applications has the advantage that heat-sensitive compounds are not affected, preserving taste and quality (Sánchez et al., 2011). In addition, biological activity will be low at temperatures below zero. Moreover, at low temperatures fouling, scaling and corrosion issues will be less (Williams et al., 2015). In our previous work, we investigated the possibility of using EFC for the recovery of lactose at sub-zero conditions (Halfwerk et al., 2021). It was shown on a

laboratory scale that it is possible to recover lactose and ice simultaneously from a saturated lactose solution. It was demonstrated that although highly saturated conditions were used at sub-zero temperatures, crystal growth was the dominating process rather than nucleation.

Although it was previously proven that EFC of lactose was possible, the small-scale laboratory batch setup did not allow for proper separation of ice, lactose and mother liquid due to the large volume of ice(Halfwerk et al., 2021). For upscaling EFC of lactose, it is necessary to use a continuous system, continuously removing ice and lactose. By doing so the slurry density will be decreased, allowing for separation by gravity of ice/liquid and lactose.

In this study, a continuous pilot-scale setup is used to crystallize and separate lactose and ice simultaneously from a whey permeate solution. The properties of the crystals produced by the EFC plant were investigated regarding crystal size distribution and morphology. Furthermore, a conceptual design is proposed to improve yield and reduce energy consumption.

5.2 Materials and methods

5.2.1 Pilot plant eutectic freeze crystallizer

Figure 5-1 shows the flow diagram for the EFC pilot setup. Its main components are the crystallizer, separator, ice centrifuge and belt filter.

The feed solution is prepared in the feed vessel, and then transferred to the buffer vessel and subsequently to the crystallizer. The EFC crystallizer is a 325 L vessel with three cooling plates inside. Inside, coolant is circulated to achieve heat removal. A chiller (Tamson)is used to cool the coolant to the desired temperature. The temperature of the solution in the crystallizer and coolant is measured continuously by sensors with an accuracy of ±0.1°C. The flow rate of the coolant is measured continuously by flowmeter (Siemens

Sitrans MAG6000) with an accuracy of ±0.2%.Mechanical scrapers on the plates ensure the removal of ice from the plate as well as mixing of the solution.

The separator is a 2.5-m long tube, where the solution can settle; the heavier solids sink to the bottom and the light ice floats over the top of the separator. Further separation of the ice from the mother liquid is achieved using a pusher centrifuge (Krauss-Maffei). Mother liquid from the centrifuge is collected in a receiver vessel and then recycled to the buffer vessel and ice goes to the melting vessel. The solids at the bottom of the separator can be retrieved using a belt filter with a filter layer. The belt filter uses a slight vacuum to remove the mother liquid, which is then recycled to the buffer vessel. The solids can be retrieved and further processed. Liquid is transported by a peristaltic pump (Watson Marlow).

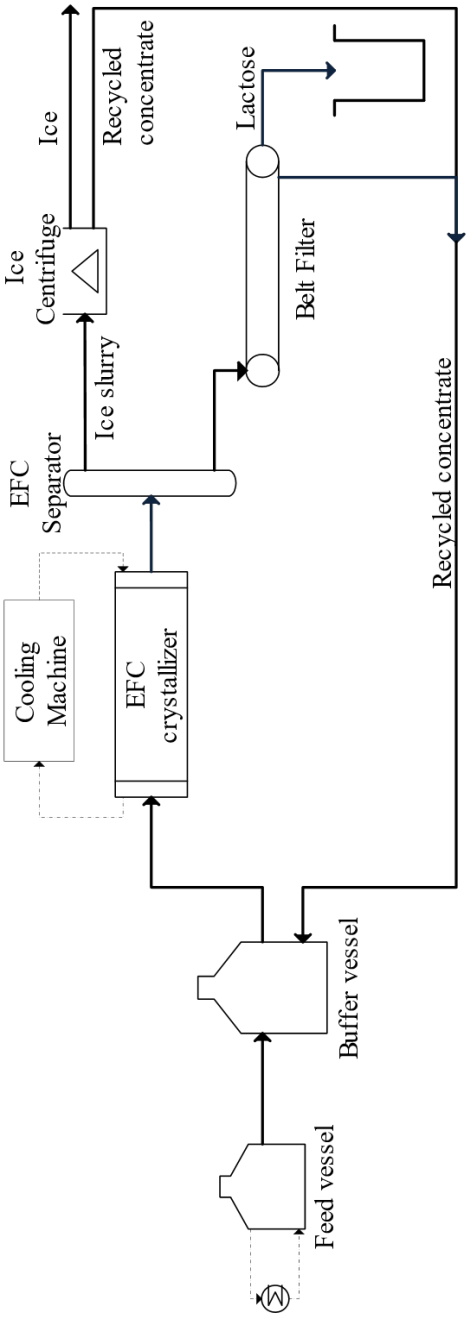

Figure 5-1 Process flow diagram of the continuous EFC pilot plant.

5.3 Materials

5.3.1 Seed material

As active seed, crystallized material obtained from a whey permeate solution in a 120-L cone crystallizer experiment was used. The whey permeate solution with an initial concentration of 30% lactose was kept at a temperature of −1°C for 22 h, after which the solids were recovered by a belt filter. The average size of the crystals was 10 µm, and they had a prism/parallelogram-like shape. Figure 5-2 shows the scanning electron microscopy images of the seed crystals and Figure 5-3 shows the crystal size distribution.

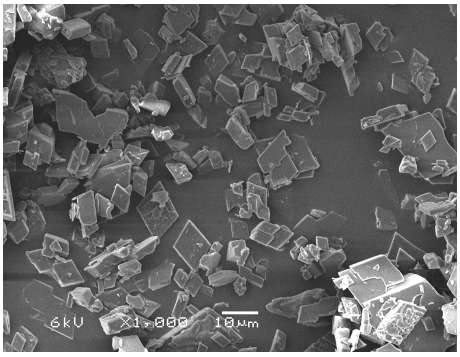

Figure 5-2 Scanning electron microscopy image of the seed.

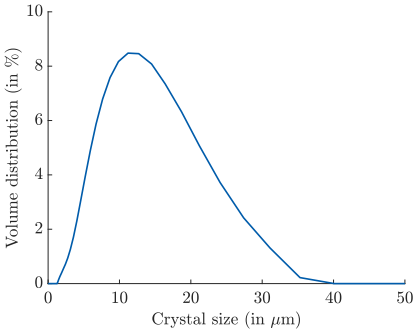

Figure 5-3 Crystal size distribution of the seed.

5.3.2 Whey permeate solution

A solution with 30wt% whey permeate (corresponding to a solution with 22 wt.% lactose) was made by first heating 700 L of water to 60°C and then adding 300 kg of whey permeate powder (WheyCo permeate powder). The solution was stirred continuously using an air mixer while adding the powder to the solution. The concentration was checked by measuring the refractive index/°Brix using a manual refractive meter (Kruss).

5.4 Experimental procedure

Two independent experimental runs were done. The experimental procedure can be divided into three steps: (5.4.1) start-up, (5.4.2) freeze concentration, (5.4.3) simultaneous crystallization of lactose and ice (EFC). An overview of the conditions used during the runs is presented in Table 5-1.

Table 5-1 Overview of the operating conditions used in runs A and B.

	Time elapsed (in hours)		Temperature in the crystallizer (°C)	
	Run A	Run B	Run A	Run B
Start-up	0	0	40	40
Ice nucleation	1.4	1.6	−2.75	−3
Start centrifuge	2.6	2	−3.8	−3.4
Seeding	4.6	2.9	−4.9	−4.2
Started belt filter	9.9	7.7	−5.9	−5.0

5.4.1 Start-up

During the start-up of the process, the reactor, separator, chiller, and tubes were filled with the feed solution, and the chiller was started at a cooling rate of 11–14 kW and set to a chiller temperature of −16.5°C. The scrapers were set to 60 rpm to achieve sufficient stirring of the solution and proper heat transfer. During start-up, the solution was pumped continuously from the crystallizer to the buffer tank at a rate of 360 L/h to maintain a uniform concentration. The start of the experiment (t = 0) was assumed when the chiller was turned on.

5.4.2 Freeze concentration

After a few hours, there was a clear increase in the torque of the scrapers, indicating that ice was starting to form on the cooling plates and the freeze

concentration of the solution was reached. Ice was removed from the plates by scrapers resulting in a suspension of ice crystals. To give ice time to grow, the system was allowed to run for 0.5–1 h after which the centrifuge was started to remove ice continuously. The freeze concentration was continuously monitored by measuring the refractive index. Samples were taken every 30 min and investigated by microscopy to determine whether lactose nucleated.

5.4.3 Eutectic freeze crystallization

The exact optimum operating conditions for the process were not exactly known. Therefore, experiment A served as first trial and the operating conditions for experiment B were adjusted accordingly. In our previous batch study, we found that at a concentration of 30 wt.% lactose, crystal growth was the dominant process rather than nucleation (Halfwerk et al., 2021). Therefore, the concentration in run A was stabilized by adjusting the feed rate to reach a concentration of ±30% lactose. However, after running for 8h the quantity/slurry density of the crystals was insufficient to be separated by the belt filter, although it was observed by microscopy that the crystals grew in size. Although all operating conditions were maintained, the temperature suddenly increased after 9 h, at a concentration of 32 wt.%, indicating that lactose crystallized, and that latent heat was released. When investigated under the microscope, a large number of crystals were visible; however, the size of the crystals seemed to be reduced.

In run B, the solution was immediately concentrated to the concentration of run A (32 wt.% lactose). Furthermore, a lower amount of seed material (0.5kg vs 5kg) was used to give the individual crystal more time to grow. After adding seed, 3 h after starting the chiller, there was no apparent effect on the temperature or concentration. When the concentration reached 32 wt.%, a large number of crystals was visible under the microscope. After 8 h, the slurry

density of lactose crystals was high enough to use the belt filter, and the feed was adjusted to maintain a constant concentration.

5.5 Analysis

During the experiments, samples were collected continuously from the crystallizer, separator, and buffer vessel to determine the refractive index/°Brix of the solution. A calibration curve was made to convert the °Brix to lactose concentration. When solids (ice/lactose) were present, 0.45-µm filter units were used to retrieve a clear solution. All samples were measured at least twice for accuracy. Every 30 min, a sample from the crystallizer was taken and investigated by microscope for the presence of crystals in the solution. The pH was determined at the start of the experiment.

Every few hours, duplicate samples were taken from the crystallizer and filtered through a 0.45-µm filter and subsequently diluted 10× and 200× for analysis of the salt and lactose concentrations over time. The sugar content in the samples was determined by high-performance liquid chromatography and the mineral content by ion chromatography.

The dried lactose crystals were further investigated with scanning electron microscopy and brightfield microscope (Leica dm 750 with polarized light) to determine the morphology. Particle size was analysed by laser diffraction (Malvern Mastersizer3000) with a hydro unit (120 mL). Analyses in the particle sizer were performed with saturated lactose solution (18 wt.%), which was cooled continuously at 12°C. The samples were first treated for 10 min with ultrasound (100%) to break any agglomerates.

5.6 Results and discussion

The use of EFC for the recovery of lactose was investigated in two independent runs at pilot scale. The characteristics of the two runs are discussed below; the initial freeze concentration stage is described for these two runs in section 5.6.1. The EFC stage is described in Section 5.6.2 An analysis is made into the morphology and size of the lactose crystals. Furthermore, in section 5.6.3 the mass and energy balance of pilot test are given.

5.6.1 Freeze concentration

Figure 5-4 shows the concentration profiles during ice formation in the EFC crystallizer and continuous ice removal in the separator. The interstitial mother liquid was recycled to a buffer tank. During freeze concentration, samples of the water phase were taken and examined under the microscope. The liquid could be concentrated without formation of a large amount of crystals for the first ±6 h. When the concentration reached ±30%wt%, a few crystals became visible in the solution in both runs. During freeze concentration, the purity of ice was high; after centrifugation, the lactose content was only 1–3 wt.% due to the remaining mother liquid present in the interstitial space between the ice crystals.

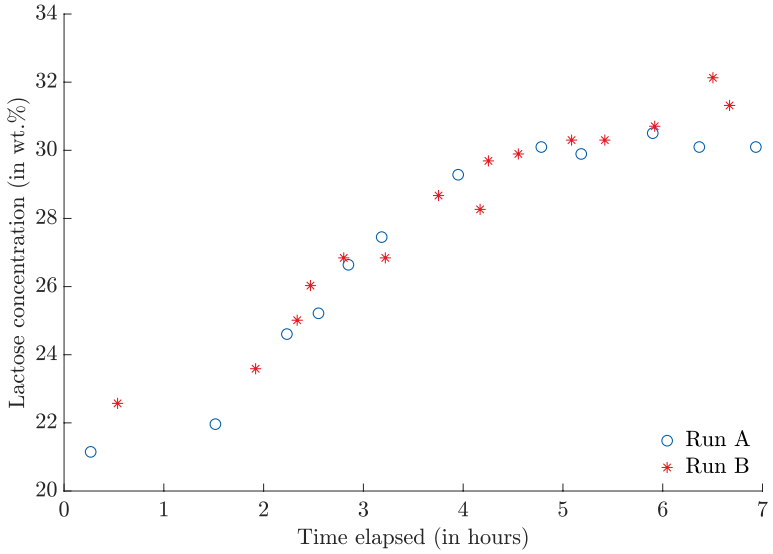

Figure 5-4 Concentration profile of lactose during freeze concentration, based on refractive index measurements.

5.6.2 Eutectic freeze crystallization

When the solution reached ±30% lactose, seeds were added to initiate the crystallization process; 5 kg of seed was used in run A and 0.5 kg of seed was used in run B. To give the crystals time to grow, the system was kept in recirculation mode for a few hours until the crystals could be filtered, after which the band filter was started. Figure 5-5 shows the concentration profiles of the two runs after 7h.

After ±8/9 h, the belt filter was started to recover the lactose from the slurry (Figure 5-6). A lactose sample was taken from the belt filter, and the lactose slurry was filtered over a vacuum filter and then washed with 2-propanol to remove any moisture. The solids were analysed for size and morphology.

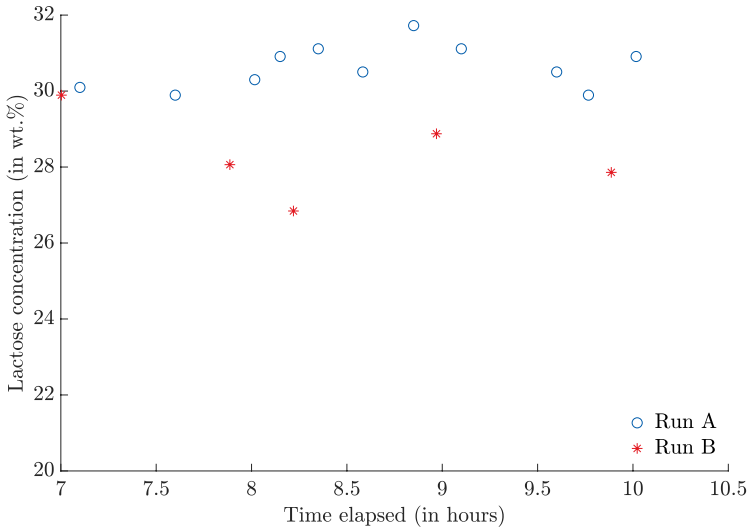

Figure 5-5 Lactose concentration in the crystallizer during EFC, based on refractive index measurements

Figure 5-6 Lactose produced by the belt filter at the end of the day.

The average volume particle size (d43) of the two runs was 12 and 7 µm for runs A and B, respectively. In both runs, seed was used to start the process and to maximize crystal growth rather than nucleation. However, during both runs, a large amount of nucleation was seen when the concentration increased above 32 wt.%. This is probably the reason for the relatively small particle size. However, it also indicates that if the process was run for a longer time at a lower supersaturation, larger crystals could be grown.

Figure 5-7 and Figure 5-8 show microscopy images of the crystals produced during the pilot run. The crystal size for run B is visibly larger than for run A and the main morphology of the crystals is rhombic plates/parallelogram plates. Lactose can exist in a wide range of morphologies; the most common morphologies for an industrial process are triangle-shaped crystals and tomahawks. Furthermore, prisms or needle-like crystals are often observed. The morphology variations of lactose are due to variations in the growth rate of the different faces (Parimaladevi and Srinivasan, 2014). The morphology can depend on supersaturation, cooling rate, α-/β-lactose concentration and impurities (Raghavan et al., 2000). The crystals in this study seem to have grown mainly in the length direction rather than developing a triangular morphology. It is expected that one of the impurities in this specific whey permeate stream, is the cause of this. It is not expected that the low temperature or mineral content is the cause as in previous studies at low temperatures and high mineral content only tomahawk crystals were produced(Halfwerk et al., 2021) and (Halfwerk et al., 2023a).

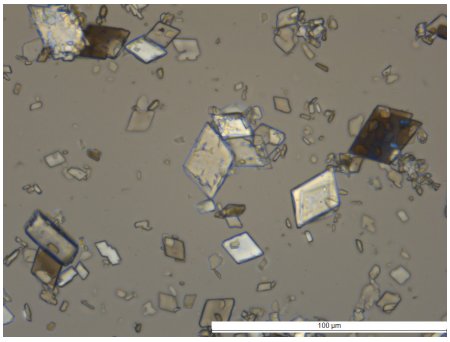

Figure 5-7 Crystals produced in run A.

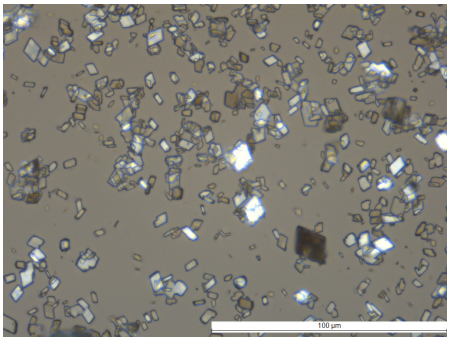

Figure 5-8 Crystals produced in run B.

5.6.3 Mass and energy balance

During the runs, the mass fractions of ice, mother liquid and lactose were determined. Based on this, the flow rates were determined of ice and lactose. Average production rates of lactose monohydrate of 15±1.0 (run A) and 17±0.7 kg/h (run B) were found. A fraction of the mother liquid in the process is lost in the lactose and ice cake; in our setup, around 80% of the lactose could be recovered. This could be further optimized by increasing the separation efficiency of the belt filter and centrifuge.

In this experiment, ice was continuously removed at a rate of 60 kg/h, and during the process, the lactose concentration in the ice fraction was 1–3 wt.%, but this increased to 8 wt.% in both runs at the end the day, indicating pollution of the ice with lactose crystals. This could be due to the high load of small particles in the mother liquor that slipped through the ice separator.

During the pilot test, the heat transferred from the cooling plates was measured continuously; on average, 12 kW of heat was removed by the system for both runs. The heat that needs to be removed is the sum of sensible heat for cooling down the solution from 20°C to −5°C, the latent heat for crystallization of ice (334 kJ/kg) and lactose (55 kJ/kg) and the heat loss. Based on the mass flows,

a total of 8 kW of heat needs to be removed as the sum of sensible and latent heat. This implies that 4 kW thermal power is lost in the pilot plant, see figure 5-9.

Although, it was shown that EFC can be used for the recovery of lactose, improvements can still be made in yield and energy consumption. The yield can be optimized by improving the separability of the crystals. In the pilot plant, some crystals were lost in the ice, the separability should improve upon increasing the residence time in the crystallizer, allowing for more growth, and by increasing the settling time in the separator. In addition, the energy consumption could be reduced by preventing heat loss with insulation and precooling of the feed by heat exchange and the use of the ice produced for cooling. In the next chapter (chapter 6) a conceptual design is made and compared with an evaporation crystallization process.

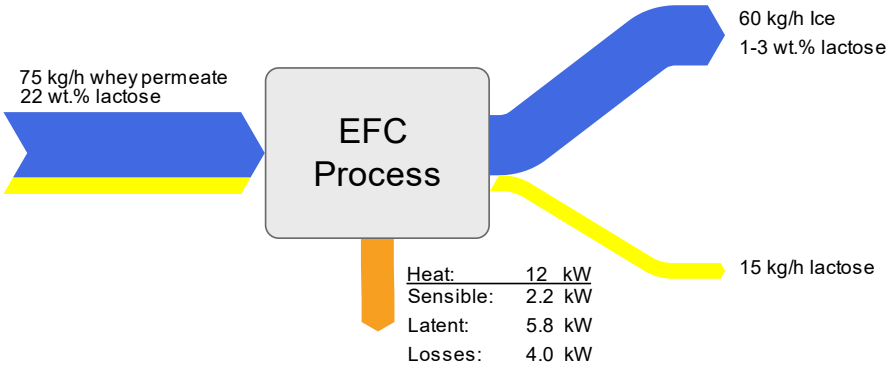

Figure 5-9 Overview of average mass and power during the pilot test

5.7 Conclusion

In this study, a continuous pilot-scale setup was used to crystallize and separate lactose and ice simultaneously from a whey permeate solution. It was shown that continuous pilot scale freeze concentration of the whey permeate was possible, and up to 30 wt% lactose, no large amount of nucleation was observed. During freeze concentration, ice had high purity, with a lactose concentration of ±2wt%.

Lactose and ice were crystallized simultaneously and removed continuously from the system by centrifuge and belt filter. The average size of the resulting crystals was ±10 µm with a parallelogram-like shape. The overall mass and energy balance was evaluated to determine the viability of the technology. Ice was recovered at a rate of 60 kg/h, lactose was recovered at a rate of 16 kg/h and yielded 80% of the feed lactose.

Acknowledgements

This work was performed in the cooperation framework of Wetsus, European Centre of Excellence for Sustainable Water Technology (www.wetsus.eu). Wetsus is co-funded by the Dutch Ministry of Economic Affairs and Ministry of Infrastructure and Environment, the European Union Regional Development Fund, the Province of Fryslân, and the Northern Netherlands Provinces. The authors would like to thank the participants of the research theme Dehydration for fruitful discussions and financial support. The authors would also like to thank Maurice Strubel for analysing the lactose content of the samples and Farah Chihi for operating the pilot plant.

*Lactose crystals recovered by the belt filter during an EFC experiment

Chapter 6

General Discussion

This chapter is part of a publication published as:
Halfwerk, R., Verdonk, L., Yntema, D., Van Spronsen, J., Van der Padt, A., (2023). Scaling up continuous eutectic freeze crystallization of lactose from whey permeate: A pilot plant study at sub-zero temperatures. Food Research International.

6.1 Introduction

The objective of this thesis was to show the applicability of eutectic freeze crystallization for the recovery of lactose from whey permeate and delactosed whey permeate. In this chapter, an overview of the main findings is given. Furthermore, the EFC process is compared to conventional evaporation + slow cooling crystallization and an outlook is made for future research.

6.2 Main Findings

The use of eutectic freeze crystallization for the recovery of lactose was investigated by doing batch experiments, modelling, and a pilot test. In the second chapter the working regime for EFC of lactose was explored. It was proven that simultaneous crystallization of lactose and water (ice) is possible, producing tomahawk shaped crystals with an average size of 10 µm. Although operating deep in the labile zone, known for being responsible for excessive nucleation, it was found that crystal growth is the predominant process rather than nucleation.

The results shown in chapter two showed that the crystallization behaviour at sub-zero temperature differs from conventional slow-cooling crystallization. To explore this further, the kinetics and the mechanisms behind crystallization of lactose at sub-zero temperatures were investigated in chapter three. Batch experiments at different operating conditions were combined with a population balance model combing mutarotation, nucleation, and crystal growth. It was discovered that mutarotation was rate-limiting when the crystallization was fast. The conversion of beta lactose could not keep up with the fast depletion of α-lactose. An empirical model was developed to describe the concentration profile and particle size over time.

In chapters two and three the use of EFC was explored for pure lactose-water solutions; however, in the industry the majority is recovered from whey permeate, producing lactose and remaining mother liquor, often referred to as delactosed whey permeate (DLP). The replacement of the current slow-cooling process can be challenging as EFC is still in the developing stage for food systems, EFC is therefore most suitable for residual streams like DLP. DLP still contains around 20 wt.% of lactose. In chapter four it was proven that still a significant portion of lactose from DLP could still be recovered at sub-zero temperatures. Furthermore, precipitation of calcium phosphate was found to be low on the first 24h. The crystallization rate of lactose recovered from DLP was increased compared to the crystallisation of pure lactose. This was caused by the increase in rate of mutarotation; where the conversion of beta-lactose was not fast enough for pure lactose, the minerals present in DLP seem to increase the mutarotation rate as it did not limit the crystallization rate. This resulted in fast crystallization; after 24h the yield was 85%.

In the chapters 2-4, batch crystallization was studied. However, batch EFC experiments proved to be challenging; for EFC continuous removal of ice and lactose is essential. For this purpose, a continuous operated pilot setup was discussed in chapter 5. Whey permeate was continuously fed to the crystallizer and ice and lactose was recovered by a centrifuge and belt filter. With two independent runs it was proven that lactose could be recovered by EFC.

6.3 Comparison of EFC and evaporation

Although it was proven that the EFC process could efficiently separate lactose from whey permeate and DLP, the question could be raised how it compares with the conventional process. In the next section, the mass and energy balances of EFC are compared with an evaporation process to assess the viability of the process.

EFC has been proposed as an energy-efficient replacement for the conventional evaporation process by different researchers, see Table 6-1. The energy efficiency, however, depends on the solution used, the operating temperatures and the concentration. Furthermore, the traditional evaporation processes have been optimized using multi-effect evaporation and mechanical vapor recompression systems, reducing energy consumption significantly. In literature, EFC has not yet been compared to the current state of the art in evaporation, mechanical vapor recompression, see Table 6-1.

Table 6-1 Literature overview of studies into the energy consumption of EFC compared to evaporation

Salt produced	Energy reduction	Compared to	Author
$NaNO_3$	30%	3-effect	(van der Ham et al., 1998)
$CuSO_4.5H_2O$	65%	3-effect	(van der Ham et al., 1998)
KNO_3	70%	3-effect	(Vaessen, 2003)
$MgSO_4.7H_2O$	60%	2-effect	(Himawan, 2005)
Na_2SO_4	85%	3-effect	(Fernández-Torres et al., 2012)

Therefore, an analysis is made to compare EFC with state-of-the-art evaporation + slow cooling crystallization process to produce lactose. The conditions, the mode of operation of EFC and slow cooling crystallization differ, a comparison between these two is therefore not straightforward as EFC is usually performed at isothermal conditions in a continuous reactor, simultaneously removing solute and solvent, to maintain a low slurry density. Whereas a slow-cooling process is operated batch wise, decreasing the temperature to maintain a constant supersaturation. To overcome this issue, the lactose production and energy consumption will be determined both per kg of whey permeate processed and per kg lactose produced.

6.3.1 Mass and energy balances

Energy

Crystallization from aqueous solutions is usually a combination of concentrating, crystallization, and purification. The energy requirement of any crystallization process is mainly due to removal of water to produce a supersaturated liquid.

The required energy can be dictated by a pressure difference (RO) or thermal energy (cooling/heating). The most common way for treating whey permeate is by evaporation. For evaporation, energy (heat) is added to evaporate water, whereas in freeze concentration heat needs to be . In both cases, it is a combination of sensible heat and latent heat from water and crystals. The latent heat of evaporating water is 2256 kJ/kg (Baehr and Stephan, 2011), whereas for crystallization water (e.g. ice) is 334 kJ/kg(Williams et al., 2015). The energy removal/addition from a crystallization process is thus a combination of heating/cooling the feed and the latent heat of lactose and vapor or ice:

$$Q_{total} = Q_{sensible} + Q_{latent} \tag{6-1}$$

The sensible heat can be calculated from the enthalpy difference:

$$Q_{sensible} = m_{total} \cdot c_p \cdot \Delta T \tag{6-2}$$

With m_{total} the mass of the solution, c_p the specific heat, the value of water is used (4.18 kJ/kg) and ΔT temperature difference of the cooled/heated solution. The latent heat can be determined from the amount of water converted into ice or vapor and heat of fusion, for evaporation and EFC:

$$Q_{latent,evap} = H_{vapor} \cdot m_{vapor} + H_{lactose} \cdot m_{lactose|\text{solid}} \tag{6-3}$$

$$Q_{latent,EFC} = H_{ice} \cdot m_{ice} + H_{lactose} \cdot m_{lactose|\text{solid}} \tag{6-4}$$

With m_{vapor}, $m_{lactose|\text{solid}}$, m_{ice} the mass of vapor, lactose crystals and ice. H is the heat of fusion of the vapor, ice and lactose (55 kJ/kg based on (Dilworth et al., 2004)).

Yield

The yield is the ratio of the lactose crystals obtained and the total amount of lactose in the starting material:

$$Yield = \frac{m_{lactose|\text{solid}}}{m_{lactose|\text{aq},crystallizer\ (t=0)}} \cdot 100\% \qquad (6\text{-}5)$$

With $m_{lactose|\text{solid}}$ the mass of lactose crystals produced (kg) in the crystallizer and $m_{lactose|\text{aq},crystallizer}\ (t=0)$ the mass of lactose dissolved in the solution at the start (kg). In literature a maximum yield of 82% is usually reported (Wong and Hartel, 2014) although actual industrial yields are reported to be significantly lower around 65%(Paterson, 2009).

For a continuous system, like EFC, in theory a recovery of 100% could be achieved, the actual recovery will be lower due to a bleed stream for non-crystallizing compounds and general losses. The system is continuous regarding the supply and removal of ice and lactose; however, minerals will accumulate and can reach supersaturation and will inevitably precipitate as a result. In addition, an increased mineral content will cause an increase in viscosity, affecting the mass transport and thus growth and nucleation. Furthermore, minerals will affect the growth of crystals, which will result in changes in both the crystallisation rate and the final morphology(Paterson, 2017)(Wong and Hartel, 2014).

To circumvent the issues above, there are two approaches, a so-called bleed stream could be used to keep the mineral concentration at the right level, or at a certain moment the continuous process is switched to batch mode for further

depletion of lactose and eventually emptying the system for separation of lactose crystals and the remaining mother liquor. In this chapter we use the latter strategy to calculate the lactose yield. In this case the final yield of lactose will be mainly determined the volume of the remaining mother liquor. In our previous study the recovery of lactose from the mother liquid of lactose crystallization, delactosed whey permeate (DLP), was investigated; only calcium phosphate precipitation was observed, the remaining minerals stayed in the solution (Halfwerk et al., 2023b). It is thus expected that the system can at least be run until it reaches the concentrations of lactose depleted DLP, i.e. the mother liquor that remains after sub-zero crystallization of lactose from conventional DLP.

Removal of minerals can be done by removing the mother liquid in the crystallizer and replacing it by fresh feed, this results in a loss of lactose which is still in the removed liquid. Based on our previous study, the total feed and reaming mother liquid quantities could be based on the mineral balance:

$$m_{feed} = FR \cdot m_{crystallizer} \tag{6-6}$$

$$w_{x,RM} = w_{x,ML\ dlp}$$

$$w_{x,RM} = \frac{m_{feed} \cdot w_{x,feed} + m_{crystallizer} \cdot w_{x,crystallizer}}{m_{RM}} \tag{6-7}$$

With m_{feed} the amount of mass added to the crystallizer, $m_{crystallizer}$ the mass in the crystallizer and m_{RM} the mass lost as remaining mother liquid (kg), $w_{x,feed}$ the weight fraction of mineral x in the feed, $w_{x,ML\ dlp}$ the weight fraction of minerals in DLP, $w_{x,crystallizer}$ the weight fraction of mineral x present in the crystallizer at the start and $w_{x,RM}$ the weight fraction of mineral x in the remaining mother liquid (kg/kg solution). FR is the feed ratio, this ratio can be determined numerically and the use of different mass balances, see Appendix 6.A for an overview of all calculation.

The yield of crystalized lactose can be calculated based on the initial load of the crystallizer, the lactose in solution fed to the reactor and the amount of lactose leaving the system in the remaining mother liquid:

$$Yield = \frac{m_{lactose|aq,feed} + m_{lactose|aq,crystallizer} - m_{lactose|aq,RM}}{m_{lactose|aq,feed} + m_{lactose|aq,crystallizer}} * 100\% \quad (6\text{-}8)$$

With $m_{lactose|\mathrm{aq},feed}$, $m_{lactose|\mathrm{aq},crystallizer}$, $m_{lactose|\mathrm{aq},RM}$ the mass of lactose added to the system by the feed, in the crystallizer at the start and removed in the remaining mother liquid (kg).

6.3.2 EFC

Removal of mother liquid

To maximize yield, it is proposed in this conceptional design to first operate the system as a continuous EFC process until the mineral content of the mother liquid reaches a certain threshold. Next the temperature is raised above the freeze point and system is then operated batch wise, still recovering a part of the lactose from the mother liquid, see Figure 6-1.

Figure 6-2 shows the relative increase in mineral content compared to the start concentration, as indicated in section 6.3.1, minerals will build up and they need to be removed before precipitation occurs.

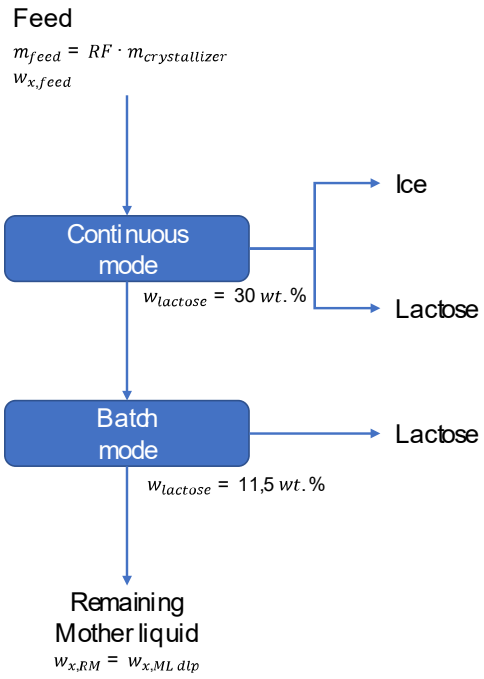

Figure 6-1 Proposed EFC process; first operate the system as a continuous EFC process, after which it is operated as batch process without ice formation

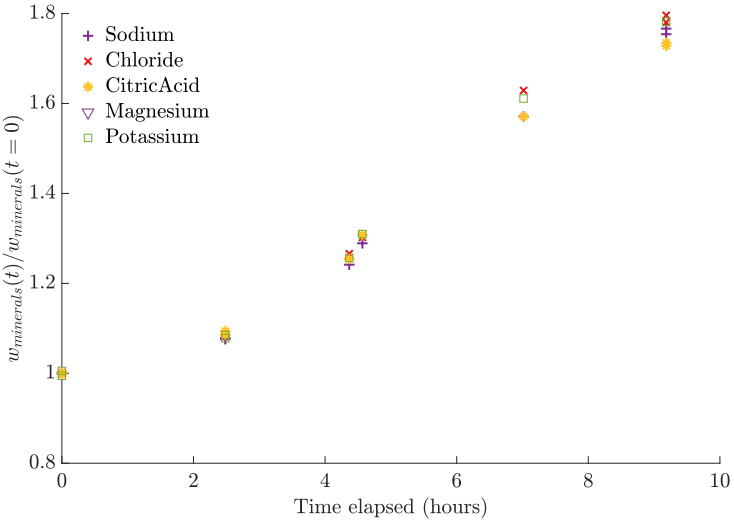

Figure 6-2 Relative increase of mineral content over time for the second run of the pilot test

The final mineral and lactose content are assumed to be equal to the composition of the mother liquid after crystallization of lactose from DLP. Table 6-2 shows the comparison with the mineral content of whey permeate with 20 wt.% lactose (feed solution) with the mother liquor after lactose crystallization from DLP. Furthermore, it gives the feed ratio (FR) and the corresponding yield found for this feed ratio. A feed ratio between 1.1 and 8 is found, the differences can be explained by the difference in source material. Furthermore, in our previous study we observed precipitation of calcium phosphate after 24h resulting in a lower calcium value (Halfwerk et al., 2023b).

For the feed ratios found in Table 6-2 the yields are around 90%, with a slightly lower value for calcium of 82%. The lower value is mainly due to the low calcium phosphate found after 48h in our previous study, which was caused by the precipitation of calcium phosphate. It can thus be expected that using higher feed ratios than 1.1, calcium phosphate will precipitate at some point. This however did not affect the crystallization of lactose in the batch system and is therefore expected it is neither the case for a continuous system.

Table 6-2 Comparison between whey permeate with 20 wt.% lactose and the mother liquid after lactose crystallization from delactosed whey permeate

	WP 20wt.%	ML after crystallization from DLP	Feed ratio *FR*	Yield
	(gram/kg)	(gram/kg)	(-)	%
Chloride	4.5	39.9	5.7	93.5
Phosphate	2.4	26.7	7.6	94.8
Citric Acid	4.3	30.8	4.3	92
Calcium	0.6	1.9	1.1	81.8
Potassium	5.9	51.7	5.6	93.4
Sodium	1.8	14.4	5	92.8
Lactose	200.0	115.0		

Based on our previous observation calcium will be the first mineral to precipitate, if this is taken as the maximum mineral level, the yield is around 80%. However, if the crystals are recrystallized it may contain some mineral load, hence three different scenarios are evaluated, 80%, all minerals in solution, 90% all but calcium in solution and finally 95% all but phosphate at supersaturation conditions.

Energy

Figure 6-3 shows the main mass and energy streams of an EFC process. Whey permeate contains around 5 wt.% lactose; it is assumed that, like an evaporation process, it is first concentrated with nanofiltration/reverse osmosis to 20wt.%(Paterson, 2017). Before the crystallizer, the solution is precooled from 20°C to 5°C using the latent heat of melting of the ice produced in the process. Next, it is fed to the EFC crystallizer where it is further cooled and concentrated to around 30wt.%. At this point, ice and lactose is crystallization simultaneous. After the crystallizer, the solution is separated into two fractions, ice slurry and lactose slurry. This is fed to two centrifuges were separation of solid is achieved, the mother liquid is recycled to the crystallizer. The ice is fed to a heat exchanger to recover a part of cold for precooling the feed solution, see Figure 6-3.

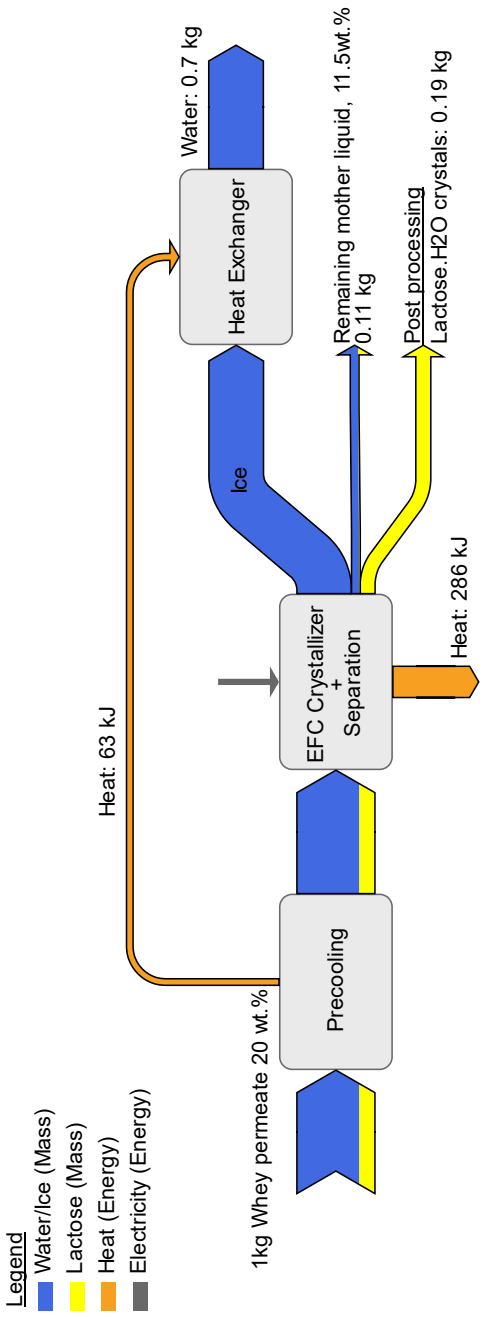

Figure 6-3 Flow diagram of mass and energy streams of the EFC process, based on 90% yield

The main energy consumption is due to the chiller. The additional consumption of the pumps, centrifuges and stirrers are neglected. Table 6-3 shows the mass and energy flows per kg of whey processed. To recover 90% of the lactose in the feed, 350 kJ of heat needs to be removed per kg whey, ±60 kJ of this can still be retrieved by precooling the feed by the latent heat of ice. If a chiller with a coefficient of performance of 5 is used, it will require ±60 kJ of electricity per kg of whey, detailed calculation can be found in Appendix 6.A.

Table 6-3 Overview of mass and energy flows for an EFC process different yields

Mass				
Start amount	1			kg
Start Concentration	20			wt.%
Crystallizer concentration	30			wt.%
Final concentration	11.5			wt.%
Yield	80	90	95	%
Water removed	0.54	0.70	0.78	kg/kg starting material
α-lactose.H2O produced	0.17	0.19	0.20	kg/kg starting material
Energy				
Temperature Start	20			°C
Temperature Precooling	5			°C
Temperature EFC	-5			°C
Sensible heat	105	105	105	kJ/kg whey permeate
Heat of fusion ice	181	234	260	kJ/kg whey permeate
Heat of fusion lactose	9	10	11	kJ/kg whey permeate
Precooling solution	-63	-63	-63	kJ/kg whey permeate
Total heat requirement	232	286	313	kJ/kg whey permeate
Chiller				
COP	5	5	5	-
Energy consumption	46	57	63	kJ/kg whey permeate
Energy consumption	276	302	313	kJ/kg lactose

6.3.3 Evaporation

Industrially lactose is recovered from whey permeate, its production steps can be separated into concentrating, crystallization, washing and drying(Wong and Hartel, 2014). Figure 6-4 shows a simplified process scheme to produce lactose. At the start, the whey permeate has a lactose content of 20wt.%, first it is preheated to 75°C, then it is further heated to around 85°C and water is evaporated until a concentration of 55 wt.% lactose is reached. Subsequently, the solution is slowly cooled to approximately 20°C in the 20h, by doing so a driving force for crystallization is created. At 20°C, the solubility is 18 wt.%, and the maximum yield that can be achieved is 83%; for every kg of whey permeate, 0.17 kg of α-lactose.H_2O is produced. After crystallization, the lactose is separated by a centrifuge, washed, and subsequently dried in a fluidized bed dryer(Paterson, 2017).

The values in Figure 6-4 show the amount of energy required for evaporating water from the system. In practice, though the energy consumption is lower due to the use of multiple-effect evaporation and mechanical vapor recompression systems. As Mechanical vapor recompression is, at time of writing, the state of the art in the industry therefor it will be used for the comparison with EFC. In Appendix 6.A however, the calculations are also shown for multiple-effect evaporation. Mechanical vapor recompression uses compression/mechanical work to increase the temperature of the vapor, similar to EFC it uses electricity as energy source. For 1 joule of electricity 20J of evaporation can be achieved (Heldman, D.R., 2019). Table 6-4 shows an overview of the mass and energy consumption of a mechanical vapor recompression system. MVR is given with and without preheating; if a source of rest heat is available this can be used instead. Detailed calculation can be found in Appendix 6.A.

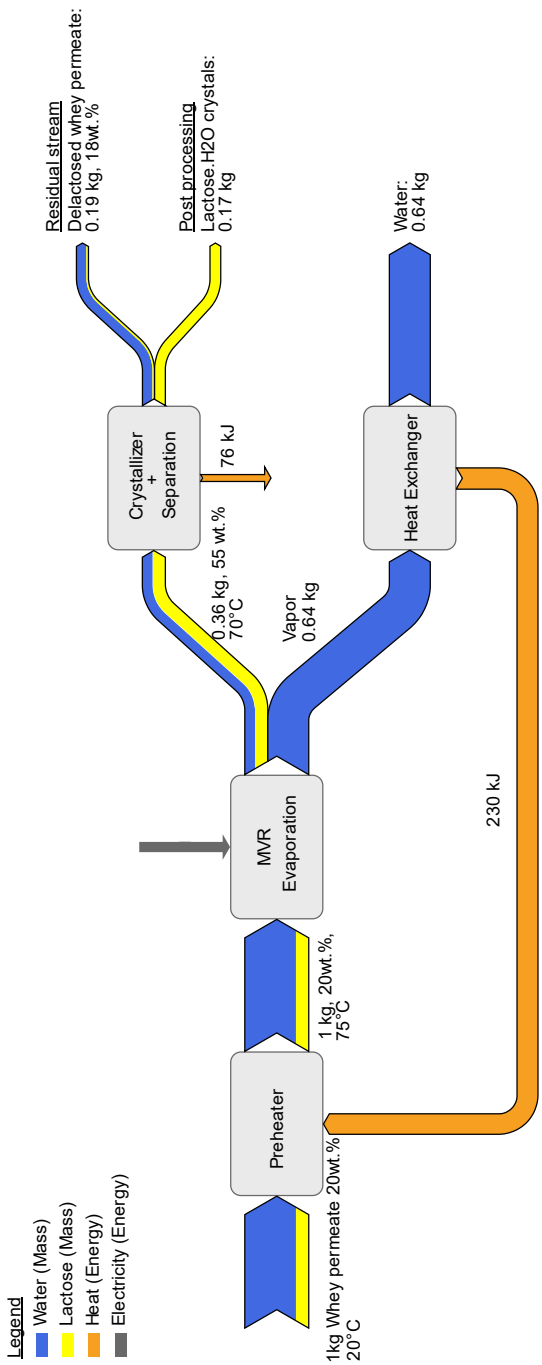

Figure 6-4 Flow diagram of mass and energy streams of the evaporation process.

Table 6-4 Overview mass and energy values for mechanical vapor recompression evaporation

Mass			
Start amount	1		kg/kg whey permeate
Start Concentration	20		wt.%
Conc. after evaporation	55		wt.%
Conc. after crystallization	18		wt.%
Water removed	0.64		kg
α-lactose.H2O produced	0.17		kg
Yield	83		%
Energy	MVR	MVR without preheating	
Efficiency MVR	20	20	J evaporation /J electricity
Sensible heat	272	0	kJ
Preheating	-230	0	kJ
Energy for evaporation	72	72	kJ
Total required	114	72	kg/kg whey permeate
Total required	651	412	kg/kg whey lactose

6.3.4 *Comparison*

Table 6-5 compares the lactose produced and energy consumption of EFC with evaporation. When preheating of the feed is required, mechanical vapor recompression is in all cases, more energy intense then EFC. With a similar yield of 80% EFC is more than twice as efficient. Depending on the location, waste/remaining heat might be available to preheat the feed, decreasing the energy consumption. However, compared to EFC it is still 30% higher. The lower energy consumption can be explained by the large difference in latent heat between the phase change to ice and vapor (2256 vs 334 kJ/kg).

Furthermore, as EFC is a continuous process, higher yields are possible, resulting in a lower energy consumption per kg of lactose.

Table 6-5 Comparison of energy consumption between EFC and evaporation

	MVR	MVR with heat recuperation	EFC 80%	EFC 90%	EFC 95%
Yield	83	83	80	90	95
Energy (kJ/kg whey)	114	72	46	57	63
Energy (kJ/kg lactose)	651	412	276	302	313

6.4 Outlook

Chapter 5 of this thesis shows that lactose can be recovered using EFC in a continuous mode at a pilot plant. Although a significant proportion of lactose could be recovered, the mineral content in the liquid builds up (Figure 6-2). Removal of minerals is thus required, resulting in a loss of mother liquid and thereby loss in lactose. The yield is mainly determined by how much mother liquid needs to be removed to lower the mineral content sufficiently. In section 6.3.2 different scenarios were investigated with different feed ratios, resulting in an 80-95% yield. However, further research is needed on the limits of mineral build-up; how much it can be concentrated before precipitation of salts occurs and how the minerals affect the crystallization process of both lactose and ice. An important parameter to consider is viscosity; if the solution becomes too viscous, it will lead to limitations in mass transfer and/or the separation of ice/lactose crystals can become difficult.

After running the EFC process for a certain time, a residual stream is thus generated with an even higher mineral content. This stream can be seen as waste or must be downstream processed to recover minerals and water. Minerals could be removed from this stream by a demineralization step like ion-

exchange(Nie et al., 2017) or the use of a supercritical fluids (Leusbrock, 2011). Another option would be to explore the use of a second EFC step for the crystallisation of salts or to combine an EFC step with a demineralisation step. For proper reuse it is important that pure salts can be extracted from the mother liquid rather than a mixture of salts. To realize, the EFC system could be seeded, for example with a citrate salt. Most crystalline materials exhibit a metastable behaviour; i.e. if the supersaturation is mild and no crystals are present it will take long before crystallization occurs. By seeding the crystallization of one compound could be realized while maintaining the other compounds in the solution. More research is needed into the crystallization of pure salts, the interaction of the different minerals on the crystallization process and how their eutectic points are affected.

Lactose and minerals can be recovered by EFC while at the same time pure water is produced in the form of ice. Water footprint of companies has become more and more important. With evaporation processes, water is usually not recovered since it is often polluted with (organic) impurities. Whereas with EFC, ice can be melted producing pure water. It gives EFC a significant advantage compared to evaporation. In chapters 2 and 5 it was shown that high-purity ice can be obtained. Further research is needed to know whether this high purity can be maintained for the full operation time and how it will be affected at different salt concentrations. Furthermore, for an in-depth comparison between EFC and other separation technologies, water usage should be considered.

In industry, heat reuse between different processes or production plants is very common, reducing the total heat input. However, in most industries there is no excess cold, making integration of EFC in a production line less easy. A major source of cold is the degasification of liquefied natural gas (LNG),

about 860 kJ/kg of heat needs to be added to degasify LNG (Khor et al., 2018). In conventional LNG regasification, direct heat exchange takes place between the LNG and seawater or other heat sources, which means cold energy is lost (Khor et al., 2018). If an EFC plant can operate close to the degassing plant, the cold demand can be significantly reduced, giving EFC a potentially significant advantage. More investigation is needed on the integration of different systems with EFC.

Although there is a need for further optimization of the Eutectic Freeze Crystallization of lactose, this thesis shows that EFC systems are, based on energy and yield, a viable alternative for the industrial process.

Nomenclature

c_p	Specific heat, 4.18 kJ/kgK
H_{ice}	Latent heat of ice, 334 kJ/kg
$H_{lactose}$	Latent heat of lactose monohydrate, 55 kJ/kg
H_{vapor}	Latent heat of water vapor, 2256 kJ/kg
FR	Feed ratio, -
$m_{crystallizer}$	Mass of the solution in the crystallizer, kg
m_{feed}	Mass of the solution in the feed, kg
m_{ice}	Mass of ice, kg
$m_{lactose\|aq,RM}$	Mass of dissolved lactose in the bleed, kg
$m_{lactose\|aq,crystallizer}$	Mass of dissolved lactose in the crystallizer, kg
$m_{lactose\|aq,feed}$	Mass of dissolved lactose in the feed, kg
$m_{lactose\|solid}$	Mass of lactose monohydrate crystals, kg
m_{RM}	Mass of the remaining mother liquid, kg

m_{vapor}	Mass of vapor, kg
m_{total}	Total mass of the solution, kg
Q_{latent}	Latent heat production/requirement from lactose, vapor and ice, kJ
$Q_{sensible}$	Sensible heat requirement/removal, kJ
Q_{total}	Total heat requirement/removal, kJ
$w_{x,crystallizer}$	Concentration of different minerals in the crystallizer, kg/kg solution
$w_{x,feed}$	Concentration of different minerals in the feed, kg/kg solution
$w_{x,ML\ dlp}$	Concentration of different minerals of depleted delactosed whey permeate, kg/kg solution
$w_{x,RM}$	Concentration of different minerals in the remaining mother liquid kg/kg solution
$Yield$	Yield of lactose recovery, %
ΔT	Temperature difference of the heated solution, K

6.A Appendix: Mass and energy calculations

EFC

An overview of all mass and energy balances of a continuous EFC process is given below.

Mass analysis

As described in section 6.3 the yield is dependent on how much mass can be added to the system with respect to the bleed stream that is used to remove the minerals. Although the exact maximum level of mineral content is not exactly known. However, in our previous study it was proven that lactose could be recovered from depleted whey permeate, e.g. the mother liquid from the lactose crystallization process called delactosed whey permeate (DLP)(Halfwerk et al., 2023b). It was found in this study that crystallization of lactose was possible at high mineral content. Therefore, it is assumed that crystallization can at least be ran until it reaches the mineral content after crystallization of lactose from DLP. To maximize the yield it is proposed to operate the system as a continuous EFC process until the mineral content reaches a certain threshold. Following, the temperature is raised above the freeze point and the system is further operated batch wise, recovering lactose from the mother liquid.

Continuous mode

The amount of mass that can be added to the system before the mineral content reaches the mineral content of DLP, see Table 6-2, after crystallization of lactose was defined as:

$$m_{feed} = FR \cdot m_{crystallizer} \qquad 6.A\text{-}1$$

With FR the feed ratio to be determined, m the masses of feed and crystallizer. It is assumed that at time zero the mother liquid in the crystallizer has the composition of concentrated whey permeate of 30 wt.% lactose, the feed solution has a concentration of 20wt.% lactose. If only lactose crystallizes and there are no losses, the mineral content after the EFC process can be determined with:

$$w_{x,crystallizer}(t) = FR \cdot w_{x,feed} + w_{x,crystallizer}(t = 0) \qquad 6.A\text{-}2$$

With w_x the concentration of different minerals x in the feed and crystallizer in kg/kg solution. After the continuous EFC process the liquid reaches a concentration of 30 wt.% which can then be treated in the batch modus. With EFC the feed is fully converted, the mass of lactose crystals produced can be determined with:

$$m_{lactose|\text{solid}} = m_{feed} \cdot w_{lactose,feed} \qquad 6.A\text{-}3$$

With $m_{lactose|\text{solid}}$ the mass of lactose monohydrate crystals, $w_{lactose,feed}$ the concentration of lactose of the feed in kg/kg solution

Batch mode

After the continuous process it is proposed to increase the temperature just above the freeze point, so no ice will form but only lactose crystallizes. A final lactose concentration of 11.5 wt.% is assumed as found in section 4.2.1, see Table 6-2. While the lactose crystallizes the amount of mother liquid in the crystallizer decreases:

$$m_{ML}(t) = m_{crystallizer}(t=0) * (1 - w_{lactose,crystallizer}(t=0) + w_{lactose,crystallizer}(t)) \quad 6.A\text{-}4$$

The decrease in amount of mother liquid affects the mineral concentration and thus the mineral content in the remaining mother liquor. As described in section 2.2 it is assumed that the weight fraction of minerals in the final mother liquor equals the concentration in depleted DLP:

$$w_{x,RM} = w_{x,ML\ dlp}$$
$$w_{x,RM} = \frac{m_{feed} \cdot w_{x,feed} + m_{crystallizer} \cdot w_{x,crystallizer}}{m_{ML}} \quad 6.A\text{-}5$$

Equation A-5 is numerically solved by changing the value of the feed ratio (X). The amount of lactose that is lost in the bleed stream and that is recovered by the batch process can be calculated as:

$$m_{lactose|aq,RM} = m_{ML}(t) \cdot w_{lactose,RM}(t) \quad 6.A\text{-}6$$

$$m_{lactose|solid} = \left(m_{crystallizer}(t=0) \cdot w_{lactose,crystallizer}(t=0) - m_{lactose,RM}\right) \cdot \frac{M_{lactose.H_2O}}{M_{lactose}} \quad 6.A\text{-}7$$

The yield becomes:

$$Yield = \frac{m_{lactose|aq,feed} + m_{lactose|aq,crystallizer} - m_{lactose|aq,RM}}{m_{lactose|aq,feed} + m_{lactose|aq,crystallizer}} * 100\% \quad 6.A\text{-}8$$

Energy analysis

The energy removal/addition from a crystallization process is a combination of heating/cooling the feed and the latent heat of lactose and ice:

$$Q_{total} = Q_{sensible} + Q_{latent} \qquad 6.A\text{-}9$$

The sensible heat can be calculated from the enthalpy difference:

$$Q_{sensible} = m_{total} \cdot c_p \cdot \Delta T \qquad 6.A\text{-}10$$

With m the mass of the solution, c_p the specific heat, the value of water is used (4.18kJ/kg) and ΔT temperature difference of the cooled solution(K). The latent heat can be determined from the amount of water converted into ice and the heat of fusion:

$$Q_{latent} = H_{latent,ice} \cdot m_{ice} + H_{latent,lactose} \cdot m_{lactose.H_2O} \qquad 6.A\text{-}11$$

With H the heat of fusion (kJ/kg).

The ice can be used for precooling the feed from 20°C to 5°C:

$$Q_{precooling} = m_{total} \cdot c_p \cdot \Delta T \qquad 6.A\text{-}12$$

Heat is removed by a chiller, with electricity consumption:

$$E = \frac{Q_{total}}{COP} \qquad 6.A\text{-}13$$

E is the electrical energy usage of the chiller, the coefficient of performance (COP) and Q_{total} the total heat transport that is required.

Evaporation

Mass analysis

Lactose is usually recovered via a batch-wise slow cooling process, before the crystallization step, a concentration step is applied using evaporation. The amount of water converted into vapor and the amount of mother liquid after the evaporation step can be calculated with:

$$m_{ML} = m_{total} \cdot \frac{w_{lactose,feed}}{w_{lactose,after\ evaporation}} \qquad 6.A\text{-}14$$

$$m_{vapor} = m_{total} - m_{mother\ liquid} \qquad 6.A\text{-}15$$

During the crystallization, mass of water is taken up as hydrate, thus reducing the amount of water in the mother liquid. Therefor three mass balance were made for the total mass during slow cooling and the amount of lactose and water in the mother liquid:

$$m_{slow\ cooling} = m_{ML} + m_{lactose|\text{solid}} \qquad 6.A\text{-}16$$

$$m_{lactose|\text{aq},crystallizer} = m_{ML} \cdot w_{lactose,after\ evaporation} - m_{lactose|\text{solid}} \cdot \frac{M_{lactose}}{M_{lactose_{H2O}}} \qquad 6.A\text{-}17$$

$$m_{water} = m_{ML} \cdot \left(1 - w_{lactose,after\ evaporation}\right) - m_{lactose|\text{solid}} \cdot \frac{M_{H_2O}}{M_{Lactose.H2O}} \qquad 6.A\text{-}18$$

Based on the start concentration before crystallization and the final solubility equation A-14 tot A-16 is solved for the amount of lactose.H_2O crystallized. Next, the yield can be determined from:

$$yield = \frac{m_{lactose|\text{solid}}(t) \cdot \frac{M_{lactose}}{M_{lactose_{H2O}}}}{m_{total} \cdot w_{lactose,feed}} \qquad 6.A\text{-}19$$

Energy analysis

Similar to the EFC process, the energy consumption of an evaporation process is a combination of sensible and latent heat, equation A-1 and A-2 are valid. Where water is converted into ice for EFC with evaporation, water needs to be converted into vapor:

$$Q_{latent} = H_{vapor} \cdot m_{vapor} + H_{lactose} \cdot m_{lactose|\text{solid}} \qquad 6.A\text{-}20$$

Prior to the evaporation step the feed needs to be preheated to around 75°C:

$$Q_{preheating} = m_{total} \cdot c_p \cdot \Delta T \qquad 6.A\text{-}21$$

A multi-effect evaporation or mechanical vapor recompression system is usually used to concentrate whey permeate. An estimation of the energy consumption of multiple effect evaporation process can be expressed as the amount of steam required for evaporating 1 kg of water (Bylund, 2015):

$$Q_{steam} \approx \frac{H_{latent,vapor} \cdot m_{vapor}}{n} \qquad 6.A\text{-}22$$

With Q_{steam} the energy of steam in kJ per kg of water evaporated and n a limit number of stages. For example, a 3-effect evaporation process requires 0.33 kg of steam to evaporate 1 kg of water. Thus, the total heat requirement for a multi-effect evaporation process becomes

$$Q_{\text{multi effect}} = \text{Q}_{\text{steam}} + Q_{sensible} \qquad 6.A\text{-}23$$

Or

$$Q_{\text{multi effect}} = H_{steam} \cdot m_{steam} + Q_{sensible}$$

With H_{steam} the enthalpy of saturated steam at 140°C, 4 bar.

Mechanical vapor recompression uses compression/mechanical work to increase the temperature of the vapor; similar to EFC it uses electricity as an energy source. For 1 joule of electricity 20J of evaporation can be achieved (Heldman, D.R., 2019).

Table 6A-6 Overview of mass and energy flow of an evaporation process per kg whey permeate (WP) and lactose

Mass					
Start amount	1				kg
Start Concentration	20				wt.%
Conc. after evaporation	55				wt.%
Conc. after crystallization	18				wt.%
Water removed	0.64				kg
α-lactose.H2O produced	0.17				kg
Yield	83.0				%
Energy	3 step	5 step	MVR	MVR without preheating	
Steam required	0,21	0,13	-	-	kg
Sensible heat	272	272	272	0	kJ
Preheating	-230	-230	-230	0	kJ/kg WP
Energy evaporation	582	349	72	72	kJ/kg WP
Total required	624	391	114	72	kJ/kg WP
Total required	3571	2238	651	412	kJ/kg lactose

Nomenclature

c_p	Specific heat, 4.18 kJ/kgK
COP	Coefficient of performance, efficiency of the chiller, -
E	Energy consumption chiller, kJ
FR	Feed ratio, -
H_{ice}	Latent heat of ice, 334 kJ/kg
$H_{lactose}$	Latent heat of lactose monohydrate, 55 kJ/kg
H_{vapor}	Latent heat of vapor, 2256 kJ/kg
m_{bleed}	Mass of the bleed solution, kg
$m_{crystallizer}$	Mass of the solution in the crystallizer, kg
m_{feed}	Mass of the solution in the feed, kg
$m_{lactose\|aq,bleed}$	Mass of dissolved lactose in the bleed, kg
$m_{lactose\|aq,crystallizer}$	Mass of dissolved lactose in the crystallizer, kg
$m_{lactose\|aq,feed}$	Mass of dissolved lactose in the feed, kg
$m_{lactose\|solid}$	Mass of lactose monohydrate crystals, kg
m_{ML}	Mass of mother liquid, kg
$M_{lactose}$	Molecular mass of lactose, 342.3 g/mol
$M_{lactose.H_2O}$	Molecular mass of lactose monohydrate, 360.31 g/mol
$m_{slow\ cooling}$	Total mass during slow cooling, kg
m_{total}	Total mass of the solution, kg
m_{vapor}	Mass of vapor, kg
m_{water}	Mass of water in the mother liquid, kg
n	Number of effect for multi effect evaporation, -

Q_{latent}	Latent heat production/requirement from lactose, vapor and ice, kJ
$Q_{\text{multi effect}}$	Energy requirement multi-effect evaporation, kJ
$Q_{sensible}$	Sensible heat requirement/removal, kJ
Q_{steam}	Energy of steam, kJ
Q_{total}	Total heat requirement/removal, kJ
$w_{x,bleed}$	Concentration of different minerals in the bleed stream, kg/kg solution
$w_{x,crystallizer}$	Concentration of different minerals in the crystallizer, kg/kg solution
$w_{x,feed}$	Concentration of different minerals in the feed, kg/kg solution
$w_{x,ML\ dlp}$	Concentrations of different minerals of depleted delactosed whey permeate kg/kg solution
$w_{lactose,after\ evaporation}$	Concentration of lactose after the evaporator, kg/kg solution
$w_{lactose,feed}$	Concentration of lactose in the feed, kg/kg solution
$w_{lactose,crystallizer}$	Concentration of lactose in the crystallizer, kg/kg solution
$Yield$	Yield of lactose recovery, %
ΔT	Temperature difference of the heated solution, K

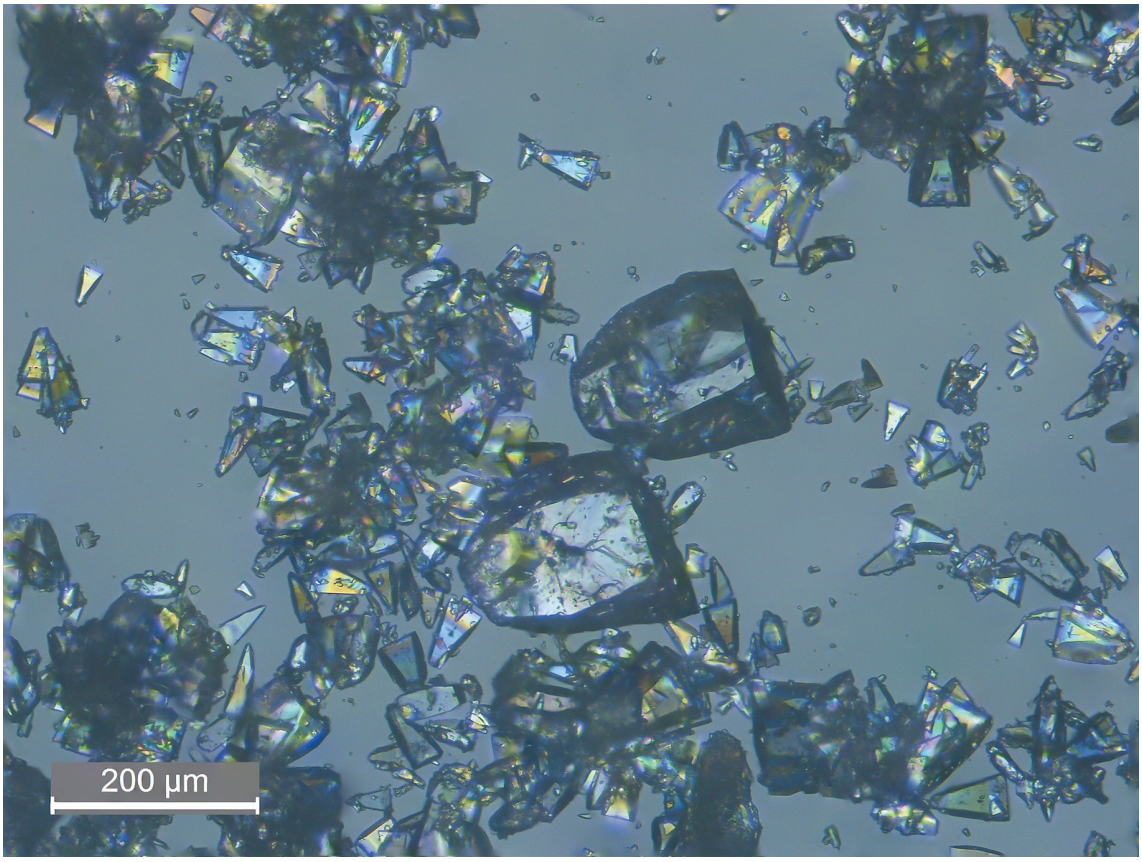

*Lactose crystals grown from an undefined seed

Bibliography

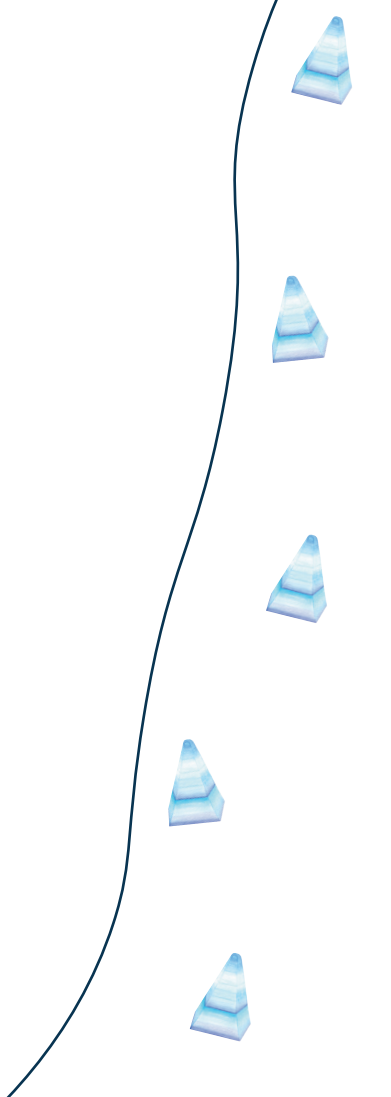

Adhikari, B.M., Truong, T., Bansal, N., Bhandari, B., 2018. Influence of gas addition on crystallisation behaviour of lactose from supersaturated solution. Food Bioprod. Process. 109, 86–97. https://doi.org/10.1016/j.fbp.2018.03.003

Agrawal, S., Paterson, A. (Tony), McLeod, J., Jones, J., Bronlund, J., 2015. Mathematical modelling and analysis of an industrial scale evaporative crystallizer producing lactose monohydrate. J. Food Eng. 154, 49–57. https://doi.org/10.1016/j.jfoodeng.2014.12.025

Alexander, L.D., Stout, M.A., Drake, M., Beckman, S.L., Metzger, L., 2016. Membrane fractionation of delactosed permeate to enhance salty taste. J. Anim. Sci. 94, 248. https://doi.org/10.2527/jam2016-0518

Baehr, H.D., Stephan, K., 2011. Heat and mass transfer. https://doi.org/10.1007/978-3-642-20021-2 LK

Berg, H.E., 1993. Reactions of lactose during heat treatment of milk : a quantitative study. Wageningen University.

Burton, W.K., Cabrera, N., Frank, F.C., 1951. The Growth of Crystals and the Equilibrium Structure of their Surfaces. Philos. Trans. R. Soc. London. Ser. A, Math. Phys. Sci. 243, 299–358.

Bylund, G., 2015. Dairy Processing Handbook. (Tetra Pak International S.A.).

Cloidt, R., Lehmann, H., 2006. Process for the preparation of lactose from whey.

Dilworth, S.E., Buckton, G., Gaisford, S., Ramos, R., 2004. Approaches to determine the enthalpy of crystallisation, and amorphous content, of lactose from isothermal calorimetric data. Int. J. Pharm. 284, 83–94. https://doi.org/10.1016/j.ijpharm.2004.07.016

Dincer, T.D., Ogden, M.I., Parkinson, G.M., 2014a. Investigation of growth rate dispersion in lactose crystallisation by AFM. J. Cryst. Growth 402, 215–221. https://doi.org/10.1016/j.jcrysgro.2014.06.027

Dincer, T.D., Ogden, M.I., Parkinson, G.M., 2009. In situ investigation of growth rates and growth rate dispersion of α-lactose monohydrate crystals. J. Cryst. Growth 311, 1352–1358. https://doi.org/10.1016/j.jcrysgro.2009.01.016

Dincer, T.D., Zisu, B., Vallet, C.G.M.R., Jayasena, V., Palmer, M., Weeks, M., 2014b. Sonocrystallisation of lactose in an aqueous system. Int. Dairy J. 35, 43–48. https://doi.org/10.1016/j.idairyj.2013.10.001

Durham, R.J., 2009. Modern approaches to lactose production, in: Woodhead Publishing Series in Food Science, Technology and Nutrition. pp. 103–144. https://doi.org/10.1533/9781845697198.1.103

Fernández-Torres, M.J., Randall, D.G., Melamu, R., von Blottnitz, H., 2012. A comparative life cycle assessment of eutectic freeze crystallisation and evaporative crystallisation for the treatment of saline wastewater. Desalination 306, 17–23. https://doi.org/10.1016/j.desal.2012.08.022

Gänzle, M.G., 2011. Lactose and Oligosaccharides | Lactose: Derivatives, in: Fuquay, J.W.B.T.-E. of D.S. (Second E. (Ed.), . Academic Press, San Diego, pp. 202–208. https://doi.org/10.1016/B978-0-12-374407-4.00275-2

Genceli, F.E., Gärtner, R., Witkamp, G.J., 2005. Eutectic freeze crystallization in a 2nd generation cooled disk column crystallizer for MgSO4·H2O system. J. Cryst. Growth 275, e1369–e1372. https://doi.org/10.1016/j.jcrysgro.2004.11.172

Gernigon, G., Baillon, F., Espitalier, F., Le Floch-Fouéré, C., Schuck, P., Jeantet, R., 2013. Effects of the addition of various minerals, proteins and salts of organic acids on the principal steps of α-lactose monohydrate crystallisation. Int. Dairy J. 30, 88–95. https://doi.org/10.1016/j.idairyj.2012.12.005

Haase, G., Nickerson, T.A., 1966a. Kinetic reactions of Alpha and Beta Lactose. I. Mutarotation1. J. Dairy Sci. 49, 127–132. https://doi.org/10.3168/jds.S0022-0302(66)87811-6

Haase, G., Nickerson, T.A., 1966b. Kinetic Reactions of Alpha and Beta Lactose. II. Crystallization1. J. Dairy Sci. 49, 757–761. https://doi.org/10.3168/jds.S0022-0302(66)87941-9

Halfwerk, R., Yntema, D., Van Spronsen, J., Keesman, K., Van der Padt, A., 2023a. Crystallization kinetics of lactose recovered at sub-zero temperatures: A population balance model combining mutarotation, nucleation and crystal growth. J. Food Eng. 111412. https://doi.org/doi.org/10.1016/j.jfoodeng.2023.111412

Halfwerk, R., Yntema, D., Van Spronsen, J., Van der Padt, A., 2023b. Recovery of lactose from delactosed whey permeate by a low-temperature crystallization process. J. Dairy Sci. Accepted.

Halfwerk, R., Yntema, D., Van Spronsen, J., Van der Padt, A., 2021. A sub-zero crystallization process for the recovery of lactose. J. Food Eng. 308, 110677. https://doi.org/10.1016/j.jfoodeng.2021.110677

Hargreaves, J., 1995. Characterisation of lactose in the liquid and solid state using nuclear magnetic resonance and other methods. Massey University.

Hartel, R.W., 2019. Crystallization in Foods, in: Lee, A.Y., Myerson, A.S., Erdemir, D. (Eds.), Handbook of Industrial Crystallization. Cambridge University Press, Cambridge, pp. 460–478. https://doi.org/DOI: 10.1017/9781139026949.015

Hartel, R.W., Shastry, A. V, 1991. Sugar crystallization in food products. Crit. Rev. Food Sci. Nutr. 30, 49–112. https://doi.org/10.1080/10408399109527541

Heldman, D.R., L., 2019. Handbook of Food Engineering (3rd ed.). https://doi.org/10.1201/9780429449734

Herrington, B.L., 1934. Some physico-Chemical properties of lactose: I. The spontaneous crystallization of supersaturated solutions of lactose. J. Dairy Sci. 17, 501–518. https://doi.org/10.3168/jds.S0022-0302(34)93265-3
Himawan, C., 2005. Characterization and Population Balance Modelling of Eutectic Freeze Crystallization. Delft University of Technology.
Hudson, C.S., 1908. Further studies on the forms of milk-sugar. J. Am. Chem. Soc. 30, 1767–1783. https://doi.org/10.1021/ja01953a015
Hunziker, O.F., Nissen, B.H., 1926. Lactose solubility and lactose Crystal Formation: I. lactose solubility. J. Dairy Sci. 9, 517–537. https://doi.org/10.3168/jds.S0022-0302(26)93924-6
Jennes, R.; Koops, J., 1962. Preparation and properties of a salt solution which simulates milk ultratrate. Netherlands Milk Dairy J. 16, 153–164.
Karpinski, P.H., Wey, J.S., 2002. 6 - Precipitation processes, in: Myerson, A.S.B.T.-H. of I.C. (Second E. (Ed.), . Butterworth-Heinemann, Woburn, pp. 141–160. https://doi.org/10.1016/B978-075067012-8/50008-2
Keesman, K.J., 2011. System identification : an introduction.
Khor, J.O., Dal Magro, F., Gundersen, T., Sze, J.Y., Romagnoli, A., 2018. Recovery of cold energy from liquefied natural gas regasification: Applications beyond power cycles. Energy Convers. Manag. 174, 336–355. https://doi.org/10.1016/j.enconman.2018.08.028
Lee, A.Y., Erdemir, D., Myerson, A.S., 2019. Crystals and Crystal Growth, in: Lee, A.Y., Myerson, A.S., Erdemir, D. (Eds.), Handbook of Industrial Crystallization. Cambridge University Press, Cambridge, pp. 32–75. https://doi.org/10.1017/9781139026949.002
Leusbrock, I., 2011. Removal of inorganic compounds via supercritical water: fundamentals and applications. Rijksuniversiteit Groningen.
Lewis, A.E., Nathoo, J., Thomsen, K., Kramer, H.J., Witkamp, G.J., Reddy, S.T., Randall, D.G., 2010. Design of a eutectic freeze crystallization process for multicomponent waste water stream. Chem. Eng. Res. Des. 88, 1290–1296. https://doi.org/10.1016/j.cherd.2010.01.023
Liang, B., Bund, R.K., Hartel, R.W., 2009. Effect of composition on moisture sorption of delactosed permeate. Int. Dairy J. 19, 630–636. https://doi.org/10.1016/j.idairyj.2009.04.010
Liang, B., Shi, Y., Hartel, R.W., 1991. Growth Rate Dispersion Effects on Lactose Crystal Size Distributions from a Continuous Cooling Crystallizer. J. Food Sci. TA - TT - 56, 848–854. https://doi.org/10.1111/j.1365-2621.1991.tb05397.x
Liang, B.M., Hartel, R.W., Berglund, K.A., 1987. Contact nucleation in sucrose crystallization. Chem. Eng. Sci. 42, 2723–2727. https://doi.org/10.1016/0009-2509(87)87022-7

Lifran, E. V, Vu, T.T.L., Durham, R.J., Hourigan, J.A., Sleigh, R.W., 2007. Crystallisation kinetics of lactose in the presence of lactose phosphate. Powder Technol. 179, 43–54. https://doi.org/10.1016/j.powtec.2006.11.010

Livney, Y.D., Donhowe, D.P., Hartel, R.W., 1995. Influence of temperature on crystallization of lactose in ice-cream. Int. J. Food Sci. Technol. 30, 311–320. https://doi.org/10.1111/j.1365-2621.1995.tb01380.x

MacFhionnghaile, P., Svoboda, V., McGinty, J., Nordon, A., Sefcik, J., 2017. Crystallization Diagram for Antisolvent Crystallization of Lactose: Using Design of Experiments To Investigate Continuous Mixing-Induced Supersaturation. Cryst. Growth Des. 17, 2611–2621. https://doi.org/10.1021/acs.cgd.7b00136

McSweeney, P.L.H., Fox, P.F., 2009. Advanced dairy chemistry. Volume 3. Lactose, water, salts and minor constituents.

Meenan, P.A., Anderson, S.R., Klug, D.L., 2002. 3 - The influence of impurities and solvents on crystallization, in: Myerson, A.S.B.T.-H. of I.C. (Second E. (Ed.), . Butterworth-Heinemann, Woburn, pp. 67–100. https://doi.org/10.1016/B978-075067012-8/50005-7

Mimouni, A., Schuck, P., Bouhallab, S., 2009. Isothermal batch crystallization of alpha-lactose: a kinetic model combining mutarotation, nucleation and growth steps. Int. Dairy J. 19, 129–136. https://doi.org/10.1016/j.idairyj.2008.09.006

Nickerson, T.A., 1956. Lactose Crystallization in Ice Cream. II. Factors affecting Rate and Quantity. J. Dairy Sci. 39, 1342–1350. https://doi.org/10.3168/jds.S0022-0302(56)94858-5

Nickerson, T.A., 1954. Lactose Crystallization in Ice Cream. I. Control of Crystal Size by Seeding. J. Dairy Sci. 37, 1099–1105. https://doi.org/10.3168/jds.S0022-0302(54)91373-9

Nie, X.-Y., Sun, S.-Y., Sun, Z., Song, X., Yu, J.-G., 2017. Ion-fractionation of lithium ions from magnesium ions by electrodialysis using monovalent selective ion-exchange membranes. Desalination 403, 128–135. https://doi.org/10.1016/j.desal.2016.05.010

Oliveira, D., Puri, R., Fenelon, M.A., O'Mahony, J.A., 2019. Delactosed permeate as a dairy processing co-product with major potential value: a review. Int. J. Food Sci. Technol. 54, 999–1008. https://doi.org/10.1111/ijfs.14064

Parimaladevi, P., Srinivasan, K., 2014. Influence of supersaturation level on the morphology of α-lactose monohydrate crystals. Int. Dairy J. 39, 301–311. https://doi.org/10.1016/j.idairyj.2014.08.007

Paterson, A., 2009. Production and Uses of Lactose, in: Advanced Dairy Chemistry. pp. 105–120. https://doi.org/10.1007/978-0-387-84865-5_4

Paterson, A.H.J., 2017. Lactose processing: From fundamental understanding

to industrial application. Int. Dairy J. 67, 80–90. https://doi.org/10.1016/j.idairyj.2016.07.018

Patil, G.K., Patil, P.B., Pardeshi, S.R., Rajput, R.L., Sonawane, S.H., Mujumdar, A., Naik, J.B., 2020. Effect of process parameters on the recovery of lactose in an antisolvent acetone/acetone-ethanol mixture: A comparative study based on sonication medium. Ultrason. Sonochem. 67, 105128. https://doi.org/10.1016/j.ultsonch.2020.105128

Qamar, S., Elsner, M.P., Angelov, I.A., Warnecke, G., Seidel-Morgenstern, A., 2006. A comparative study of high resolution schemes for solving population balances in crystallization. Comput. Chem. Eng. 30, 1119–1131. https://doi.org/10.1016/j.compchemeng.2006.02.012

Raghavan, S.L., Ristic, R.I., Sheen, D.B., Sherwood, J.N., Trowbridge, L., York, P., 2000. Morphology of Crystals of α-Lactose Hydrate Grown from Aqueous Solution. J. Phys. Chem. B 104, 12256–12262. https://doi.org/10.1021/jp002051o

Randall, D.G., Nathoo, J., 2018. Resource recovery by freezing: A thermodynamic comparison between a reverse osmosis brine, seawater and stored urine. J. Water Process Eng. 26, 242–249. https://doi.org/10.1016/j.jwpe.2018.10.020

Randall, D.G., Nathoo, J., 2015. A succinct review of the treatment of Reverse Osmosis brines using Freeze Crystallization. J. Water Process Eng. 8, 186–194. https://doi.org/10.1016/j.jwpe.2015.10.005

Randall, D.G., Nathoo, J., Lewis, A.E., 2011. A case study for treating a reverse osmosis brine using Eutectic Freeze Crystallization—Approaching a zero waste process. Desalination 266, 256–262. https://doi.org/10.1016/j.desal.2010.08.034

Rodriguez Pascual, M., Genceli, F.E., Trambitas, D.O., Evers, H., Van Spronsen, J., Witkamp, G.J., 2010. A novel scraped cooled wall crystallizer: Recovery of sodium carbonate and ice from an industrial aqueous solution by eutectic freeze crystallization. Chem. Eng. Res. Des. 88, 1252–1258. https://doi.org/10.1016/j.cherd.2009.07.015

Roetman, K., Buma, T.J., 1974. Temperature dependence of the equilibrium beta/alpha ratio of lactose in aqueous solution. Netherlands Milk Dairy J. 28.

Sánchez, J., Hernández, E., Auleda, J.M., Raventós, M., 2011. Review: Freeze Concentration Technology Applied to Dairy Products. Food Sci. Technol. Int. 17, 5–13. https://doi.org/10.1177/1082013210382479

Shi, Y., Hartel, R.W., Liang, B., 1989. Formation and Growth Phenomena of Lactose Nuclei Under Contact Nucleation Conditions. J. Dairy Sci. 72, 2906–2915. https://doi.org/10.3168/jds.S0022-0302(89)79441-8

Shi, Y., Liang, B., Hartek, R.W., 1990. Crystallization kinetics of alpha-Lactose Monohydrate in a Continuous Cooling Crystallizer TT -. J. Food

Sci. TA - 55, 817–820.
Spronsen, J. van, 2017. Patent: Recovery of Lactose from an Aqueous Solution (NL2016952B1) Octrooicentrum Nederland.
Stepakoff, G.L., Siegelman, D., Johnson, R., Gibson, W., 1974. Development of a eutectic freezing process for brine disposal. Desalination 15, 25–38. https://doi.org/10.1016/S0011-9164(00)82061-5
Vaessen, R.J.C. (TU D., 2003. Development of scraped eutectic crystallizers. Delft University of Technology.
Vaessen, R.J.C., Seckler, M.M., Witkamp, G.J., 2004. Heat transfer in scraped eutectic crystallizers. Int. J. Heat Mass Transf. 47, 717–728. https://doi.org/10.1016/j.ijheatmasstransfer.2003.07.028
van der Ham, F., Seckler, M.M., Witkamp, G.J., 2004. Eutectic freeze crystallization in a new apparatus: the cooled disk column crystallizer. Chem. Eng. Process. Process Intensif. 43, 161–167. https://doi.org/10.1016/S0255-2701(03)00018-7
van der Ham, F., Witkamp, G.J., de Graauw, J., van Rosmalen, G.M., 1999. Eutectic freeze crystallization simultaneous formation and separation of two solid phases. J. Cryst. Growth 198–199, 744–748. https://doi.org/10.1016/S0022-0248(98)01003-3
van der Ham, F., Witkamp, G.J., de Graauw, J., van Rosmalen, G.M., 1998. Eutectic freeze crystallization: Application to process streams and waste water purification. Chem. Eng. Process. Process Intensif. 37, 207–213. https://doi.org/10.1016/S0255-2701(97)00055-X
Van Spronsen, J., Pascual, M.R., Genceli, F.E., Trambitas, D.O., Evers, H., Witkamp, G.J., 2010. Eutectic freeze crystallization from the ternary Na2CO3–NaHCO3–H2O system: A novel scraped wall crystallizer for the recovery of soda from an industrial aqueous stream. Chem. Eng. Res. Des. 88, 1259–1263. https://doi.org/10.1016/j.cherd.2009.09.012
Visser, R.A., 1983. Crystal Growth kinetics of Alpha-Lactose hydrate. Thesis University of Nijmegen.
Visser, R.A., 1982. Supersaturation of alpha-lactose in aqueous solutions in mutarotation equilibrium. Netherlands Milk Dairy J. 36.
Vu, L.T.T., Durham, R.J., Hourigan, J.A., Sleigh, R.W., 2005. Dynamic modelling and simulation of lactose cooling crystallisation: from batch and semi-batch to continuous operations, in: European Symposium on Computer-Aided Process Engineering. pp. 493–498. https://doi.org/10.1016/S1570-7946(05)80204-4
Vu, T.T.L., Durham, R.J., Hourigan, J.A., Sleigh, R.W., 2006. Dynamic modelling optimisation and control of lactose crystallisations: Comparison of process alternatives. Sep. Purif. Technol. 48, 159–166. https://doi.org/10.1016/j.seppur.2005.07.015
Vu, T.T.L., Hourigan, J.A., Sleigh, R.W., Ang, M.H., Tade, M.O., 2003.

Metastable control of cooling crystallisation, in: European Symposium on Computer Aided Process Engineering. Elsevier, pp. 527–532. https://doi.org/10.1016/S1570-7946(03)80169-4

Wey, J.S., Karpinski, P.H., 2002. 10 - Batch crystallization, in: Myerson, A.S.B.T.-H. of I.C. (Second E. (Ed.), . Butterworth-Heinemann, Woburn, pp. 231–248. https://doi.org/10.1016/B978-075067012-8/50012-4

Williams, P.M., Ahmad, M., Connolly, B.S., Oatley-Radcliffe, D.L., 2015. Technology for freeze concentration in the desalination industry. Desalination 356, 314–327. https://doi.org/10.1016/j.desal.2014.10.023

Wong, S.Y., Bund, R.K., Connelly, R.K., Hartel, R.W., 2012. Designing a lactose crystallization process based on dynamic metastable limit. J. Food Eng. 111, 642–654. https://doi.org/10.1016/j.jfoodeng.2012.03.003

Wong, S.Y., Bund, R.K., Connelly, R.K., Hartel, R.W., 2011. Determination of the dynamic metastable limit for α-lactose monohydrate crystallization. Int. Dairy J. 21, 839–847. https://doi.org/10.1016/j.idairyj.2011.05.003

Wong, S.Y., Bund, R.K., Connelly, R.K., Hartel, R.W., 2010. Modeling the crystallization Kinetic Rates of Lactose via Artificial Neural Network. Cryst. Growth Des. 10, 2620–2628. https://doi.org/10.1021/cg100122y

Wong, Y.S., Hartel, R.W., 2014. Crystallization in lactose Refining A Review. J. Food Sci. 79, R257–R272. https://doi.org/10.1111/1750-3841.12349

Xun, A., Truong, T., Bhandari, B., 2017. Effect of Carbonation of Supersaturated Lactose Solution on Crystallisation Behaviour of Alpha-Lactose Monohydrate. Food Biophys. 12, 52–59. https://doi.org/10.1007/s11483-016-9462-3

Yuping, S., Liang, B., W. Hartel, R., 2006. Crystal Refining Technologies by Controlled Crystallization.

Zisu, B., Sciberras, M., Jayasena, V., Weeks, M., Palmer, M., Dincer, T.D., 2014. Sonocrystallisation of lactose in concentrated whey. Ultrason. Sonochem. 21, 2117–2121. https://doi.org/10.1016/j.ultsonch.2014.03.031

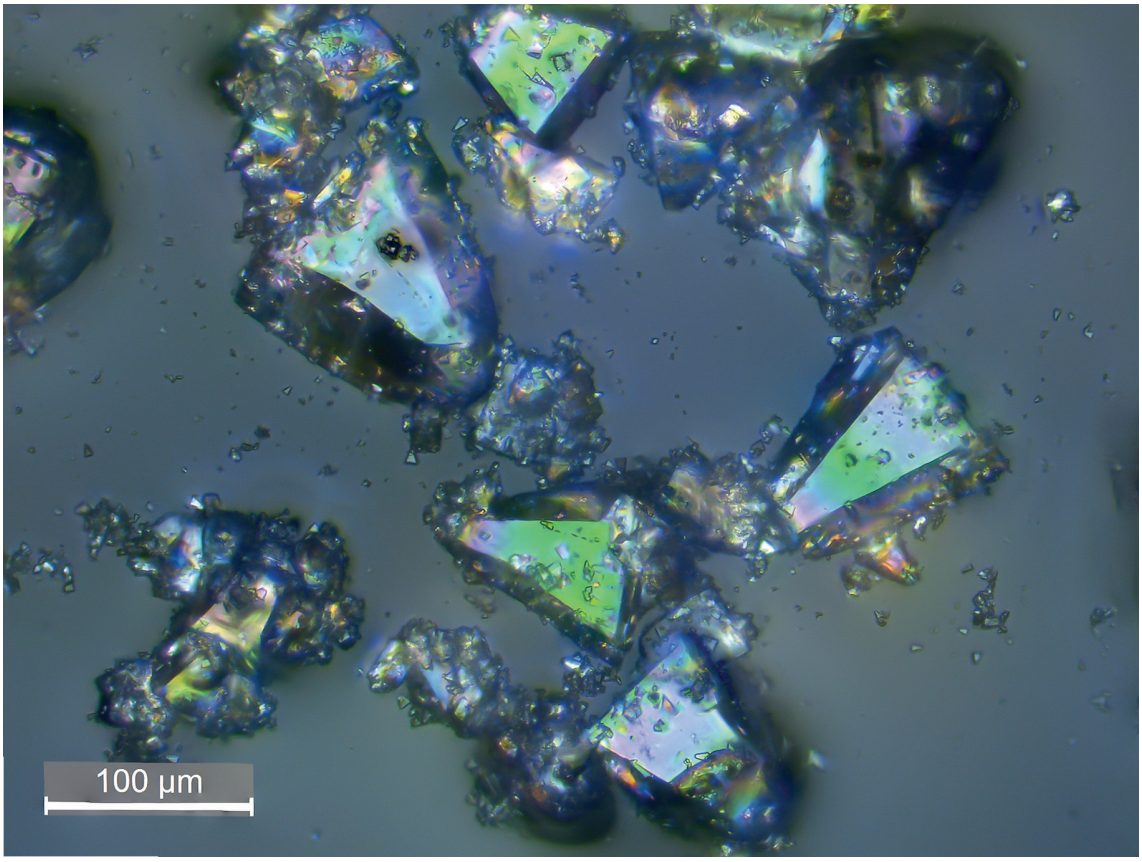

*Lactose crystals grown from an undefined seed

Summary

Samenvatting

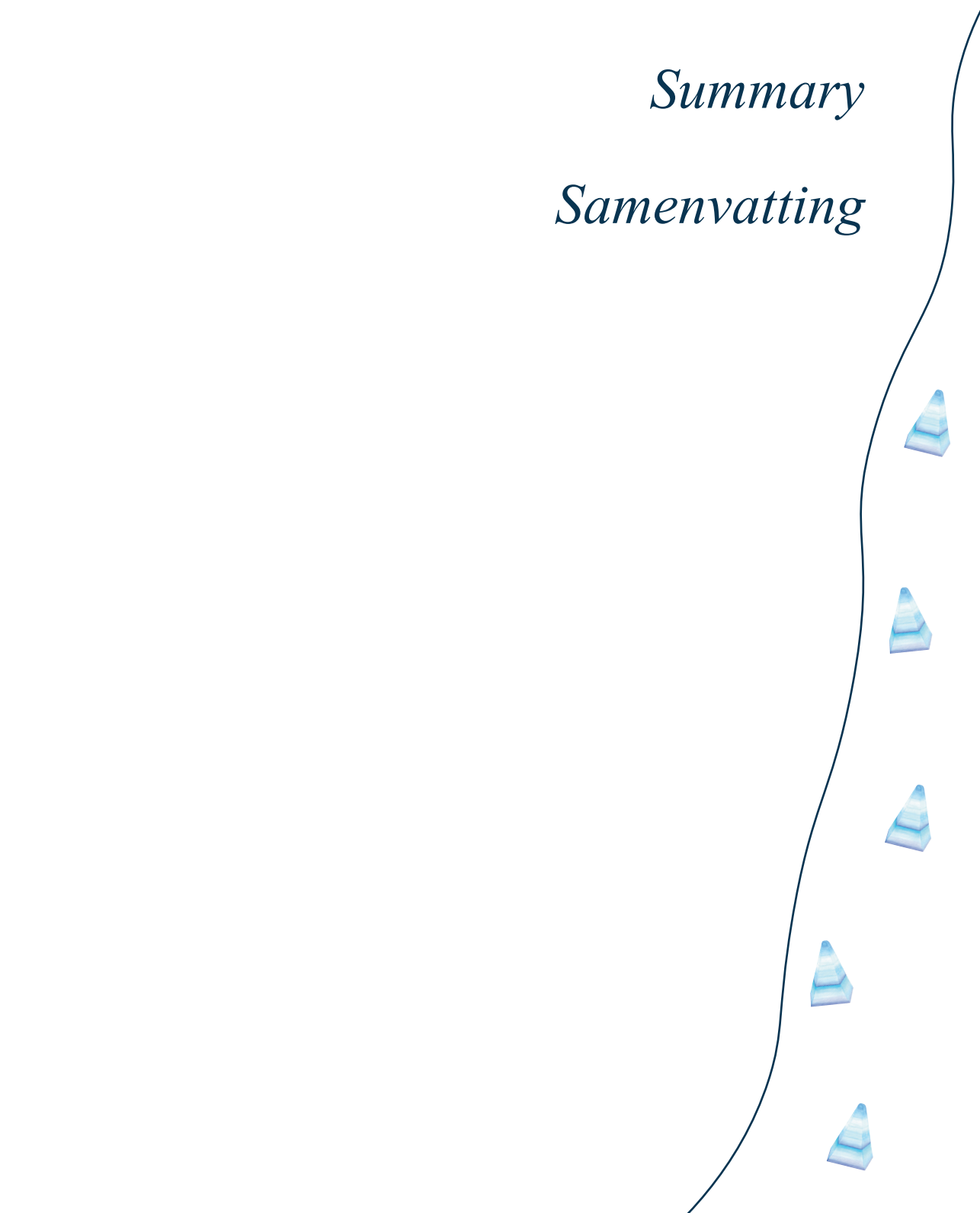

Summary

Today crystallization in the food industry is used for the production of many products, like sugars, ice, lipids and proteins. Lactose is one of the larger streams that is produced by crystallization. Although it is mainly known as a problematic ingredient for people with lactose intolerance, it is used in many everyday products like infant formula and as filler in medicine. The current production process however has some major disadvantages such as a large residual stream produced after crystallization and the use of elevated temperatures during evaporation. This results in a high energy consumption and scaling/precipitation issues on heat exchanger surfaces.

An alternative method is eutectic freeze crystallization where the stream is brought to the eutectic point, which is the concentration and temperature were solvent and solute crystallize simultaneously. By using this point a solution can in theory be fully converted. The advantages are low energy cost, low fouling, low biological activity, and no degradation of heat sensitive compounds. In chapter two of this thesis, the operational regime for EFC of lactose solutions was explored. It was proven that lactose and ice could be crystallized simultaneously, producing tomahawk shaped crystals. Furthermore, it was shown that seeding with crystals had a large influence on the final yield, crystal size and morphology. Although highly supersaturated conditions are present in the sub-zero crystallization of lactose, crystal growth is found to be the predominant process rather than nucleation.

At low temperatures there are two competing effects on the crystallization kinetics. On the one hand, mass transport and the rate of both mutarotation and nucleation are reduced, reducing the crystallization rate. On the other hand, supersaturation is increased, which increases nucleation and crystal growth and thereby increases the crystallization rate. To investigate this, the results of

batch experiments at different conditions were combined with a population balance model combing mutarotation, nucleation and crystal growth. At temperatures below zero it appeared that mutarotation was rate-limiting when the crystallization was fast. The conversion of β-lactose to α-lactose could not keep up with the fast depletion of α-lactose. An empirical model was developed to describe the concentration profile and particle size over time.

EFC is very suitable for residual streams as replacing the current slow-cooling process can be challenging. In chapter four the use of EFC was investigated for the mother liquid after lactose crystallization, delactosed whey permeate. This residual stream still contains 20wt.% lactose but due to the high mineral and water content, high viscosity and stickiness it is currently not economically feasible to further recover this stream and therefore it is usually seen as waste. It was proven that still a significant portion of lactose could be recovered at sub-zero temperatures. Furthermore, precipitation of calcium phosphate was found to be limited in the first 24 hours. Due to a higher mutarotation rate, caused by the minerals present in DLP, the crystallization rate of lactose was increased. After 24 hours a yield of 85% was found , the resulting crystals had tomahawk morphology and an average size of around 30μm.

Batch EFC experiments proofed to be challenging; for EFC continuous removal of ice and lactose is essential. For this purpose, a continuous pilot setup was investigated in Chapter 5. Whey permeate was continuously fed to the crystallizer and ice and lactose was recovered by a centrifuge and belt filter. During two independent runs it was proven that lactose could be recovered by EFC. A conceptual design was proposed where lactose was recovered in a continuous way and energy consumption was reduced by using the latent heat of ice.

The mass and energy balances were further analysed in chapter 6, comparing EFC with the state of the art in industry: mechanical vapor recompression (MVR) evaporation. It was shown that at a comparable yield of 80% EFC is twice as efficient than a slow-cooling crystallization process with MVR. Depending on the location rest heat might be available to preheat the feed to the MVR. This would decrease the energy consumption of MVR, however, compared to EFC it was found to be still 30% higher.

Samenvatting

Kristallisatie wordt in de voedingsindustrie gebruikt voor de productie van veel producten, zoals suikers, ijs, lipiden en proteïnen. Lactose is een van de grotere stromen die wordt geproduceerd door kristallisatie. Hoewel het vooral bekend is als probleemcomponent voor mensen met lactose-intolerantie, wordt het gebruikt in veel alledaagse producten zoals babyvoeding en als vulmiddel in geneesmiddelen. Het huidige productieproces heeft echter enkele nadelen, waaronder een reststroom die achterblijft na de kristallisatie en het gebruik van hoge temperaturen tijdens de verdamping. Dit resulteert in een hoog energieverbruik en schaling/precipitatieproblemen op de warmtewisselaars.

Een alternatieve methode is eutectische vrieskristallisatie , waarbij de stroom naar het eutectische punt wordt gebracht, dat is de concentratie en temperatuur waarbij zowel het oplosmiddel als de opgeloste stof gelijktijdig kristalliseren. Door dit punt te gebruiken kan in theorie een oplossing volledig worden omgezet. Voordelen zijn de lage energiekosten, weinig schaling en precipitatie, lage biologische activiteit en geen afbraak van warmtegevoelige componenten. In hoofdstuk twee van dit proefschrift werd het werkingsregime voor EFC van lactose onderzocht. Er werd aangetoond dat lactose en ijs gelijktijdig konden worden gekristalliseerd, waarbij tomahawkvormige kristallen werden geproduceerd. Verder werd aangetoond dat de hoeveelheid ent een grote invloed had op de uiteindelijke opbrengst, kristalgrootte en morfologie. Hoewel bij temperaturen onder nul er sprake is van sterk oververzadigde omstandigheden, blijkt kristalgroei het overheersende proces te zijn in plaats van nucleatie.

Bij lage temperatuur zijn er twee concurrerende effecten op de kristallisatiekinetiek. Enerzijds worden massatransport en de snelheid van zowel mutarotatie als nucleatie verminderd, waardoor de kristallisatiesnelheid afneemt.

Anderzijds wordt de oververzadiging verhoogd, waardoor de nucleatie en de kristalgroei toenemen en de kristallisatiesnelheid stijgt. Om dit te onderzoeken werden batch-experimenten onder verschillende omstandigheden gecombineerd met een populatie balansmodel dat mutarotatie, nucleatie en kristalgroei combineert. Bij temperaturen onder nul bleek dat mutarotatie snelheidsbeperkend was wanneer de kristallisatie snel verliep. De omzetting van bèta-lactose kon de snelle afname van α-lactose niet bijhouden. Er werd een empirisch model ontwikkeld om het concentratieprofiel en de deeltjesgrootte in de tijd te beschrijven.

Aangezien de vervanging van het huidige kristallisatie proces een uitdaging kan zijn is EFC het meest geschikt voor reststromen. In hoofdstuk vier werd het gebruik van EFC onderzocht voor de moederloog na lactose kristallisatie, delactosed whey permeate of DLP. Deze reststroom bevat nog 20wt.% lactose, maar vanwege het hoge mineraal- en watergehalte, de hoge viscositeit en kleverigheid is het momenteel economisch niet haalbaar om deze stroom verder terug te winnen. Daarom wordt deze stroom daarom meestal gezien als afval. In hoofdstuk vier werd aangetoond dat een aanzienlijk deel van de lactose kan worden teruggewonnen bij temperaturen onder nul. Bovendien bleek de neerslag van calciumfosfaat in de eerste 24 uur beperkt te zijn. Door een hogere mutarotatie snelheid, veroorzaakt door de in DLP aanwezige mineralen, werd de kristallisatiesnelheid van lactose verhoogd ten opzichte van pure lactose oplossingen. Na 24 uur werd een opbrengst gevonden van 85%, de resulterende kristallen hadden een tomahawk morfologie en een gemiddelde grootte van ongeveer 30μm.

Batch EFC-experimenten bleken een uitdaging; voor EFC is continue verwijdering van ijs en lactose essentieel. Daarom werd in hoofdstuk 5 een continue pilot opstelling gebruikt. Wei permeaat werd continu toegevoerd aan de

kristallisator, ijs en lactose werden continu verwijderd door een centrifuge en een bandfilter. Tijdens twee onafhankelijke runs werd bewezen dat lactose kon worden teruggewonnen door EFC. Er werd een conceptueel ontwerp voorgesteld waarbij lactose continu werd teruggewonnen en het energieverbruik werd verminderd door gebruik te maken van de latente warmte van ijs.

De massa- en energiebalansen werden verder geanalyseerd in hoofdstuk 6, hierbij werd EFC vergeleken met de huidige stand van de techniek in de industrie: mechanical vapor recompression (MVR) verdamping. Er werd aangetoond dat bij een vergelijkbaar rendement van 80% EFC tweemaal zo efficiënt is als een kristallisatieproces met MVR. Afhankelijk van de locatie kan restwarmte beschikbaar zijn om de toevoer naar de MVR voor te verwarmen. Hierdoor zou het energieverbruik van MVR significant afnemen, maar in vergelijking met EFC nog steeds 30% hoger liggen.

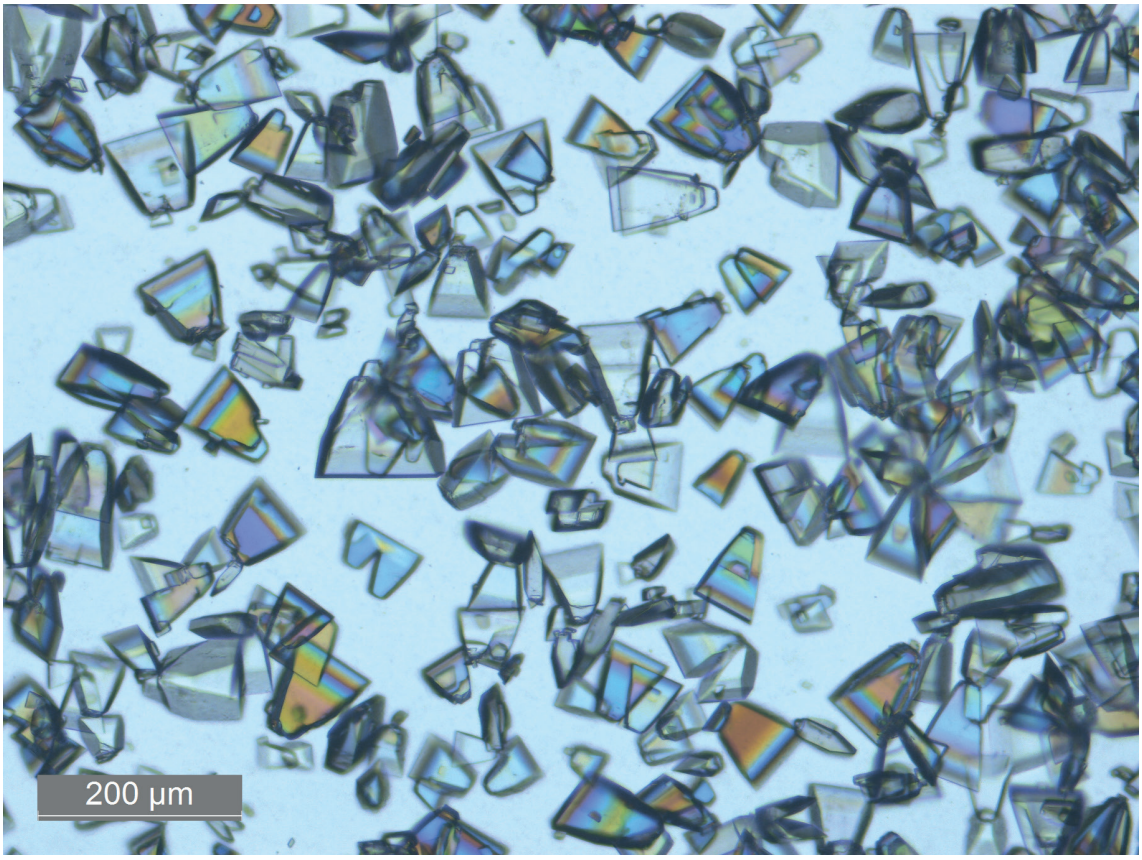

*Lactose crystals obtained from synthetic delactosed whey permeate

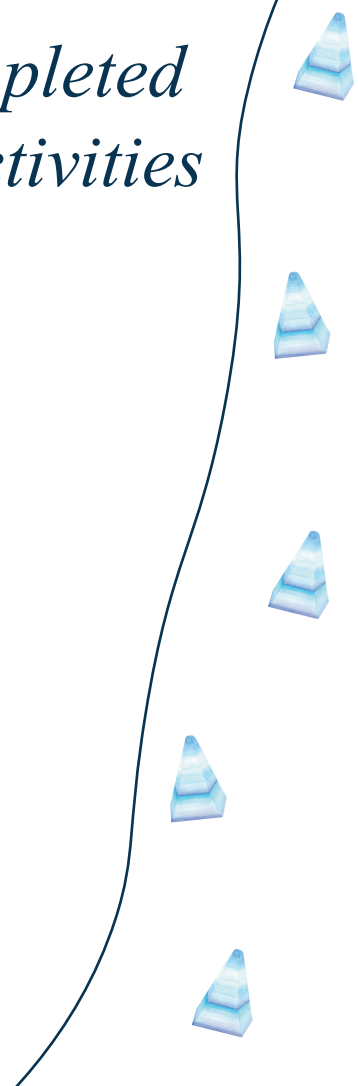

Acknowledgements

After four years my PhD journey comes to end, with this thesis as a result. Although the PhD proved challenging at times I have enjoyed it very much. A big part of this joy was the collaboration and the time I spent with the people I met at Wetsus. I could not have finished this thesis without the help and support of many others.

I would first like to thank my promotor and supervisors. **Albert**, dank voor alle steun de afgelopen vier jaar en inhoudelijke discussies. Onze overleggen waren meestal lang en intens maar de tijd vloog voorbij, ik heb onze discussies als zeer prettig ervaren. Ik heb het enorm gewaardeerd hoeveel tijd je voor mij en ons project vrijmaakte. **Doekle**, dank dat ik altijd bij je terecht kon met al mijn grote en kleine problemen in mijn onderzoek. Je gaf me vaak een andere kijk op dingen, je liet mij zien dat bij veel dingen het wellicht minder ingewikkeld is dan het op het eerste gezicht voor mij leek. Ik kijk met veel plezier terug op onze samenwerking de afgelopen vier jaar. **Jaap**, bedankt voor de begeleiding en inhoudelijke discussies over EFC en je praktische ervaring in het lab. **Henk**, dank voor alle discussies en je input als thema coördinator voor mijn project. **Karel**, dank voor je hulp met alle statistiek en modeleer problemen, ik heb hiervan veel geleerd en ik heb onze samenwerking als prettig ervaren.

I would like to thank the MSC students who did their internship for my project, **Sander**, **Louise** and **Igy**. Working on this PhD was so much more fun with your collaboration, thank you for all your hard work in the lab, effort and input. Special thanks for **Louise** for helping me with the pilot test we did in Rotterdam, it was a really nice experience.

I would like to thank the analytical team and technical support. Having limited lab experience at the start I got a lot of help from the analytical team, something I am very grateful for. Thank you for answering all my questions and for all the support throughout my PhD. The technical support team was always ready to help out, special thanks for **Ernst**, who was always ready when I wanted to modify my setup or to help me when, once again, the system stopped working. **Cees**, **Johannes** and **Bert** thank you for the amazing place Wetsus has become. Also, thanks for the support staff, secretaries, human resources and canteen team; without you Wetsus would not be so organized and nice as it is.

Working in Leeuwarden, it was sometimes challenging to keep in touch with Wageningen University. I would like to thank all the support I got from the food process engineering department. **Marjan**, **Ilona**, **Esther**, **Evelyn** and **Martin** thank you for all the support throughout my PhD. A part of the analysis was done in the laboratory at Wageningen, thank you **Jos**, **Maurice** and **Wouter** for doing the analysis and answering all my questions although I was far away.

I had the luck of working in one of the best offices of Wetsus. Starting all more or less at the same time we grew close. I will cherish the time we spent together and hope we can stay in touch. In random order: **Angel** thanks for all the nice discussions and talks we had during our breaks, lunches and dinners. I wish you all the best in Gent. **Vania**, I enjoyed our many discussions and your different views on subjects. **Xiaoxia**, your enthusiasm about science always inspired me, I wish you lot of happiness. **Carlo**, you are one of the kindest persons I met in Wetsus, always willing to help or to have a chat, I enjoy spending time together. **Anthony**, I am glad we were officemates in two

different offices, I wish you a lot of happiness with Virgin. **Yicheng**, although you started at the end of my PhD it soon felt like you were already part of the office for years. I enjoyed our talks and climbing together. **Olga** I will treasure our many talks, walks, coffee breaks, dinners and climbing session together. You were a great support in my PhD for the last five years.

Special thanks for my paranymphs **Yujia** and **Nouran**, for helping me to arrange everything around the defence. **Yujia**, I like how you bring out my spontaneous side. I enjoy the time we spent together during our many climbing sessions, dinners and our trip to London. I hope there are many more to come. **Nouran**, although we have completely different backgrounds, I felt we had a good connection from the start, and I really enjoyed talking to you. After hearing all the stories about Egypt, I would love to visit it one day.

The final phase of the thesis can be very stressful, writing the thesis and at the same time looking for the next step in your career. **Shuyana**, thank you for supporting me in this, I really enjoyed our writing sessions together and the many chats we had. **Ruizhe**, thank you for the many lunches and climbing sessions together. I wish you a lot of fun in Switzerland and expect to see you as a professor in a few years. **Barbara**, **Nandini** and **Anthony** I am happy we were in the writing office together. Also thank to the mindfulness group within Wetsus for bringing me some peace of mind, **Shuyana, Barbara**, **Jolanda**, **Alicia** and **Carlo**.

Amanda, **Liang-shin**, **Shuoguang, Rouel** thank you for the fun games of badminton. Climbing has become a big part of my live at Wetsus, I really enjoy it but even more importantly the company during climbing: **Ruizhe**, **Yujia**, **Sam**, **Kestral**, **Loes**, **Olga**, **Jasper**, **Angel** and **Yicheng** I hope we will have many more climbing sessions together. I also would like to thank **Carlos**, **Wokke**, **Raquel**, **Philip**, **Sara**, **Suyash**, **Catarina**, **Chris**, **Qingdian**, **Ragne**,

Sophie. Perhaps I forgot to put your name in this acknowledgement however I really enjoyed the interaction I had with all the people in Wetsus.

Als laatste wil ik mijn familie bedanken. **Tamara** dank voor het maken van de cover, het is supermooi geworden. **Wayra** dank voor alle lange wandelin-gen voor als het even te veel was. **Mam**, **Pap**, **Jochem**, **Laura**, **Tamara**, dank dat jullie altijd voor mij klaar staan.

List of publications

Halfwerk, R., Yntema, D., Van Spronsen, J., Van der Padt, A., (2023). Recovery of lactose from simulated delactosed whey permeate by a low-temperature crystallization process. *Accepted for publication in Journal of Dairy Science*

Halfwerk, R., Verdonk, L., Yntema, D., Van Spronsen, J., Van der Padt, A., (2023.) Scaling up continuous eutectic freeze crystallization of lactose from whey permeate: A pilot plant study at sub-zero temperatures. *Food Research International.* 168, 112764.

Halfwerk, R., Yntema, D., Van Spronsen, J., Keesman, K.J., Van der Padt, A., (2023). Crystallization kinetics of lactose recovered at sub-zero temperatures: A population balance model combining mutarotation, nucleation and crystal growth. *Journal of Food Engineering*. 11412.

Halfwerk, R., Yntema, D., Van Spronsen, J., Van der Padt, A., (2021). A sub-zero crystallization process for the recovery of lactose. *Journal of Food Engineering,* . 308, 110677.

Louwes, A.C., **Halfwerk, R.B**., Bramer, E.A., Brem, G., (2019). Experimental Study on Fast Pyrolysis of Raw and Torrefied Woody Biomass. *Energy Technology*.

About the author

Ruben Halfwerk was born on December 23th in Dalfsen, the Netherlands. From 2009-2013 he did his bachelor Mechanical Engineering at Windesheim University of applied Science in Zwolle. In 2013 he started the master Mechanical Engineering with specialization thermal engineering at the University of Twente. The graduation thesis was an experimental research on the effect of torrefaction as biomass pre-treatment on the reaction rates of flash pyrolysis reactions. After graduation he was employed as a consultant 'energy and process technology' at KWA bedrijfsadviseurs. In 2018 he had the opportunity to start a PhD research investigating the use of eutectic freeze crystallization on the recovery of valuable, heat sensitive products and concentrates in agriculture and food industry. This project was a collaboration with university of Wageningen and research institute Wetsus under the supervision of Doekle Yntema, Jaap van Spronsen and Albert van der Padt.

Overview of completed training activities

Discipline specific activities

Courses

Downstream Processing	Biotech Delft, The Netherlands	2019
Rheology course	Vlag, The Netherlands	2021

Conferences

European Water Tech Week[o]	Wetsus, The Netherlands	2018[o] 2022[o]
Symposium DACG	DACG, The Netherlands	
Symposium NWGD[p]	NWGD The Netherlands	2018
Internal congres Wetsus	Wetsus, The Netherlands	2018 2019 2020 2021[o]
International Symposium on Industrial Crystallization	ISIC, Germany	2021

General courses

Personal development program for PhD	Wetsus, The Netherlands	2018
Communication styles	Wetsus, The Netherlands	2018
Presentation course	Wetsus, The Netherlands	2018
"Illustrations for scientific publications	Wetsus, The Netherlands	2018
Supervision course	Wetsus, The Netherlands	2018
Talent course	Wetsus, The Netherlands	2019

Scientific writing course	In'to languages/WUR The Netherlands	2020
Business development course +presentation/pitch	Wetsus, The Netherlands	2021[o]
Mindfulness course	Wetsus, The Netherlands	2021
Introduction to R	VLAG, The Netherlands	2021
Applied statistics	VLAG, The Netherlands	2021
Career perspectives	Wageningen graduate school, The Netherlands	2021

Other Activities

Writing research proposal	Wetsus, The Netherlands	2018
Theme meetings Wetsus[o]	Wetsus, The Netherlands	2018-2022
Particulate products (MSc-course)	University of Groningen The Netherlands	2018

[p]poster presentation, [o]oral presentation